

**PLASMODESMATA AND SYMPLASTIC TRANSPORT  
IN ONION (*ALLIUM CEPA* L.) ROOTS**

**By**

**Fengshan Ma**

**A thesis  
presented to the University of Waterloo  
in fulfillment of the  
thesis requirement for the degree of  
Doctor of Philosophy  
in  
Biology**

**Waterloo, Ontario, Canada, 2000**

**© Fengshan Ma 2000**



National Library  
of Canada

Acquisitions and  
Bibliographic Services

395 Wellington Street  
Ottawa ON K1A 0N4  
Canada

Bibliothèque nationale  
du Canada

Acquisitions et  
services bibliographiques

395, rue Wellington  
Ottawa ON K1A 0N4  
Canada

*Your file Votre référence*

*Our file Notre référence*

The author has granted a non-exclusive licence allowing the National Library of Canada to reproduce, loan, distribute or sell copies of this thesis in microform, paper or electronic formats.

The author retains ownership of the copyright in this thesis. Neither the thesis nor substantial extracts from it may be printed or otherwise reproduced without the author's permission.

L'auteur a accordé une licence non exclusive permettant à la Bibliothèque nationale du Canada de reproduire, prêter, distribuer ou vendre des copies de cette thèse sous la forme de microfiche/film, de reproduction sur papier ou sur format électronique.

L'auteur conserve la propriété du droit d'auteur qui protège cette thèse. Ni la thèse ni des extraits substantiels de celle-ci ne doivent être imprimés ou autrement reproduits sans son autorisation.

0-612-51210-X

Canada

The University of Waterloo requires the signatures of all persons using or photocopying this thesis. Please sign below and give address and date.

## ABSTRACT

The structure of onion (*Allium cepa* L. cv. Ebenezer) roots was studied by light and electron microscopy, with special reference to the plasmodesmata and their functions in symplastic transport. In young zones (< 50 mm from the root tip), all living cells were linked by plasmodesmata. In old zones (> 50 mm from the root tip), all plasmodesmata in the exodermal long cells were severed by the developing suberin lamellae. Observations were focused on zones 100 mm and farther from the root tip where all long cells of the exodermis had formed suberin lamellae and the endodermal cells were at various stages of wall modification. Hydrophobic substances were also incorporated into epidermal cell walls. All these three cell layers had a low permeability, and this represented an enormous challenge for preserving cellular structures for transmission electron microscopy. One of the major contributions of the present study was the establishment of suitable techniques that made possible a series of investigations at the ultra-structural level.

A complete assessment of plasmodesmatal frequencies was performed for all cell types 100 mm from the root tip. Along the inward path (*i.e.* that taken by ions), the frequencies at the interfaces of epidermis-exodermal short cells-central cortex-central cortex-endodermis-pericycle-stelar parenchyma were 0.21, 1.03, 1.59, 0.58, 0.70, and 0.12 plasmodesmata per  $\mu\text{m}^2$  wall surface, respectively. When converted into numbers of plasmodesmata per mm root length, the numerical values for the interfaces of epidermis-exodermis-central cortex-endodermis-pericycle-stelar parenchyma were  $8.96 \times 10^4$ ,  $4.05 \times 10^5$ ,  $5.13 \times 10^5$ ,  $5.64 \times 10^5$ , and  $1.25 \times 10^5$ , respectively. These numbers were believed to be the most instructive for assessing the degree of symplastic connection as all cell layers (except for those of the central cortex) were organized in concentric cylinders and the surface area traversed by ions was gradually decreasing. The data for the central cortex was not obtained because the cells were connected to each other in

all directions, but the number of plasmodesmata available for radial transport was postulated to be high enough to support symplastic transport across this tissue. Therefore, significant symplastic transport was possible from the short cells of the exodermis up to the pericycle. From the epidermis to the short cells, much less symplastic transport was anticipated, and even less from the pericycle to the stelar parenchyma. Accordingly, a combination of symplastic and transmembrane transport was postulated to occur across the interface of the epidermis and short cells, and little transport from the pericycle to the stelar parenchyma.

In the phloem, the highest plasmodesmatal frequency was observed at the interface of metaphloem sieve elements and companion cells. The rest of the interfaces had much lower yet constant frequencies. This result suggested that photosynthates would be first transferred from the metaphloem sieve elements to companion cells and then distributed to the surrounding cells.

Ultrastructural observations and plasmodesmatal frequency analysis indicated that the pericycle could more intensively contribute to the transport process than previously envisioned. The high plasmodesmatal frequency on the radial walls of this layer implied that a significant transfer of solutes was occurring in the tangential direction. This would be beneficial to the overall transport in the root in which the xylem and phloem are arranged alternately.

By using an ultrastructural ion precipitation technique, chlorine movement in the root was monitored. It was shown that all ranks of plasmodesmata were functional in transferring ions from the culture media to the stele. The precipitation pattern was approximately parallel to the plasmodesmatal frequencies. Under nutrient deficiency, the phloem was involved in reallocating chlorine from the shoot to the root tissues. Stelar parenchyma might play a role in transferring these ions from the companion cells to the pericycle. Also, epidermal cells sometimes developed wall ingrowths on their outer tangential side (*i.e.* transfer cells), which was regarded as a mechanism of enhancing transport across the boundary of the

apoplast and symplast. When grown in a  $\text{CaSO}_4$  solution, the nutrient deficiency symptoms were remarkably alleviated. Calcium was postulated to have enhanced the reallocation of phloem-mobile ions (including chloride).

The development of wall modifications was investigated in the endodermis and exodermis. In the endodermis, Casparian bands, suberin lamellae, and tertiary walls formed in succession at increasing distances from the root tip. During band initiation, the tight binding of the plasma membrane to the anticlinal walls was established before the hydrophobic components could be detected in ultrathin sections. Casparian bands exhibited increased electron density with age. Mature bands never exceeded half the length of the radial walls. Suberin lamella formation started first along the outer tangential walls and then along the inner tangential walls. At the site of the Casparian band, the plasma membrane was detached from the wall, then hydrophobic substances were laid down. Tertiary wall formation commenced immediately afterwards. Large populations of dictyosomes and ER profiles were observed during suberin lamella and tertiary wall formation. These membrane systems were also found in association with the plasma membrane. This was suggestive of the involvement of membrane systems in the synthesis and delivery of wall materials. None of the wall modifications interrupted the symplastic connections of the endodermis. In the exodermis, Casparian bands were detected with fluorescence microscopy, but were not positively defined with the electron microscopy. The radial walls were extremely thin and alterations (if any) of their electron density were not apparent. Suberin lamellae were formed only in long cells, in which dictyosomes and ER were prominent. No tertiary walls had developed in the exodermis. All plasmodesmata in long cells were severed once suberin lamellae were laid down and the cells eventually died. Therefore, in a root with a mature exodermis, the epidermis was linked to the cortex only through the short cells without suberin lamellae.

## **ACKNOWLEDGEMENTS**

I am very grateful to my supervisor, Dr. Carol Peterson, for offering me the opportunity to work in her laboratory. Her skillful guidance was invaluable to me. She has been very kind and considerate as well.

My appreciation goes to my committee, Drs. Frédérique Guinel, Larry Peterson and John Thompson. I learned so much from the many discussions, both at my yearly committee meetings and in informal settings. They have been a source of encouragement to carry on my struggle against the difficulties encountered during the program.

The TEM work was supported by Dale Weber. His skills in communicating with the machines were very impressive. His care and efficiency ensured the high quality of the hundreds of negatives. I enjoyed so much working with him. Thank you, Dale!

Many thanks to my colleagues in the laboratory. Daryl's advice and assistance significantly contributed to the success of my research. Ewa had generously offered her ideas and expertise. Dave, Jeff, Jeanine and Lydia were all very nice and helpful. I will miss the team greatly.

I thank the University of Waterloo for awarding me the International Graduate Student Scholarships, Graduate Student Scholarships and Teaching Assistantships.

I want to say a BIG "THANK YOU" to Professor Wendian Li at the Chinese Academy of Forestry in Beijing. She first showed me the proper way of doing science during my B.Sc. thesis research in her laboratory.

I am particularly indebted to my parents, sisters, brothers and family. Without their caring and suffering, my education would be otherwise impossible.

## TABLE OF CONTENTS

TITLE PAGE .....	i
AUTHOR'S DECLARATIONS.....	ii
BORROWER'S PAGE .....	iii
ABSTRACT .....	iv
ACKNOWLEDGEMENTS .....	vii
TABLE OF CONTENTS .....	viii
LIST OF TABLES .....	xiii
LIST OF FIGURES .....	xiv

### Chapter 1

<b>General introduction .....</b>	<b>1</b>
1.1 Scope of the thesis .....	1
1.2 Transport pathways: a literature review .....	2
1.2.1 Membrane transport .....	2
1.2.2 Apoplastic transport .....	3
1.2.3 Symplastic transport .....	4
1.2.3.1 Structure and function of plasmodesmata .....	4
1.2.3.2 Regulation of plasmodesmata .....	8
1.2.4 Structure of the root: relation to radial ion transport pathways .....	11
1.2.4.1 Epidermis .....	11
1.2.4.2 Central cortex .....	12
1.2.4.3 Endodermis .....	12
1.2.4.4 Exodermis .....	13
1.2.4.5 Pericycle .....	16
1.2.4.6 Stellar parenchyma .....	16
1.2.4.7 Xylem vessels .....	17
1.2.4.8 Phloem .....	17
1.2.4.9 Control steps for radial ion transport in roots: a summary .....	17



1.3	Plasmodesmata in the root .....	19
1.3.1	General considerations .....	19
1.3.2	A case study of onion roots .....	20

## Chapter 2

	<b>Plasmodesmata in onion roots: a study enabled by improved fixation and embedding techniques .....</b>	<b>24</b>
2.1	Abstract .....	24
2.2	Introduction .....	25
2.3	Materials and methods .....	27
2.3.1	Plant material .....	27
2.3.2	Transmission electron microscopy .....	28
2.3.3	Histochemical detection of suberin .....	29
2.3.4	Observation of pit fields and wound pit callose .....	29
2.4	Results .....	30
2.4.1	Light microscopic observations of endodermal and exodermal development .....	30
2.4.2	Primary pit fields and wound pit callose in the exodermis .....	30
2.4.3	Transmission electron microscopic observations of wall modifications in endodermis and exodermis .....	31
2.4.4	Protoplasts of long and short cells .....	36
2.4.5	Plasmodesmata .....	36
2.4.5.1	In tangential walls (radial symplastic path) .....	39
2.4.5.2	In transverse and radial walls .....	39
2.5	Discussion .....	44
2.5.1	The TEM technique for suberized cells .....	44
2.5.2	Plasmodesmata .....	47
2.5.3	Short cells .....	49
2.6	Conclusion .....	50

## Chapter 3

### **Plasmodesmatal frequencies in onion roots:**

<b>implications for transport pathways</b> .....	51
3.1 Abstract .....	51
3.2 Introduction .....	52
3.3 Materials and methods .....	54
3.3.1 Transmission electron microscopy .....	54
3.3.2 Calculation of plasmodesmatal frequencies along the inward path (from the epidermis to the stelar parenchyma) .....	54
3.3.3 Calculation of plasmodesmatal frequencies associated with the phloem .....	58
3.3.4 Statistics .....	58
3.4 Results .....	63
3.4.1 Plasmodesmatal frequencies along the path of ions .....	63
3.4.2 Plasmodesmatal frequencies associated with the phloem .....	63
3.5 Discussion .....	68
3.5.1 Plasmodesmatal frequencies: implications for transport of ions .....	71
3.5.2 On phloem unloading and post-phloem transport of photosynthates in the old zone .....	73
3.5.3 A further note on the pericycle .....	75
3.6 Conclusion .....	75

## Chapter 4

### **Plasmodesmata in the symplastic transport of chloride**

<b>in onion roots: an ultrastructural ion localization study</b> .....	81
4.1 Abstract .....	81
4.2 Introduction .....	82
4.3 Materials and methods .....	83

4.3.1	Growth conditions and treatments .....	83
4.3.2	Chloride precipitation for the TEM .....	84
4.4	Results .....	85
4.4.1	Plants grown in vermiculite (experiment 1) .....	85
4.4.2	Plants in vermiculite with an additional incubation in NaCl (experiment 2) .....	88
4.4.3	In pure water (experiment 3) .....	88
4.4.4	Cultured in pure water, and later treated with NaCl (experiment 4) ....	91
4.4.5	In CaSO <sub>4</sub> solution (experiment 5) .....	91
4.4.6	Grown in CaSO <sub>4</sub> solution, and later incubated in NaCl solution (experiment 6) .....	94
4.5	Discussion .....	94
4.5.1	The plasmodesmata are functional in the radial transport of ions toward the stele .....	94
4.5.2	The function of the pericycle and stelar parenchyma .....	98
4.5.3	Function of the various vessel members .....	99

## Chapter 5

	<b>Development and ultrastructure of cell wall modifications in the endodermis and exodermis of onion roots .....</b>	<b>100</b>
5.1	Abstract .....	100
5.2	Introduction .....	101
5.3	Materials and methods.....	103
5.4	Results .....	103
5.4.1	Casparian bands in the endodermis .....	103
5.4.2	Suberin lamellae in the endodermis .....	106
5.4.2.1	Along the tangential walls .....	106
5.4.2.2	Along the radial walls .....	106
5.4.3	Tertiary walls in the endodermis .....	111
5.4.4	Suberin lamellae in the exodermis .....	111

5.5	Discussion .....	116
5.5.1	Casparian bands and suberin lamellae in the endodermis .....	119
5.5.2	Wall modification in the exodermis .....	121
5.5.3	The relationships of suberin lamellae to other cellular structures .....	122

## Chapter 6

<b>General Discussion</b> .....	128
6.1 Root development, transport, and wall modifications .....	128
6.2 The distribution of plasmodesmata in the old zone of the root .....	129
6.2.1 On the inward direction .....	129
6.2.2 Plasmodesmatal frequencies: implications for phloem unloading and post-phloem transport .....	131
6.3 Plasmodesmata in ion transport .....	132
6.4 Wall modifications in the endodermis and exodermis .....	133
6.5 Conclusions .....	135
<b>References</b> .....	137

## LIST OF TABLES

<b>Table 2.1</b>	<b>Pit fields and wound pit callose in the exodermis of onion roots</b>	<b>..... 34</b>
<b>Table 3.1</b>	<b>Plasmodesmatal frequencies along the radial files of onion root tissues</b>	<b>..... 59</b>
<b>Table 3.2</b>	<b>Plasmodesmatal frequencies associated with the phloem</b>	<b>..... 66</b>

## LIST OF FIGURES

<b>Fig. 1.1</b> Schematic representation of the structure of a plasmodesma (longitudinal section) .....	5
<b>Fig. 1.2</b> Schematic representation of an onion root (cross section) .....	21
<b>Fig. 2.1</b> Light microscopic preparations of onion root tissues .....	32
<b>Fig. 2.2</b> Ultrathin cross sections of old zone showing wall modifications in endodermis and exodermis .....	37
<b>Fig. 2.3</b> Median longitudinal ultrathin section taken 2 mm from the root tip .....	40
<b>Fig. 2.4</b> Plasmodesmata in tangential walls of cells in a radial file of the root (cross sections) .....	42
<b>Fig. 2.5</b> Plasmodesmata in radial walls of endodermis and pericycle .....	45
<b>Fig. 3.1</b> Diagram of a cross section of onion root showing cell and tissue interfaces studied for plasmodesmatal frequencies .....	55
<b>Fig. 3.2</b> Plasmodesmogram of onion roots: plasmodesmatal frequencies from the epidermis to the stele .....	61
<b>Fig. 3.3</b> Structure of phloem and surrounding tissues .....	64
<b>Fig. 3.4</b> Plasmodesmogram of onion roots: plasmodesmatal frequencies associated with the phloem .....	69
<b>Fig. 3.5</b> Pericycle as “annular collector” for ions .....	77
<b>Fig. 3.6</b> Pericycle as “annular disperser” for photosynthates .....	79
<b>Fig. 4.1</b> AgCl precipitation in onion roots grown in vermiculite .....	86
<b>Fig. 4.2</b> Chloride in roots grown in vermiculite and later treated in NaCl .....	89
<b>Fig. 4.3</b> Chloride in roots grown in pure water and later treated in NaCl .....	92
<b>Fig. 4.4</b> Roots grown in pure water or CaSO <sub>4</sub> solution and later treated In NaCl .....	95
<b>Fig. 5.1</b> Casparian band formation in the endodermis of onion roots .....	104
<b>Fig. 5.2</b> Suberin lamella development along the endodermal tangential walls ..	107
<b>Fig. 5.3</b> Suberin lamella deposition over the Casparian band in the endodermis .....	109
<b>Fig. 5.4</b> Tertiary wall formation in the endodermis .....	112

<b>Fig. 5.5</b>	<b>Suberin lamella deposition in the exodermal long cells (early stage)...</b>	<b>114</b>
<b>Fig. 5.6</b>	<b>Suberin lamella deposition in the exodermal long cells (late stage) ..</b>	<b>117</b>
<b>Fig. 5.7</b>	<b>Schematic reconstruction of suberin lamella formation in the endodermis (illustrated in the literature) .....</b>	<b>123</b>
<b>Fig. 5.8</b>	<b>Schematic representation of suberin lamella formation in the endodermis of onion roots .....</b>	<b>125</b>

# Chapter 1

## General Introduction

### 1.1 Scope of the thesis

Among the functions that a root system performs, nutrient uptake and transport are the most fundamental to the life of a plant. In the study of transport physiology, the root has been traditionally viewed as consisting of two compartments, the apoplast and symplast (Münch 1930). The apoplast is composed of cell walls, intercellular spaces, and lumina of dead cells including tracheary elements. The symplast is the totality of plasmodesmata-linked cytoplasms. These two compartments are demarcated by the plasma membrane. Three transport pathways have been characterized, namely apoplastic, symplastic and transmembranous, which may be used individually or in combination. Across the root tissues, from the soil solution (or culture medium) to the stele, water flows through cell walls and membranes (see Steudle and Peterson 1998). Solutes move (passive diffusion) freely in the apoplast (until blocked by hydrophobic barriers), less freely through plasmodesmata, and the least freely across the membrane. This thesis will be primarily concerned with the radial symplastic transport of ions (Chapters 2, 3, 4).

A second topic of the project is concerned with phloem unloading in the old zones of roots. Some interest has centered on the root apex (Oparka et al. 1994, Zhu et al. 1998a) which, because of the active cell division and growth, is a significant sink. In the old zones, the bulk of the tissues are composed of living cells; therefore, phloem unloading is also a necessity. Respiration, biosynthesis and all other metabolic processes can only be sustained by a



continuous supply of food. Apparently, plasmodesmata play an important role in food distribution as they do in other organs (*e.g.*, leaves and fruits). A comprehensive analysis of plasmodesmatal connections inside and around the phloem will help understand the photosynthate movement pathways (Chapter 3).

Whether or not the observed plasmodesmata are functional has always been a concern. There are several methods to probe the functionality of plasmodesmata, among which, however, only the ultrastructural ion localization technique allows a thorough examination of ion movement in all cells of the root tissues. This topic will be detailed in Chapter 4.

Cell wall modifications, in the forms of Casparian bands and suberin lamellae, normally occur in the endodermis and frequently also in the exodermis. These wall structures produce a profound effect on the overall transport pathways and mechanisms. An investigation of the cytological events of wall development has been undertaken (Chapter 5). Wall ingrowths can occur in the root, *e.g.*, during nutrient deficiency or salinity (see § 1.2.4.1).

## **1.2 Transport pathways: a literature review**

### **1.2.1 Membrane transport**

Both passive and active transport pathways for ions across membranes have been characterized in a number of systems. The plasma membrane represents a significant permeability barrier for ions (*i.e.*, for their passive diffusion through the lipid bilayer). Diffusion can be facilitated by specific channels. Active transport is accomplished by carrier (at the expenditure of energy). Channel-mediated transport has high rates and low specificities, while carrier-mediated transport has low rates and high specificities. These two mechanisms occur down and against an electrochemical gradient, respectively. In terms of radial ion movement in the root, membrane transport is restricted to certain locations, *e.g.*, the epidermis and probably some other tissues as well.

## 1.2.2 Apoplastic transport

Apoplastic transport occurs mainly in cell walls and these are chemically and structurally complex. Even primary walls contain cellulose and matrix materials (hemicelluloses, pectic polysaccharides, and structural proteins). Cellulose molecules are organized into microfibrils (10-30 nm in diameter), each containing regions of crystalline micelles and paracrystalline arrays (Frey-Wyssling 1969). Hemicelluloses are tightly bound to the cellulose microfibrils, forming the framework of a cell wall (Hayashi et al. 1987), which is immersed in the gel-like pectic polysaccharides. The major component of the pectic substances is polygalacturonic acid, the carboxyl groups of which are the origin of the large majority of negative charges of cell walls. In the wall, there are two categories of channels, large and small (Frey-Wyssling 1969). The large channels are formed between the microfibril-wrapped bundles. Inside each bundle are small channels (see Peterson and Cholewa 1998). In well-hydrated states, both categories of channels are filled with water, either free (in large ones) or bound (in small ones). Water and ions are assumed to move in large channels. To determine the diameters of the channels, cells and tissues of various origins were incubated in solutions of known molecular sizes and the wall pores (large channels) were estimated at 3.5-5.2 nm in diameter, permitting the passage of molecules with molecular weights of 1-7.5 kD (Carpita et al. 1979).

Diffusion is one mode of apoplastic transport across the apoplast for both ions and water (Läuchli 1976) and was generally thought to be the only one. But, in the case of root cortex of dicots, there is evidence that bulk water flow also occurs in transpiring plants (Aloni et al. 1998). However, when hydrophobic, long chain molecules are incrustated into cell walls (as in the case of Casparian bands), the channels will be diminished both in size and in number, or even totally blocked; thus, the apoplastic transport can be severely affected (§ 1.2.4.3 and 1.2.4.4).

## **1.2.3 Symplastic transport**

### **1.2.3.1 Structure and function of plasmodesmata**

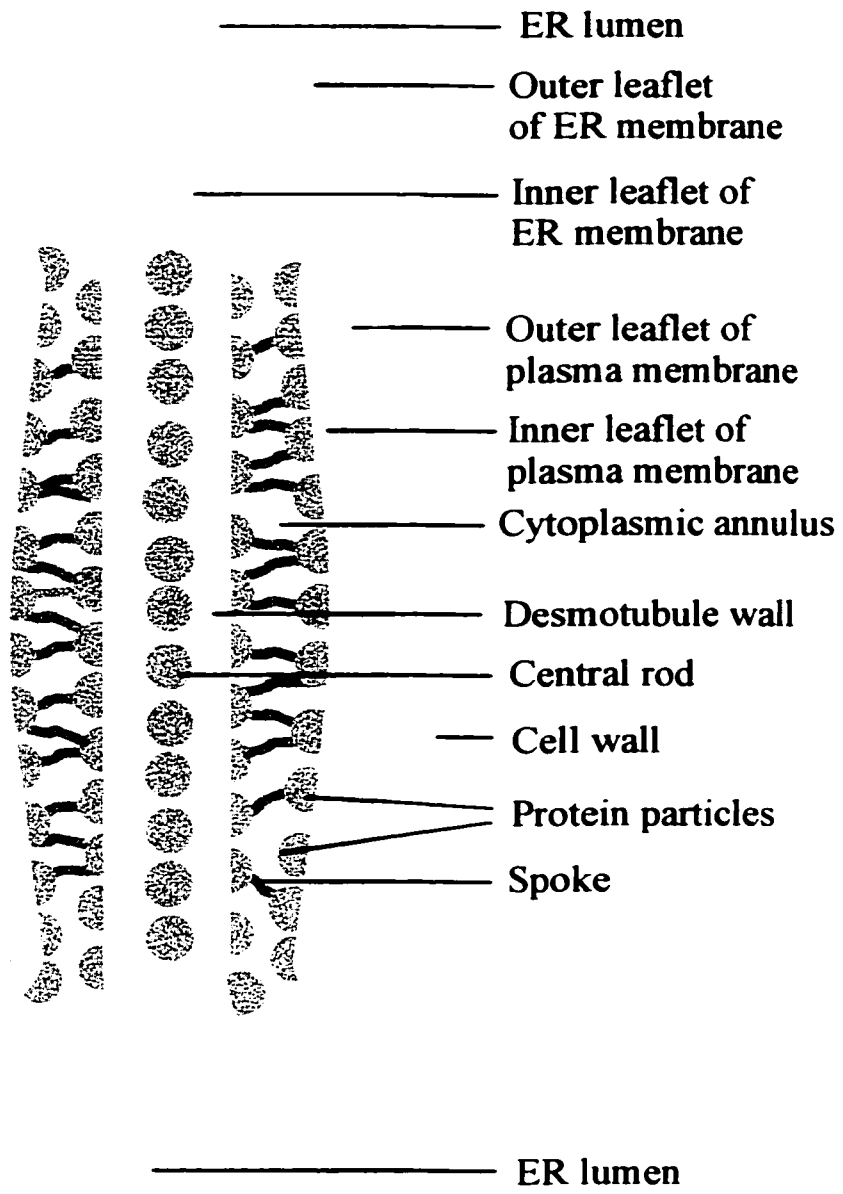
Plasmodesmata are cytoplasmic structures that link neighbor cells and provide a low-resistance transport pathway, the symplastic pathway. Large numbers of plasmodesmata are always associated with a huge amount of symplastic transport, as exemplified in salt glands (Campbell and Thomson 1975) and nectaries (Gunning and Hughes 1976). In leaves, high numbers of plasmodesmata are usually associated with the symplastic mode of phloem loading (van Bel et al. 1992, Turgeon 1996). While it is well known that plasmodesmata are extensively involved in numerous biological processes (in addition to phloem loading and unloading), our knowledge of their structure is still rudimentary.

Our knowledge about the structure of plasmodesmata has evolved over time. Plasmodesmata were initially named “offene Communicationen” (open communications) by Tangl in 1879 and later termed “Plasmodesmen” (plasmodesmata) by Strasburger in 1901 (cited in Carr 1976b). However, due to the small dimension (diameter  $\approx$  50 nm) and delicateness of plasmodesmata, their structure has not been clearly resolved. At the light microscopical level, plasmodesmata were viewed as cytoplasmic threads. At the electron microscopical level, many details were added into these “threads”. Over history, several models have been produced, among which were those of López-Sáez et al. (1966), Robards (1976) and Gunning and Overall (1983). It is recognized that plasmodesmata are lined with plasma membrane, and are traversed by a tubule, the desmotubule. Both ends of the desmotubule are connected with the endoplasmic reticulum (ER).

During recent years, the model published by Ding et al. (1992) has been the most frequently cited (Fig. 1.1); this is attributed to the reliability of cryofixation and freeze-substitution in preserving cellular structures. Computer-aided image-enhancement has further resolved the subcellular details. In this model, both the wall of the desmotubule (appressed ER) and the inner leaflet of the plasma membrane contain regularly spaced electron-dense particles (diameter  $\approx$  3 nm, presumably proteinaceous) embedded in lipid.

**Fig. 1.1 Schematic representation of the structure of a plasmodesma**

Longitudinal median sectional view (adapted from Ding et al. 1992). The plasma membrane is continuous, lining the pore of the plasmodesma between neighboring cells. Electron dense particles (presumably proteinaceous) are partially embedded in the lipid of the inner leaflet of the plasma membrane. The desmotubule, as appressed ER, is continuous with the ER at both ends of the plasmodesma. Both the desmotubule wall and the central rod are composed principally of proteinaceous particles. There are spoke-like extensions between the plasma membrane and the desmotubule. Between the desmotubule wall and the central rod, there are filamentous connections (not shown in the diagram).



The central rod is also particulate. The appressed ER and plasma membrane are bridged by spoke-like extensions. Symplastic transport is thought to take place through the cytoplasmic annulus (*i.e.*, the space between the plasma membrane and the appressed ER). The effective pore size is determined and regulated by the relative position of protein particles in the two sets of membranes (Ding et al. 1992). Shortly after this publication, it was shown that conventional fixation in conjunction with image enhancement produced essentially the same picture of plasmodesmatal structure (Botha et al. 1993).

The exact path through plasmodesmata appears to be variable, although the chief mechanism of symplastic transport has long been surmised to be by diffusion (Tyree 1970). It is quite widely accepted that the cytoplasmic annulus is a path for symplastic communication. During osmotic stress, the widening of the plasmodesmatal cytoplasmic annulus accompanies the increased symplastic phloem unloading in the root tip (Schulz 1995). Nevertheless, the cytoplasmic annulus is apparently not the sole path. Tubular ER, instead of appressed ER, has long been detected (see Robards 1976) and has been a topic of interest in the more recent literature (*e.g.*, Waigmann et al. 1997). This implies the possibility that the ER lumen is available for symplastic transport (Gamalei et al. 1994). In addition, lipids have been shown to diffuse through the appressed ER membrane (Grabski et al. 1993).

The functionality of plasmodesmata has been tested by a number of approaches. In the early years, experiments with microelectrodes established that living cells are electronically coupled through plasmodesmata (Lou 1955, Spanswick and Costerton 1967, Spanswick 1972, Overall and Gunning 1982). Now, plasmodesmatal functioning is routinely visualized by using plasma membrane-impermeable fluorescent tracer dyes, such as fluorescein isothiocyanate (FITC), Lucifer Yellow CH (LYCH) and trisodium 8-hydroxyl-1,3,6-pyrene trisulfonate (PTS). Furthermore, exciting advances have been made by microinjecting tracer-conjugated molecules of known molecular sizes into plant cells. These experiments showed that the symplast is not a uniform system all over the plant body; rather, it is composed of a number of domains with varying molecular size exclusion limits (SELs), in the range of 600-1000 Da (Goodwin 1983, Erwee and Goodwin 1985, Erwee et al. 1985, Terry and Robards

1987). The sieve elements and companion cells make up a special case, where much larger SELs were found (*e.g.*, 3 kD in *Cucumber maxima*, Kempers et al. 1993; 10 kD in *Vicia faba*, Kempers and van Bel 1997). All these results indicate that the individual domains are physiologically independent to each other, to a certain extent. The signaling patterns characterized in the shoot (Rinne and van del Schoot 1998, Gisel et al. 1999) and root apices (van den Berg et al 1995, 1997) probably correspond to the domain formation.

Plasmodesmata are selective for molecules. In addition to the molecular sizes (see above), there are some additional factors that govern transport. Particularly, plasmodesmata are selective for molecules by their charge(s) and, especially, their structures (Tucker and Tucker 1993). These results could explain the findings on plant hormone transport. For example, it was found that gibberellic acid was transported through plasmodesmata (Drake and Carr 1979, Kwiatkowska 1991), but auxin was not (Drake and Carr 1978). It is interesting to note that gibberellins share certain structural similarities with fluorescein that is a symplastic tracer dye. Auxin is a derivative of tryptophan which is one of those amino acids that cannot move symplastically (in the staminal hair cells of *Setcreasea purpurea*, Tucker and Tucker 1993). It must be emphasized that we are still in a very early stage of resolving the selectivity of plasmodesmata. For instance, it is rather common in the plant body that cells that are interconnected by plasmodesmata can be dramatically different from each other structurally (and thus physiologically). It is not clear how the identity of each type of cell is maintained when symplastic communication normally occurs.

### **1.2.3.2 Regulation of plasmodesmata**

The dynamic nature of plasmodesmata has been a subject of intense investigation. The traditional view of the functional control of plasmodesmata is that sphincters at the neck region modulate symplastic transport through the cytoplasmic annulus (Olesen 1979), although the presence of sphincters is not a constant feature of all observed plasmodesmata. In a recent report, Rinne and van der Schoot (1998) have shown that, during induction of dormancy in the shoot apical meristem of *Betula pubescens* Ehrh.,

callose deposition at the neck of plasmodesmata is associated with plasmodesmatal closure (and thus symplastic isolation of the component cells from each other). Several factors can alter the permeability of plasmodesmata, such as pressure gradient (Cote et al. 1987, Oparka and Prior 1992), ATP level (Cleland et al. 1994), light intensity (Epel and Bandurski 1990), and cytoplasmic free calcium concentration (Tucker 1990). Signaling molecules, albeit unidentified yet, probably play a significant role in regulating plasmodesmatal functioning (see Crawford and Zambryski 1999).

The plasmodesmata could be remarkably expanded during intercellular movement of macromolecules. As early as half a century ago, nuclear extrusion through plasmodesmata was observed in bright optics microscopes (well before the plasmodesmata were ultrastructurally examined) and was believed to be a normal phenomenon of common occurrence (Lou et al. 1956, and literature cited therein). Recently, trafficking of either endogenous proteins (see review by McLean et al. 1997) or virus-related macromolecules has been observed in a number of systems (see Ghoshroy et al. 1997, Ding 1998, Ding et al. 1999, Lucas 1999). SELs can be 10 kD (Wolf et al. 1989) and even 45 kD (Kikuyama et al. 1992). These kinds of results were obtained by conjugating either a fluorescent dye (above) or the green fluorescent protein (Oparka et al. 1996) to a given molecule. The interaction between the macromolecules and the plasmodesmata has not been elucidated.

Recent research is expanding our vision of plasmodesmatal function and regulation. The frequently observed neck constriction in plasmodesmata could be an artifact due to physical wounding and glutaraldehyde fixation. For example, in pretreated tissues of onion roots with 2-deoxy-D-glucose (DDG, an inhibitor of callose synthesis), the plasmodesmata exhibited a funnel-shaped configuration, *i.e.*, without neck constriction (Radford et al 1998). Special wall material of an unknown chemical nature was found associated with the plasmodesmatal plasma membrane, which was postulated to help regulate the plasmodesmatal permeability (Badelt et al. 1994). Actin (White et al. 1994, Ding et al. 1996, Blackman and Overall 1998) and myosin (Radford and White 1998,



Blackman and Overall 1998) were detected in the plasmodesmata, and these are surmised to play a role in the regulation of plasmodesmatal function.

The regulation of plasmodesmatal functioning also lies in structural alteration during ontogenesis. Initially, plasmodesmata are formed at cytokinesis when endoplasmic reticulum (ER) is incorporated into the growing cell plate (Jones 1976, Hepler 1982), which is referred to as the primary formation. These plasmodesmata are simple channels without branching. Primary plasmodesmata can be modified in structure, usually by forming branches. This occurs in particular locations, probably depending on the function of the tissues in the plant body (see Jones 1976, Robards and Lucas 1990). Plasmodesmata can also be created *de novo*, either during natural morphogenesis (Seagull 1983, Wang et al. 1998, Zhu et al. 1998b) or during tissue fusion (van der Schoot et al. 1995). Secondary plasmodesmata were also commonly observed in plant chimeras (see Jones 1976, Robards and Lucas 1990, Ehlers and Kollmann 1996). Cellulase (a hydrolytic enzyme) probably plays a critical role in the creation of secondary plasmodesmata (Wang et al. 1998). Secondary plasmodesmata usually exhibit branches, but not necessarily. Therefore, the formation of secondary plasmodesmata can be better recognized by checking the number (frequency) than by observing their structure (Zhu et al. 1998b). All the changes listed above are positive (augmentation). It is also well known that negative changes (diminution) do occur in certain circumstances. This is exemplified by the developing roots of *Azolla*, in which this phenomenon was considered related to the determinate growth of the root (Gunning 1978). The significance of the control of plasmodesmatal numbers during plant development has been stressed in numerous studies (see Carr 1976a). In extreme cases, plasmodesmata can be totally removed, as in mature stomata (*e.g.*, Peterson and Hambleton 1978, Wille and Lucas 1984). The guard cells are symplastically isolated from each other and from the surrounding epidermal cells (Palevitz and Hepler 1985) and communication between these two types of cells will be regulated through membrane mechanisms.

Regulation of plasmodesmata has to be regarded as an integral mechanism of plant function, at the tissue or the whole-plant level. The delicate design of plasmodesmata is suggestive of their sensitive response to both internal and external environments.

#### **1.2.4 Structure of the root: relation to radial ion transport pathways**

Radial transport in the root consists of a series of complicated steps. Research on ion movement has been focused on (1) the site(s) of uptake (epidermis, cortex, or endodermis), (2) pathway(s) across the cortex (symplastic or apoplastic), and (3) the site (from pericycle or from stelar parenchyma) and mechanism (active or passive) of xylem loading. In light of the structural diversity of the roots among different species, a uniform mechanism/pathway is definitely not employed by all plants.

##### **1.2.4.1 Epidermis**

Epidermal cell walls are permeable to ions as demonstrated by fluorescent tracer dyes (Peterson et al. 1978). Evidence has indicated that the epidermis is the first and probably the most important, if not the sole, cell layer for ion uptake into the symplast (van Iren and Boers-van der Sluijs 1980, Vakhmistrov 1981). The root epidermis in barley has a high level of plasma membrane  $H^+$ -ATPase (Samuels et al. 1992). The significance of the epidermis in ion uptake has been further demonstrated by the formation of wall ingrowths (*i.e.*, transfer cells) in saline conditions (Kramer 1981) or during ion deficits (Kramer 1981, Landsberg 1986, Schmidt and Bartels 1996). Transfer cells are specialized to increase short-distance transport across the apoplast-symplast boundary (Gunning and Pate 1969). Another common feature is the formation of root hairs on the epidermis (in the zone that xylem vessels are mature), which significantly increases the absorbing surface area, thus leading to the general idea that the root hair zone is the most rapid absorption region of the root (Peterson and Farquhar 1996).

#### **1.2.4.2 Central cortex**

The cell walls and intercellular spaces of this multi-layered tissue comprise the bulk of the apoplast in a primary root. Symplastic transport is also possible as plasmodesmata link all living cells together. Crafts and Broyer (1938) suggested that ions are first accumulated in cortical cells and are subsequently transported in the symplast. Vakhmistrov (1981) maintains that cortical cells play a role in absorbing ions (*e.g.*,  $K^+$ ) from the apoplast when the external concentration is high. (At moderate external concentrations, ions are taken up mainly by epidermal cells.) There is evidence that ions can also be accumulated in the vacuole that will eventually contribute to the symplastic transport (Hodges and Vaadia 1964, Anderson et al. 1974). Recent advances in specimen preparation and analytical technology have firmly established that the cortical cell vacuoles have a very high capacity for accumulating ions (Storey and Walker 1987, Stelzer et al. 1988, Huang and van Steveninck 1989). In the cytoplasm, ions can be involved in various processes (depending on the species of the ions). So, from the viewpoint of transport, the cortex appears to hinder the inward transport (Vakhmistrov 1981).

#### **1.2.4.3 Endodermis**

This is the innermost cell layer of the cortex. In some species, the endodermis develops through states I, II and III, marked by the deposition of Casparian bands in the anticlinal walls, additional formation of suberin lamellae and tertiary cellulosic walls, respectively (Clarkson and Robards 1975). The hydrophobic components of the bands are suberin and lignin (Schreiber et al. 1999). The plasma membrane is tightly attached to the bands, as evidenced by band plasmolysis after treatment with hypertonic solutions. The Casparian band is a major apoplastic barrier between the cortex and the stele. This has been best demonstrated by the blockage of tracer ions at the outer edge of the band (DuPont and Leonard 1977, Peterson et al. 1986). Ions that diffused from the soil solution through the cortical apoplast must converge into the symplast of the endodermis to gain access into the stele. There must be special features in the endodermal plasma membrane to cope with the hypothesized membrane transport across the endodermis. There is some indication that the plasma

membrane of the endodermal cells has more protein and glycoprotein particles than that of cortical cells in maize roots (see Clarkson 1993). However, the mechanism of membrane transport across the endodermis is not known.

Although the Casparian bands function as one of the plant's most important mechanisms to exercise selectivity towards molecules and ions, not all substances are affected by the bands (and the later suberin lamellae and tertiary walls). Phosphate transport, for example, is not changed by these wall modifications in barley, suggesting that phosphate moves in the symplast (Clarkson et al. 1971). This result gained support from anatomical studies. In all species examined with the electron microscope, the endodermis' plasmodesmatal continuity is preserved through all stages (Clarkson et al. 1971; Harrison-Murray and Clarkson 1973; Stelzer and Läubli 1977; Scott and Peterson 1979; Warmbrodt 1985a, b, 1986a; Barnabas and Arnott 1987; Wang et al. 1995, Verdaguer and Molinas 1997, Ma and Peterson 2000).

#### **1.2.4.4 Exodermis**

The exodermis is a specialized hypodermis with Casparian bands in the anticlinal walls (Peterson 1988, Peterson and Perumalla 1990). By definition, the concept of exodermis evolved from that of the hypodermis. The latter was first described in leaves in the late 19th century (see Kroemer 1903). In the leaves, stems and fruits of many species, one or more chlorophyll-free cell layers are present underneath the epidermis. These specialized cells usually have a "suberin lamella" in their walls. A similar cell layer(s) also develops in the roots of virtually all monocotyledonous and many dicotyledonous species. Historically, there had been a debate on the origin and terminology of this layer(s). It was either designated as the inner layer(s) of the multi-layered epidermis or the outer layer(s) of the cortex. According to Kroemer (1903), about twenty terms had been applied to describe this special layer(s). He introduced the term "Interkutis" (a hypodermis that contains suberized cells). Based on his own extensive observations and the results in the literature, he recognized 5 types of Interkutis. **Type 1** – The single-layered, homogenous Interkutis. All cells are approximately equal in length. Some cells get suberized earlier than others.

but eventually all cells become suberized. **Type 2** – The single- or multi-layered, homogenous Interkutis, with unsuberized cells between suberized ones. **Type 3** – The single- or multi-layered (homogenous) Interkutis that suberizes completely in a region close to the root tip. **Type 4** – The short cell Interkutis, containing short and long cells. The short cells become obstructed through local suberin formation in the parenchyma cells lying under a short cell, or more seldom through peculiar invaginations of the long cells in the area of the short cells. Frequently, the short cells do not undergo any changes with age. **Type 5** – Mixed Interkutis. This is a multilayered Interkutis in which the outer layer consists of short and long cells, while the remaining layers contain only elongated cells.

Von Guttenberg (1968) simplified the classification: an exodermis is either short-celled or uniform. In the former, short and long cells alternate regularly along the root axis (equivalent to Kroemer's type 4). The short cells are also named "passage cells" as they usually do not develop suberin lamellae and thus provide a path for transport. A multiseriate short-celled exodermis is found in very few taxa (as in Amaryllidaceae, Iridaceae and Liliaceae), in which short cells are present only in the outermost layer (equivalent to Kroemer's type 5). In the uniform type, all cells are elongate (a collective of all of Kroemer's first three types).

Shishkoff (1987) referred to the "short-celled Interkutis" (Kroemer 1903) and the "short-celled exodermis" (von Guttenberg 1968) as the "dimorphic hypodermis". According to the recent concept about exodermis, this type of hypodermis was designated as a dimorphic exodermis (Peterson 1988, Peterson and Perumalla 1990). Thus, an exodermis can be either dimorphic (as in onion) or uniform (as in maize).

It was a long time before the exodermal Casparian bands were identified. Scott (1928) briefly mentioned the staining properties of the hypodermal walls of *Funkia ovata* roots, which indicated the presence of a Casparian band, although she did not speculate on that. van Fleet (1950) reported that a Casparian band was observed in the hypodermis of *Pelargonium* sp., *Smilax* sp., *Berberis* sp., *Iris* sp., and *Allium sativum*. Later, the

Casparian band reported in *Pelargonium* by van Fleet (1950) was found to be actually phi thickenings (von Guttenberg 1968, Haas et al. 1976). Also, in none of the species examined with the transmission electron microscope was an exodermal Casparian band detected (Tippett and O'Brien 1976, Olesen 1978, Peterson et al. 1978). Thus, it has been since generally held that a Casparian band does not exist in the hypodermis. However, there had been some physiological results that did point to its existence (e.g., de Rufz de Lavison 1910, Ziegler et al. 1963, Huisinga and Knijff 1974). In 1982, a major contribution was made by Peterson et al. who positively detected Casparian bands in the roots of maize and onion by clearing sections in NaOH followed by staining with *Chelidonium majus* L. root extract. This result was soon confirmed by the demonstration of band plasmolysis in this layer of onion roots (Peterson and Emanuel 1983). Now, the microscopical techniques to observe Casparian bands have been further improved (Brundrett et al. 1988). The function of the exodermal Casparian band as an apoplastic barrier for ions (Peterson 1987) and for fluorescent dyes (Peterson et al. 1978) has been established. A survey study showed that Casparian bands occur widely in the plant kingdom (Perumalla et al. 1990, Peterson and Perumalla 1990). Then, why were the bands discovered so late? This could be due to several facts. (1) Suberin lamellae normally develop shortly after the Casparian band is deposited (Perumalla and Peterson 1986, Enstone and Peterson 1997). (2) The exodermal radial walls are very thin. Therefore, the Casparian bands can be obscured by the overlying suberin lamellae and, thus, cannot be detected by the routine microscopical methods.

The information on the exodermis is still rudimentary (see Peterson 1988, 1989, 1998). To better understand its structure and function, a developmental study is needed. At the present, a generalization of developmental patterns is impossible. The relationship of suberin deposition to the symplastic continuity has to be illustrated. In the dimorphic exodermis, the significance of short cells in the water and ionic relations of the roots will be an exciting area of future research.

#### **1.2.4.5 Pericycle**

Very little attention has been paid to the function of pericycle in transport. Rather, the pericycle is best known as a tissue that potentially forms lateral roots, root buds and secondary meristems (vascular and cork cambia). In the barley pericycle, many more plasmodesmata occur in the outer tangential and radial walls than in the inner tangential walls (Vakhmistrov et al. 1972, Robards and Jackson 1976). This observation led to the creation of a model for pericycle functioning (Vakhmistrov et al. 1972). In brief, the majority of ions moving from the cortex do not enter the stelar parenchyma but proceed immediately to the xylem vessels by way of the pericycle. Inside the pericycle, lateral circulation is possible through the radial walls, facilitating the inward and outward transport of ions and photosynthates, respectively (see Figs. 3.5 and 3.6). For onion roots, a larger scale measurement of plasmodesmatal frequencies has been performed and the pericycle will be viewed in the context of the overall transport in the root (Chapter 3).

#### **1.2.4.6 Stelar parenchyma**

Stelar parenchyma cells are grouped between the phloem and xylem strands. The function of these cells in the ion transfer to the xylem vessels has long been a subject of debate. Both passive and active ion transport pathways have been proposed to occur at the boundary of the stelar parenchyma and xylem vessels. The passive leakage theory was devised by Crafts and Broyer (1938) based on the idea that the stele is in a state of oxygen-deficiency. Dunlop and Bowling (1971a, b, c) have shown that both  $K^+$  and  $Cl^-$  move down an electrochemical gradient from the symplast into the xylem vessels. Results from other research groups are in favor of an active mechanism at the interface of stelar parenchyma and the xylem (Yu and Kramer 1967, 1969, Pitman 1972, Mizuno et al. 1985, Clarkson and Hanson 1986). Cytochemical experiments have shown that, in the stele, the ATP activity is mainly localized in the stelar parenchyma, with extremely high activity at the plasma membrane in the region of the half-bordered pits facing the vessels (Winter-Sluiser et al. 1977). A recent report again raised the possibility of passive loading of xylem from stelar parenchyma cells (by ion channels) in barley roots (Wegner and Raschke 1994). It is possible that different mechanisms

are used by different species. On the other hand, the above-mentioned results seem confusing as most of them were obtained from one species (barley). To resolve this matter, *in vivo*, rather than *in vitro* (Wegner and Raschke 1994), studies will be most helpful. Ultrastructural ATPase localization will show what membrane system(s) are possibly involved in the final stages of the radial ion transport.

It is apparent that the stelar parenchyma cells also have a physiological relationship with the phloem. From the anatomical point of view, stelar parenchyma cells have equal physical contact with the xylem and with phloem, but functional relationships of the three tissues have not been investigated.

#### **1.2.4.7 Xylem vessels**

The protoxylem vessels are located right internal to (or inside, as in barley) the pericycle, close to the root tip. This is followed by the formation of early and late metaxylem vessels, internal to protoxylem vessels and farther back from the tip (Esau 1977). It is firmly established that along the long axis of the root, xylem sap is pulled by the transpiration in leaves. But, the initial entry of ions into the xylem (§ 1.2.4.5 and 1.2.4.6) and the relative contribution of various categories of xylem vessels are less well understood.

#### **1.2.4.8 Phloem**

The major role of the phloem is the transport of photosynthates. Compared to the enormous number of studies in leaves, very little information is available for the root phloem (§1.1). Phloem might also act in reallocating mobile elements, such as Cl, S and Mn (Nelson et al. 1990), under certain conditions (*e.g.*, nutrient deficiency).

#### **1.2.4.9 Control steps for radial ion transport in roots: a summary**

Both the xylem sap and soil solution contain inorganic ions, but the ion compositions and concentrations in the two compartments are different from each other. This is because the



xylem sap is a result of selectivity through all cell layers external to the xylem. Ions need to cross cell walls (the apoplastic) to get contact with the plasma membranes before being taken up by living cells. This first occurs at the epidermis. The epidermal cell walls are permeable to ions, assuming that the availability and mobility of an ion in the soil solution or culture medium are not limiting, then the plasma membranes of epidermal cells (including root hairs) will be the first control step for ion uptake. There are several possibilities that an ion can traverse the membrane. Passive diffusion is not significant because of the high resistance. Ion channels could facilitate the uptake process. Active transport (by carriers) will accumulate ions from the medium. Cortical cells are theoretically capable to absorb ions from the apoplast, but this ability decreases dramatically in old zones of the root (van Iren and Boers-van der Sluijs 1980). This observation further implied the significance of epidermal cells in ion uptake (Vakhmistrov 1981). Once taking up into the symplast, ions can move through plasmodesmata, until being exported into the mature vessel members (below).

Apoplastic transport can occur as far as the endodermal Casparian bands. Then, all substances will converge into the symplast through the outer tangential plasma membranes of endodermal cells (Clarkson and Robards 1975). At this point, the endermis functions as a fine filtration system that will determine the final ion composition in vessels. If a root has an additional Casparian band in the exodermis, apoplastic transport will be blocked near the root surface (Peterson 1987), and symplastic transport will be the dominant pathway across the root. In this case, the outer tangential plasma membranes of exodermal cells will play a vital role in ion uptake. So, it is apparent that the root exerts more intense selectivity on ions at the periphery of the root in exodermal than in non-exodermal species.

In exodermal species, when suberin lamellae develop, the access of ions to the outer tangential membranes of the exodermal cells is blocked. Then uptake has to take place at the epidermal membranes and symplastic transport is initiated at the epidermis-exodermis interface. In the case of a dimorphic exodermis, when suberin lamellae are deposited in long cells, all their plasmodesmata are severed, leaving only the short cells' outer tangential plasma

membranes available for ion uptake (Chapter 2). Therefore, control steps of initial ion uptake are different both between plant species and along the root axis.

At the endodermis, in addition to the Casparian bands which interrupt the apoplastic continuity, the later-forming suberin lamellae block the access of ions to the outer tangential plasma membrane (as at the exodermis). Now only symplastic transport pathway is available except in a few passage cells where membrane transport is still possible.

The final control of ion movement is at the site of xylem loading. Traditionally, all substances will be released to vessels through stelar parenchyma cells that abut the vessels. This could be accomplished through either passive (ion channels) or active transport across the plasma membranes of stelar parenchyma cells. It is also claimed that pericycle cells might also play a role in loading the xylem (Chapters 3 and 4). Yet, both the mechanisms and pathways of xylem loading are poorly understood.

## **1.3 Plasmodesmata in the root**

### **1.3.1 General considerations**

In young zones of the root, particularly in the apical meristem, plasmodesmata are most likely playing a significant role in differentiation, probably through signaling. As studied in the model plants *Azolla* (Gunning 1978) and *Arabidopsis* (Zhu et al. 1998a, b), the distribution mode of plasmodesmata is tissue-specific and is correlated to pattern formation. In old zones, the principal role of plasmodesmata is probably to provide a symplastic path for nutrient ions taken up from the soil solution toward the stele (Ginsberg and Ginsberg 1970b, Robards and Clarkson 1976). Indeed, running from the epidermis, across the cortex, and all the way to the stele, plasmodesmata occur at all tissue interfaces, except in the long cells of a dimorphic exodermis (Walker et al. 1984, Chapter 2).

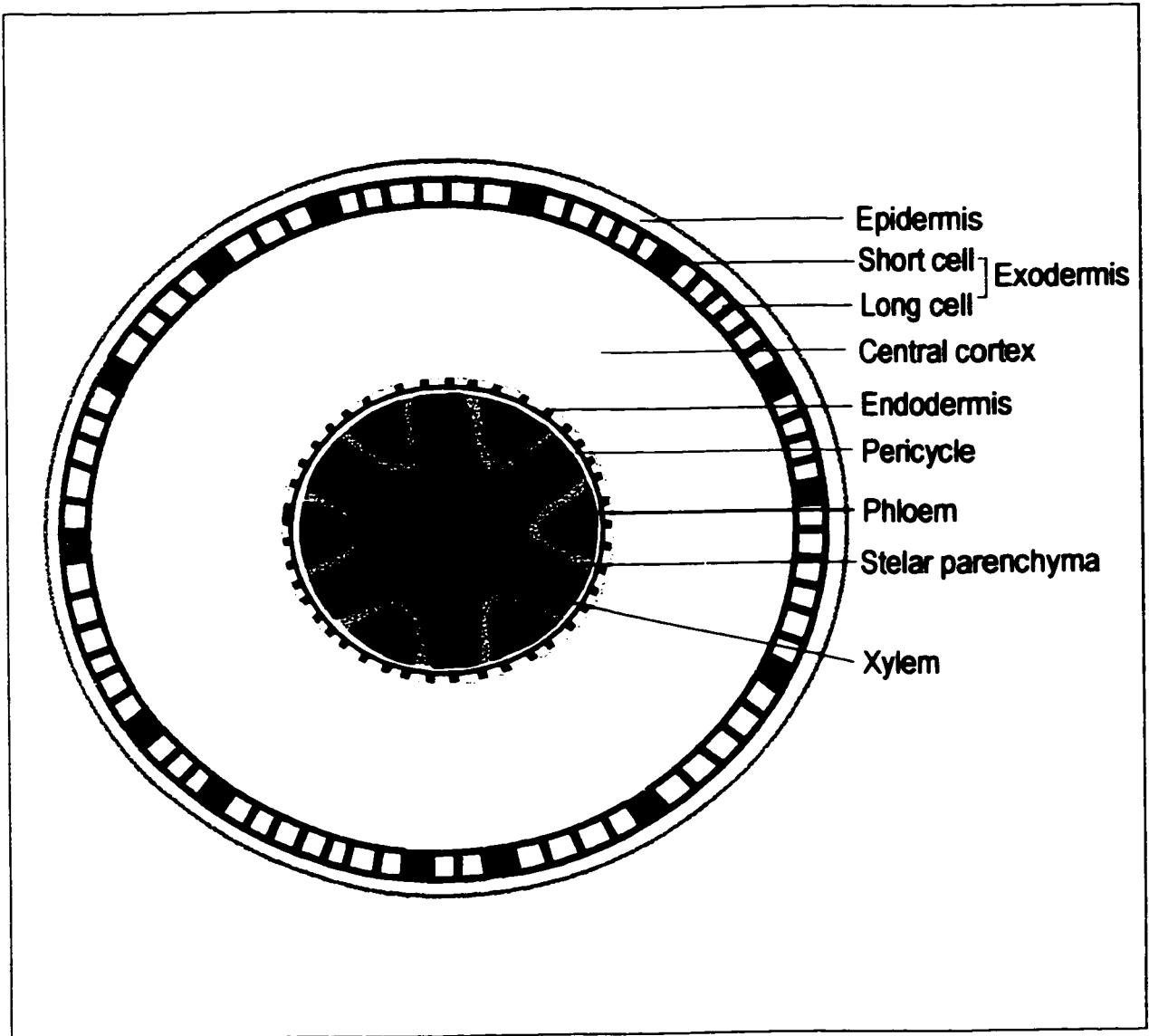
### 1.3.2 A case study of onion roots

The onion root has been a model system in the laboratory of Dr. Carol Peterson to study transport phenomenon. The anatomical features (Fig. 1.2) in relation to transport have been extensively examined, mainly with fluorescent dye tracing experiments (Peterson et al. 1982; Peterson and Emanuel 1983; Moon et al. 1984; Peterson and Perumalla 1984; Perumalla and Peterson 1986; Barnabas and Peterson 1992). As a model system, this material possesses several advantages. (1) Laboratory culture of the onion plants is simple and easy. (2) Only primary growth occurs in the roots. (3) Under favorable conditions, the roots do not produce laterals and hairs for a considerable period of time (e.g., 2 weeks).

Onion is a species with a dimorphic exodermis, and previous efforts have been focused on the physiological significance of the exodermal short cells. These particular cells are remarkably resistant to drought and are suggested to be critical for initial water absorption after a period of water stress (Stasovski and Peterson 1993; Barrowclough and Peterson 1994; Kamula et al. 1994). In *Hoya carnosa* L. (Olesen 1978) and *Citrus* sp. (Walker et al. 1984), electron microscopic observations revealed that the exodermal short cells exhibited dense cytoplasm and features typical of highly metabolically active cells. This points to an important role that the short cells might play in ion absorption and transport. Suberin lamellae in exodermal long cells have blocked the invasion of soil-originating fungi into the root tissues (Kamula et al. 1995); this seems to be a general pattern among species with a dimorphic exodermis (see Matsubara et al. 1999 and literature therein).

Little information is available on symplastic transport in onion roots. By using radiolabeled  $\text{Cl}^-$ , Hodges and Vaadia (1964) demonstrated the presence of a symplastic pathway in onion roots. Preliminary results from fluorescent tracer dye experiments inferred that there is a continuous symplastic pathway from the epidermis to the stele (Peterson and Perumalla 1984). But, the occurrence of plasmodesmata was only briefly noted in the cortex (Scott et al. 1956, Strugger 1957a, b) and a complete assessment of plasmodesmatal distribution has been lacking. In the exodermis, plasmodesmata were only occasionally seen in the transmission

**Fig. 1.2 Schematic representation of an onion root (cross section)**



electron microscope (Peterson et al. 1978). A closer examination of the exodermis by using fluorescent tracer techniques demonstrated that the short cells without suberin lamellae are symplastically connected to both the epidermis and the central cortex. At the same time, it was observed that the long cells (with suberin lamellae) are symplastically linked only to the central cortex and not to the epidermis (Peterson and Waite 1996). This study opened several questions. (1) Are there any plasmodesmata in both inner and outer tangential walls of long cells before suberin lamellae are laid down? (2) Are plasmodesmata in the outer tangential walls severed by suberin lamellae, while those in the inner tangential walls are preserved? (3) Is the development of suberin lamellae delayed at the inner tangential side?

The present study is aimed at unravelling the overall pattern of plasmodesmatal distribution in onion roots (Chapters 2 and 3). Special attention has been given to the structural differences between the exodermal short and long cells (Chapter 2). The functionality of plasmodesmata has been tested by using an *in situ* ion precipitation method followed by TEM (Chapter 4). Efforts have also been dedicated to the relationships of wall modifications to plasmodesmatal connections in the exodermis and endodermis (Chapter 5).

## Chapter 2

# **Plasmodesmata in onion roots: a study enabled by improved fixation and embedding techniques**

[Published in *Protoplasma* Vol. 211 (2000). Reproduced with permission from the publisher.]

### **2.1 Abstract**

Onion (*Allium cepa* L. cv. Ebenezer) roots from vermiculite culture were examined with transmission electron microscopy (TEM) to detect the plasmodesmata in all tissues. In young root regions, plasmodesmata linked all living cells together in all directions. In old zones, the plasmodesmatal connections of the endodermis to its neighbor tissues were not interrupted by later suberin lamella and cellulosic wall deposition. Moreover, plasmodesmata in the fully mature endodermis usually exhibited a large central cavity. In the exodermis, however, upon deposition of suberin lamellae in long cells, all plasmodesmata that initially linked them to their adjacent cells were severed. Afterwards, the long cells lost the capability of forming wound pit callose and their protoplasts began to degenerate. The mature exodermal layer was symplastically bridged to its neighbors only by the short (passage) cells that lacked suberin lamellae. Compared to the long cells, the short cells not only had thicker cytoplasm surrounding their central vacuoles but also a higher density of mitochondria and rough ER, consistent with an active involvement in the transport processes of the root. The above results were obtained using an improved, extended TEM procedure devised to analyze plasmodesmata in cells with suberin lamellae. By fixing root tissues in glutaraldehyde and acrolein, all cells were well preserved. Further fixation was carried out in osmium tetroxide at a low concentration (0.5%). Following

dehydration in acetone and transfer to propylene oxide, infiltration with Spurr's resin was accomplished by incubating samples in the accelerator-free mixture for 4 days, then infiltrating samples in the accelerator-amended mixture for an additional 4 days.

**Keywords:** *Allium cepa* L.; endodermis; exodermis; plasmodesmata; suberin lamellae; transmission electron microscopy.

## 2.2 Introduction

Plasmodesmata are thin channels that link the protoplasts of most adjacent plant cells together (see McLean et al. 1997, Ding et al. 1999). In roots, plasmodesmata in a radial file are of particular interest since they are involved in the symplastic transport of ions (and, to a lesser extent, water) from the epidermis to the stele, and of photosynthates in the reverse direction. Recently, plasmodesmata have been visualized at the ultrastructural level in all tangential walls of living cells in mature, lateral roots of maize (*Zea mays* L.; Wang et al. 1995). During the last three decades, however, it is the endodermal plasmodesmata that have received the most attention. This is due to the long-recognized significance of the endodermis for ion movement in plants (see Clarkson and Robards 1975). The symplastic continuity of the endodermis is preserved throughout its life span in all species examined by transmission electron microscopy (TEM). Examples include *Puccinellia peisonis* (Stelzer and Läuchli 1977), *Ranunculus acris* L. (Scott and Peterson 1979), *Hordeum vulgare* L. (Clarkson et al. 1971, Warmbrodt 1985a), *Cucurbita pepo* L. (Harrison-Murray and Clarkson 1973, Warmbrodt 1986a), maize (Warmbrodt 1985b, Wang et al. 1995) and *Quercus suber* L. (Verdaguer and Molinas 1997). The onion root endodermis is likely to remain symplastically connected to the cells of the central cortex and to those of the pericycle, although ultrastructural data on this point are lacking.

The exodermis is generally assumed to share certain similarities with the endodermis in terms of wall thickening (von Guttenberg 1968). In the latter, Casparian bands develop in the anticlinal walls at an early stage (State I). This is quickly followed by deposition of



suberin lamellae (State II) and later tertiary cellulosic walls (State III) all over the primary wall (see Clarkson and Robards 1975). The exodermis can be uniform; all the component cells are elongate (like those in the endodermis) and develop through State I to State III. The exodermis can also be dimorphic, consisting of both long and short cells (Kroemer 1903, von Guttenberg 1968). In onion, Casparian bands are present in all exodermal cells; suberin lamellae first develop in long cells and later occur also in short cells (Perumalla and Peterson 1986). In general, compared to the endodermis, the exodermis is much less well understood with respect to the presence and structure of plasmodesmata. One reason is that the wide occurrence of the exodermis in the plant kingdom (Perumalla et al. 1990, Peterson and Perumalla 1990) and its significance in root function (Peterson and Enstone 1996, Peterson 1998) have only recently been brought to light. The scant ultrastructural data available suggest that the uniform exodermis responds differently to the wall modifications than does the dimorphic exodermis. In maize (with a uniform exodermis), the suberin lamellae and cellulosic walls had no effect on plasmodesmatal continuity (Clarkson et al. 1987, Wang et al. 1995). This is the only ultrastructural information on a uniform exodermis. In the dimorphic exodermis, some variability among species was noticed in the mature (old) zone of the roots. In *Citrus* sp., plasmodesmata were initially present traversing the walls of all exodermal cells, but later those in the long cells were severed when additional wall materials were laid down (Walker et al. 1984). In *Hoya carnososa* L., the long cells were not connected to either the epidermis or the central cortex with plasmodesmata. The short cells were connected to the epidermal cells by plasmodesmata (Olesen 1978). But it was not stated whether or not the short cells were also linked to the central cortical cells.

A major reason for the current paucity of knowledge of plasmodesmata in the exodermis is the extreme difficulty in preparing the samples for TEM. The diffuse suberin in the epidermis, the Casparian bands and especially the suberin lamellae in the exodermis and endodermis tend to be almost impermeable to TEM chemicals (see Discussion).

The symplastic connections within the onion root exodermis have not been well resolved. To test the symplastic permeability of exodermis in the old zone (100 mm from the tip), intact root segments (end-sealed) and tangential sections were incubated in a solution of disodium fluorescein, a symplastic tracer dye (Peterson and Waite 1996). This study indicated that the exodermal short cells were connected to both the epidermis and the central cortex with plasmodesmata. However, the long cells (with suberin lamellae) were connected to the central cortex and not to the epidermis. These results do not agree with those of an earlier ultrastructural study by Peterson et al. (1978). The latter authors found that the plasmodesmata in the exodermal cells were so rare that significant symplastic transport was not anticipated.

In this study, cells of all root tissues in onion were examined for plasmodesmata, with special reference to the effect of suberin formation on the symplastic continuity in the endodermis and exodermis. Exodermal cells were also tested for their ability to produce wound pit callose in young and old zones. The ultrastructure of exodermal long and short cell protoplasts was compared. An improved method for preserving suberized cells for TEM is presented.

## **2.3 Materials and methods**

### **2.3.1 Plant material**

Bulbs of onion (*Allium cepa* L. cv. Ebenezer) were stripped of their outer, dry scales and planted to half their depth in vermiculite saturated with tap water in 200 mm-deep pots. They were sprouted under greenhouse conditions (photoperiod 16 h day/8 h night, temperature 25°C day/20°C night). Plants were irrigated daily with tap water. Roots were harvested for the experiments 7 to 14 days after planting, by which time they were 100-200 mm long.

### **2.3.2 Transmission electron microscopy**

Root segments 1 mm long were excised from four regions at various distances from the root tip: (1) 2-3 mm, (2) 50 mm, (3) 100 mm, and (4) 200 mm. Regions 1 and 2 are referred to as “young”, region 3 as “old”, and region 4 as “very old”. A variety of fixing and embedding protocols were tried, and best results were achieved with the following. Fixation was done in 4% glutaraldehyde and 2% acrolein in 25 mM Na-phosphate buffer, pH 6.8, 4°C, overnight. This was followed by further fixation in 0.5% OsO<sub>4</sub> in the same buffer at 4°C, overnight. Dehydration was achieved with acetone through a 10%-step graded series. The specimens were then transferred into propylene oxide. Samples were initially infiltrated in mixtures of propylene oxide and incomplete Spurr's resin (without the accelerator, 2-dimethylaminoethanol, DMAE, Spurr 1969) in steps of 5:1, 4:1, 3:1, 2:1, 1:1, 1:2, 1:3, 1:4, and 1:5, with 2-6 h for each step. Tissues were then incubated in pure resin for 4 d, being changed into fresh resin daily. Pure resin mixtures were kept at 4°C and were then warmed up to room temperature every time before use. Further infiltration was carried out in the complete resin (with DMAE) for another 4 d, with resin being replaced twice daily. Resin mixtures were divided into small packages (each of which was to be used up for one or several resin changes). All resin mixtures were kept at -20°C and were then warmed up to room temperature every time before use. Polymerization occurred at 65°C for 24 h. Semithin sections (cross, paradermal and median longitudinal) were cut with glass knives on a Reichert Ultracut E microtome (Leica AG Reichert Division, Austria), stained with 0.05% toluidine blue O (TBO, in 0.05% sodium borate) at about 60 °C for 30-60 s. Excess dye was thoroughly rinsed off with water. Sections were observed with bright field optics and were photographed with Kodak Elite II ASA 200 films (for colour slides). Ultrathin sections (80 nm) were then collected on Formvar-coated 75-mesh hexagonal copper grids. The Formvar film was prepared from a 0.3% chloroform solution. Sections were post-stained in uranyl acetate and lead citrate in a CO<sub>2</sub>-free small chamber. Observation and photography were accomplished in a Philips CM 10 microscope operated at 60 kV.

### **2.3.3 Histochemical detection of suberin**

Casparian bands and suberin lamellae in freehand, cross sections were recognized by autofluorescence under ultraviolet light (UV) in a Zeiss Axiophot microscope (Carl Zeiss Canada, Don Mills, Ontario) equipped with an Osram HBO 100W mercury lamp and epifluorescence optics. The filter set consisted of exciter filter G365, chromatic beam splitter FT395 and barrier filter LP420. To improve resolution and contrast, sections were slightly stained with 0.01% TBO. Casparian bands and suberin lamellae were also stained with berberine (Brundrett et al. 1988) and Sudan red 7B (Brundrett et al. 1991), respectively. The latter stain was also used for the tertiary cellulosic walls of the endodermis.

### **2.3.4 Observation of pit fields and wound pit callose**

Root segments 10 mm long were excised from two regions, an immature exodermal zone (IE zone, between 25-40 mm from the root tip) and a mature exodermal zone (ME zone, further than 100 mm from the tip). The samples were subjected to incomplete maceration in 50% sulfuric acid for 24 h. After thorough rinsing in distilled water, fragments of an outer layer (consisting of the associated epidermis and exodermis) and tissue pieces of the central cortex were prised from the segments under a dissecting microscope, spread onto microscope slides and stained in 0.05% TBO. The specimens were briefly rinsed in distilled water. To enhance staining and contrast for photography, the extracellular layer on the root surface (Peterson et al. 1978) was peeled off with a brush when the dye was applied. Staining was also performed on free-hand tangential sections. Observations were made with bright field optics.

To test whether the exodermal cells of young and old zones could synthesize wound pit callose, tangential sections were prepared free-hand through the exodermis or its immediate neighbor cell layers. Sections were stained with 0.001% aniline blue (in 10 mM phosphate buffer at pH 8.0) and observed in the fluorescence microscope as described above.

## **2.4 Results**

### **2.4.1 Light microscopic observations of endodermal and exodermal development**

The endodermal cells progressed through States I, II and III. Casparian bands had fully developed (State I) near the tip. At 100 mm from the tip (or a bit farther), suberin lamella deposition (State II) was first observed in a few endodermal cells facing the primary phloem. This process progressed laterally toward the protoxylem poles and passage cells were situated near the xylem poles (Fig. 2.1A). A tertiary cellulosic wall was formed internal to the suberin lamellae. At 200 mm from the tip, most passage cells had developed through States II and III (Fig. 2.1B). The tertiary wall was also incrustated with suberin, as evidenced by the positive staining with Sudan red 7B (Fig. 2.1B). In older regions of the root (*e.g.*, 300 mm from the tip), all endodermal cells eventually matured into State III.

In the exodermis, long and short cells resulted from an unequal division of mother cells in the proximal part of the apical meristem, about 2-3 mm from the root tip (Fig. 2.1C). In old zones, long and short cells generally alternated with each other along the root axis. Occasionally some pro-exodermal cells did not divide and instead developed directly into long cells (Fig. 2.1C, D). In other examples, a few short cells divided forming two adjacent short cells (Fig. 2.1D). In cross sections, the long and short cells were usually distinguishable by the presence or absence of suberin lamellae (Fig. 2.1A).

### **2.4.2 Primary pit fields and wound pit callose in the exodermis**

The primary pit fields of exodermal short and long cells were readily detected by TBO in the IM zone. In the ME zone, primary pit fields were observed in short cells in their inner tangential walls (Fig. 2.1E, Table 2.1), and frequently also in their outer tangential walls. In long cells in the same preparations, primary pit fields were rarely detected (Fig. 2.1E, Table 2.1). When stained with aniline blue for callose, short and long cells gave similar positive reactions in the IM zone (Table 2.1). Callose stood out as bright, whitish-green dots against a

dim background in the cell walls under the fluorescence microscope. In the ME zone, callose was readily observed in short cells (Fig. 2.1F, G) in both inner and outer tangential walls (approximately 13 callose deposits on either wall, or 6 callose deposits/1000  $\mu\text{m}^2$  wall). However, in long cells, callose was not seen in the outer tangential walls (Fig. 2.1F), but was apparent in the inner tangential walls of some cells (Fig. 2.1G). In the central cortex of the IM zone, both primary pit fields and wound pit callose were easily detected. In the ME zone, cortical cells developed secondary walls; pit membranes and wound pit callose were evident on all walls (data not shown).

### **2.4.3. Transmission electron microscopic observations of wall modifications in endodermis and exodermis**

The new TEM protocol successfully preserved all cell types in all zones examined (Fig. 2.1C, H). This method was especially useful in dealing with the exodermis and endodermis at State II development and later, and with the epidermis (Fig. 2.1H). With “standard” protocols (fixation in glutaraldehyde and osmium tetroxide, and infiltration with complete Spurr’s resin), however, cells of these layers collapsed due to poor fixation and infiltration (Fig. 2.1I), which made the ultrastructural observation of cell walls (and protoplasts) impossible. In the endodermis, suberin lamellae first appeared as a fine electron-dense wall layer situated between the plasmalemma and the existing primary wall (Fig. 2.2A). Later, the new wall could be multilayered, consisting of alternating electron-dense and electron-lucent components. A typical lamella was 40 nm thick. In the pit fields, the lamellae were about 80 nm and the multilayered configuration was obvious (Fig. 2.2B). The cellulose wall thickened unevenly around the cells, the outer tangential wall being rather thin and the inner tangential wall much thicker.

In the exodermis, deposition of suberin lamellae in the long cells was first detected 50 mm from the tip. It seemed that this commenced earlier along the outer tangential and radial walls than on the inner tangential side (Fig. 2.2C, D). Long cells had attained their full development at State II (with suberin lamellae) 100 mm from the tip (Fig. 2.2E-G). No further wall

**Fig. 2.1** Light microscopic preparations of onion root tissues

**A** Free-hand cross section (150 mm from the tip) stained with TBO and viewed under UV light. Endodermal cells in State I (passage cells; arrowheads) and State II (arrows). Casparian bands (*CB*) in all exodermal cells. Long cells (*LC*) developed suberin lamellae (*SL*) and many short cells (*SC*) did not. **B** Cross section (200 mm from the tip) stained with Sudan red 7B and viewed with a polarizing filter. Most endodermal cells in State III (arrows). Suberin lamellae (*SL*) stained red and tertiary walls (*TW*) orange. A few passage cells (arrowheads) remained near xylem poles. **C** Semithin tangential section taken 3 mm from the tip. Tissue was processed with the new protocol. Short and long cells (indicated by paired black and white arrowheads, respectively) resulted from unequal divisions of mother cells. Short cells were proximal to their sister long cells. Root tip in the direction of arrow. A long cell could also develop directly from an undivided mother cell (+). **D** Exodermis in old zone. Specimen was obtained from partial maceration and viewed with a polarizing filter. Aside from the usual one-by-one alternate positioning of long (*LC*) and short cells (*SC*) in the longitudinal file, two or more long cells (+) could be intercalated between two short cells. Twin short cells (\*) were also present. **E** Exodermis in old zone. Tangential section stained with TBO. Pits (arrowheads) in the inner tangential walls of short cells (*SC*), but not of long cells (*LC*). **F** Section from ME zone and stained with aniline blue, showing outer tangential walls of exodermis. Wound pit callose (arrowheads) in short cells (*SC*), but not in long cells (*LC*). **G** Similar to **F** but showing inner tangential walls. Callose most abundant in short cell, but also present in some long cells (*LC*). **H** Cross section from old zone processed with new protocol. All cells were properly preserved, including those of epidermis (*EP*), exodermis (*EX*), central cortex (*CC*), endodermis (*EN*), pericycle (*PE*), phloem (*PH*), xylem (*XY*), and stelar parenchyma (*SP*). **I** Similar stage as in **H**, but treated by “standard” protocol. Epidermis (*EP*), exodermis (*EX*), and State II-endodermal cells (arrows) collapsed. Other cell types were well preserved. Bars: 50  $\mu$ m

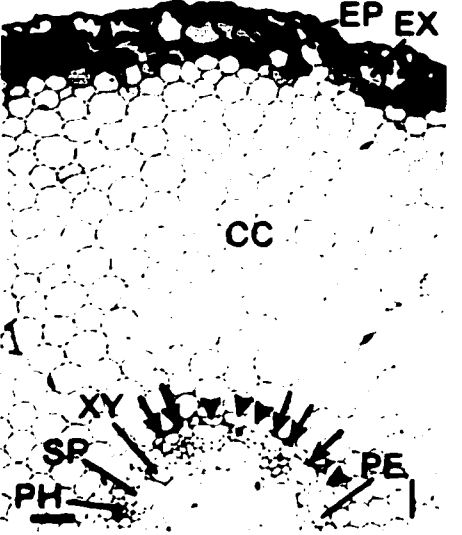
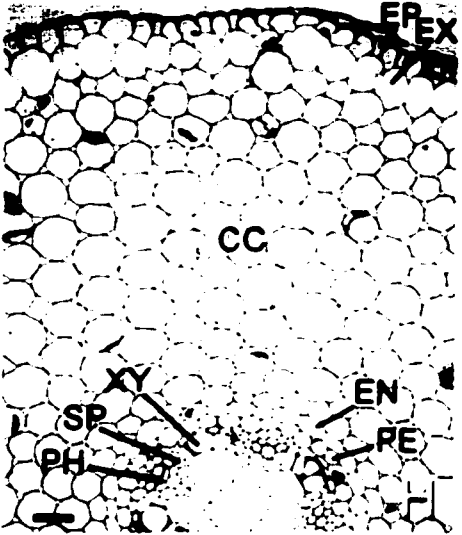
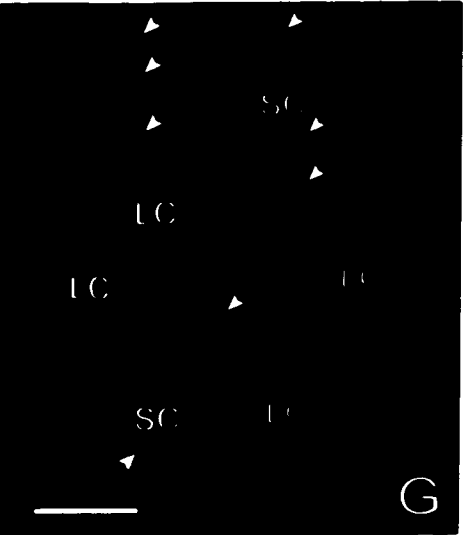
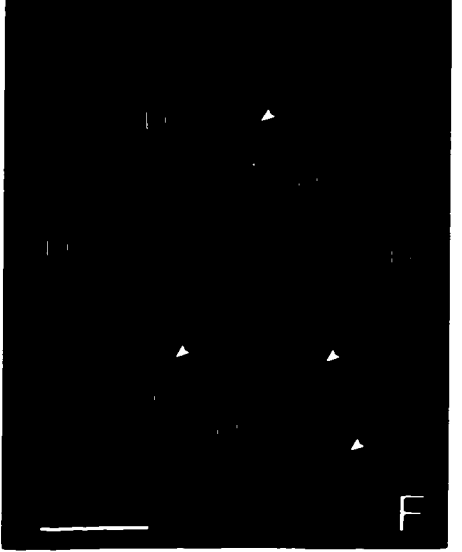
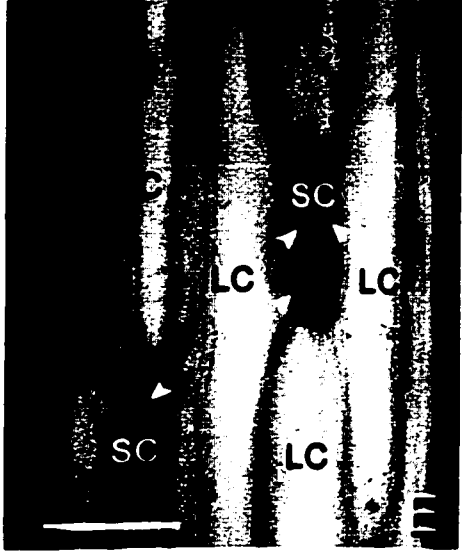
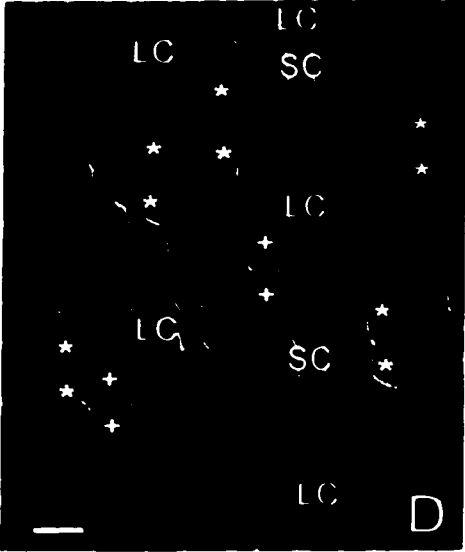
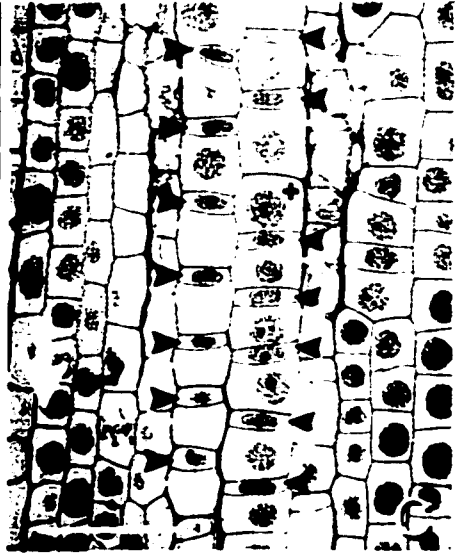
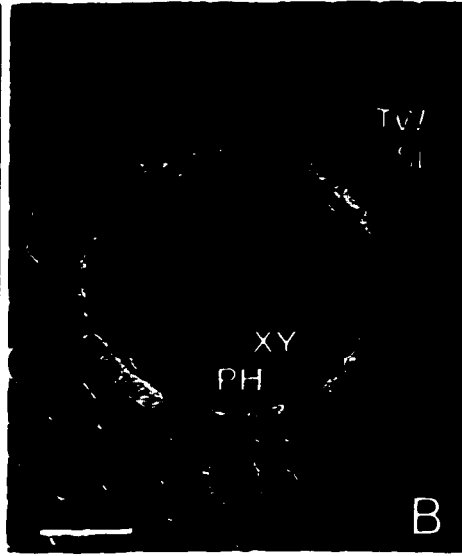




**Table 2.1 Pit fields and wound pit callose in the exodermis of onion roots**

<sup>a</sup> *OTW* and *ITW*, outer and inner tangential wall, respectively; *IE* and *ME*, immature and mature exodermal, respectively

<sup>b</sup> ++, large diameter (2-5  $\mu\text{m}$ ); ++(-), usually large diameter, occasionally not applicable (due to absence of pit fields); +, small diameter (<1  $\mu\text{m}$ ); -, not applicable (due to absence of pit fields)

<sup>c</sup> ++, high (4-7 pit fields or callose deposits per 1000  $\mu\text{m}^2$  wall); ++(-), usually high, occasionally zero; +, low (<3 pit fields or callose deposits per 1000  $\mu\text{m}^2$  wall); -(+), usually zero, occasionally low; -, zero

<sup>d</sup> ++, large diameter (2-4  $\mu\text{m}$ ); +, small diameter (<1  $\mu\text{m}$ ); -(+), usually not applicable (due to absence of callose), occasionally small diameter; -, not applicable (due to absence of callose)

Cell type	Primary pit field						Wound pit callose			
	b dimension		c frequency		d dimension		c frequency			
	<sup>a</sup> OTW	ITW	OTW	ITW	OTW	ITW	OTW	ITW	OTW	ITW
Short cell										
<sup>a</sup> IE zone	+	+	++	++	+	++	++	++	++	++
ME zone	++(-)	++	++(-)	++	++	++	++	++	++	++
Long cell										
IE zone	+	+	+	+	+	+	+	+	+	+
ME zone	-	-	-	-	-	-(+)	+	+	-(+)	-(+)

material deposition took place, even in very old zones, which would correspond to a 14 to 20-day-old region.

In the old zone, the walls of both long and short cells were uneven in thickness. The tangential, primary walls of both cell types were comparable with those of the contiguous central cortical cells, which were approximately 200 nm thick. Their radial primary walls were much thinner, only 30 nm. Suberin lamellae in the long cells resembled those in the endodermis, but generally thinner (50 nm).

#### **2.4.4 Protoplasts of long and short cells**

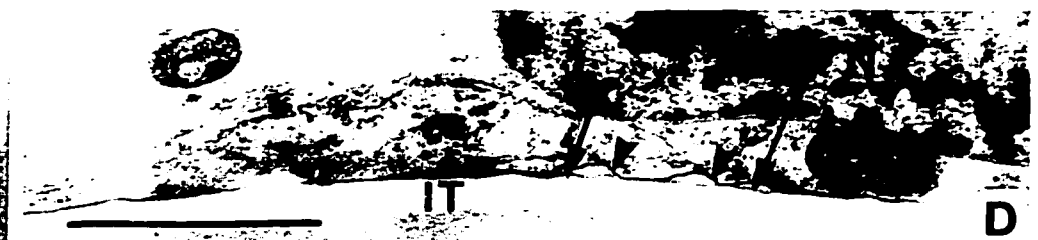
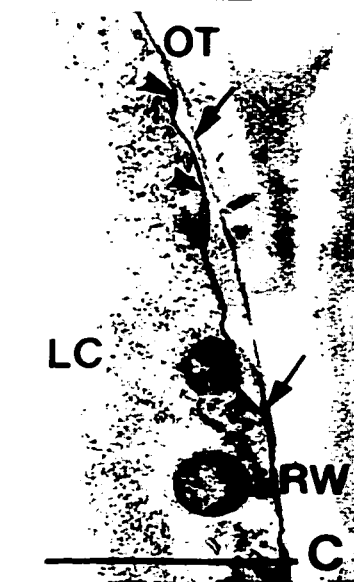
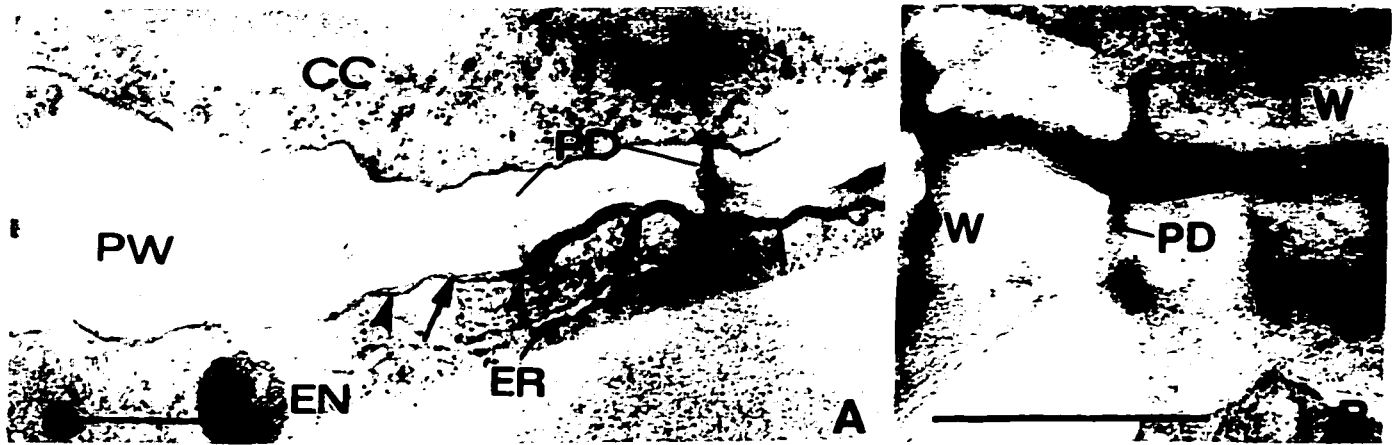
In young zones, both long and short cells have dense cytoplasm and are rich in organelles (*e.g.*, mitochondria and plastids; Fig. 2.3). Yet, long cells vacuolated earlier and faster than short cells (Fig. 2.3). In the old zone, both long and short cells were highly vacuolated, but were strikingly different from each other in the organization of their protoplasts. In living long cells, a very thin peripheral cytoplasm (150 nm on average) enveloped the large central vacuole (Fig. 2.2E). The composition of the cytoplasm was rather simple, the major organelles being mitochondria, plastids, and endoplasmic reticulum (ER). The cytoplasm could be relatively thick in the corners of these cells, but this was not coupled with an increased number of organelles (Fig. 2.2F). By contrast, short cells had a thicker cytoplasmic layer (580 nm on average) and more abundant organelles (Fig. 2.2E). Mitochondria and rough ER (rER) were most conspicuous. Plastids and dictyosomes were frequently observed. Long cells, after the deposition of suberin lamellae, looked healthy for about 5 d before degenerating. Early symptoms of degeneration were condensation of cytoplasm, disorganization of the internal membranes and loss of contents of organelles, and vanishing plasmodesmata (Fig. 2.2H).

#### **2.4.5 Plasmodesmata**

In all zones, the plasmodesmata were predominantly simple, narrow channels in longitudinal sectional view. Branched plasmodesmata were only occasionally encountered. The presence

**Fig. 2.2** Ultrathin cross sections of old zone showing wall modifications in endodermis and exodermis.

**A** Early phase of suberin lamella deposition (arrows) over the primary wall (*PW*) in endodermis (*EN*). The lamella appearing as an electron-dense wall layer external to plasmalemma (arrowheads). Plasmodesma (*PD*) intact and its diameter expanded. **B** Walls of a State III-endodermal cell. Suberin lamellae (*SL*) at the pit field clearly multi-layered. Plasmodesmata (*PD*) not affected by either suberin lamellae or tertiary walls (*TW*). **C** and **D** Exodermal long cell (*LC*). Early stage of suberin lamella formation (arrows) adjacent to plasmalemma (arrowheads). The lamellae along the outer tangential (*OT*) and radial (*RW*) portions of the cell wall were well developed (**C**), while those on the inner tangential (*IT*) side of the same cell were barely visible (**D**). **E** Cross section including radial walls of mature long (*LC*) and short cells (*SC*). Suberin lamellae (arrows) present in long but not short cells. The cytoplasm of the short cell was not only thicker but also richer in organelles than that of the long cell. **F** More details of a long cell with suberin lamellae (arrows) coating inner tangential wall. The cytoplasm could be relatively thick at cell corners, but with fewer organelles as compared to short cells (as in **E**). **G** Long cells (*LC*) in old zone. Plasmodesmata severed. It seems that tiny suberin platelets (arrowheads) act as a seal through the neck of plasmodesmata, covered by continuous suberin lamellae (arrows). The lamellar structure was more obvious at the pit field than elsewhere. **H** Cytoplasm (*CY*) of long cell (*LC*) degenerating and the damaged plasmodesmata (*PD*) vanishing. Suberin lamellae (arrows) evident. *CC* central cortical cell; *EP* epidermis; *ER* endoplasmic reticulum; *M* mitochondrion; *N* nucleus; *P* plastid; *rER* rough endoplasmic reticulum. Bars: 0.5  $\mu\text{m}$



of a desmotubule and neck constriction was a common feature. In the old zone, plasmodesmata all had similar diameters (about 60 nm).

#### **2.4.5.1 In tangential walls (radial symplastic path)**

In young zones, all living cells in the radial file (*i.e.*, those of the epidermis, immature exodermis, central cortex, endodermis, pericycle, and stelar parenchyma) had only primary walls and were all linked by plasmodesmata. (Fig. 2.3 shows plasmodesmata in the outer cell layers.) In the old zones examined, plasmodesmata were also found in all layers, from the epidermis all the way to the stelar parenchyma (Fig. 2.4A-H), but certain changes had taken place. In the endodermis, the plasmodesmatal continuity remained intact in State II (Fig. 2.2A) and State III (Figs. 2.2B, 2.4E) cells, and the diameter of the plasmodesmata expanded noticeably to about 80-90 nm at the site of central cavity (Fig. 2.2A). In the exodermis, however, long cell plasmodesmata were all severed by suberin lamellae. As seen in some sections, tiny platelets of suberin were found right at the neck as a seal through the plasmodesmata, which was followed by deposition of continuous suberin lamellae (Fig. 2.2G). At the pit fields, suberin lamellae were thicker and exhibited finer electron-dense/lucent components than elsewhere of the wall (Fig. 2.2G), similar to the endodermis (Fig. 2.2B). Thus, the long cells were isolated symplastically (and also apoplastically) from all surrounding cells. Plasmodesmatal connections of the exodermis with the epidermis and with the central cortex were preserved only through the short cells lacking suberin lamellae (Fig. 2.4A, B).

#### **2.4.5.2 In transverse and radial walls**

In transverse walls, the epidermal cells were connected end-to-end with plasmodesmata at both young (Fig. 2.3) and old ages. In the exodermis, both long and short cells, sister and non-sister, were initially linked with plasmodesmata (Fig. 2.3), but these connections were later severed by the suberin lamellae in long cells. In the central cortex, cells were all connected to each other with plasmodesmata in the longitudinal files at all stages of development. In radial

**Fig. 2.3** Median longitudinal ultrathin section taken 2 mm from the root tip

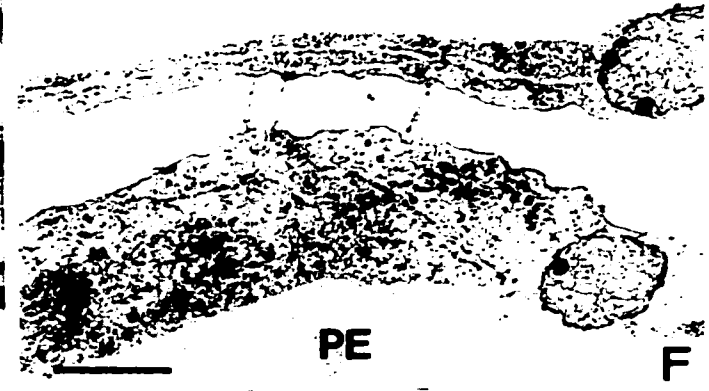
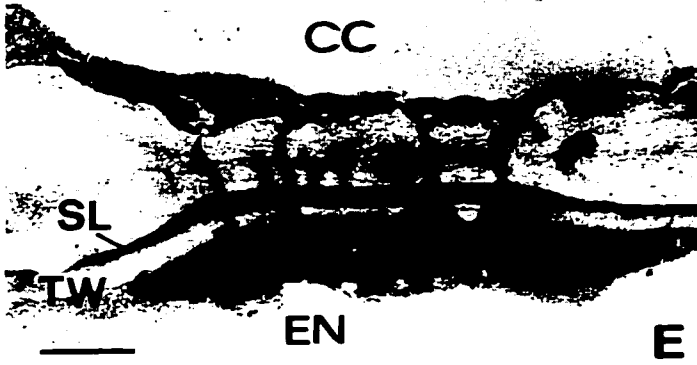
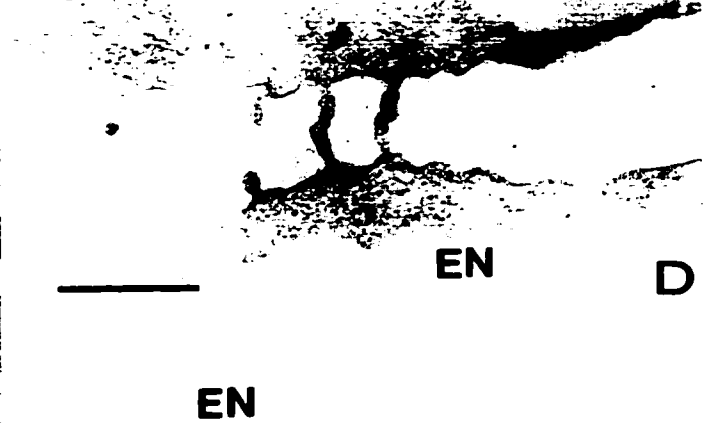
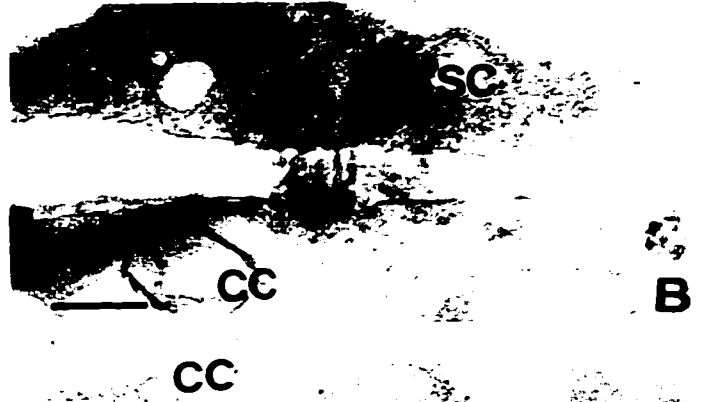
Short (*SC*) and long cells (*LC*) are recent products of unequal cell divisions. New walls between sister cells are indicated by single arrows. Wall between non-sister cells is indicated by double arrows. Long cells have larger and more numerous vacuoles (*V*) than short cells. All cells connected with plasmodesmata. Those in transverse and tangential walls are indicated by black and white arrowheads, respectively. *CC* central cortex; *EP* epidermis; *M* mitochondrion; *N* nucleus; *P* plastid. Bar: 5  $\mu\text{m}$





**Fig. 2.4** Plasmodesmata in tangential walls of cells in a radial file in the root (cross sections)

**A** Epidermal cell-short cell. **B** Short cell-central cortical cell. **C** Central cortical cells. **D** Central cortical cell-endodermal cell (State I). **E** Same interface as in **D**, but endodermal cell at State III. Plasmodesmata intact through suberin lamellae (*SL*) and tertiary cellulosic wall (*TW*). **F** Endodermal cell (State I)-pericycle cell. **G** Same interface as in **F**, but with branched plasmodesmata (arrows). **H** Pericycle cell-stelar parenchyma cell. *CC* central cortex; *EN* endodermis; *EP* epidermis; *PE* pericycle; *SC* short cell; *SP* stelar parenchyma. Bars: 0.5  $\mu\text{m}$



walls, the same pattern of plasmodesmatal connection was observed for all cell layers as in their transverse walls. It is interesting to note that the endodermal cells were poorly connected by plasmodesmata on their lateral walls (Fig. 2.5A). By contrast, pericycle cells were well connected laterally to each other (Fig. 2.5B). Between stelar parenchyma cells, very few plasmodesmata were observed.

## **2.5 Discussion**

The incomplete picture of the symplastic relationships of the dimorphic exodermis (see Introduction) can be attributed to several factors. (1) Only very few species have been investigated at the ultrastructural level. (2) The area available for examination of viable plasmodesmata is rather small. For example, in onion, short cells without suberin lamellae occupy only 13% of the exodermis (calculated from tangential sections and partial macerations) and this value declines with the formation of suberin lamellae in short cells at very old ages (Kamula et al. 1994). (3) The plasmodesmata in this small area are so few that they could be overlooked in small collections of ultrathin sections. (4) Standard TEM protocols do not produce clear images of plasmodesmata in cells with suberin lamellae. Therefore, devising an appropriate protocol was a necessary prerequisite for the present study.

### **2.5.1 The TEM technique for suberized cells**

Routine protocols consist of double fixation in glutaraldehyde and osmium tetroxide, and embedding in resins. However, as shown in the published electron micrographs, along with the distorted cell shapes, none of the protoplasts of the post-State I endodermis (Stelzer and Läubli 1977, Mackenzie 1979, Scott and Peterson 1979) and other suberized cells (*e.g.*, mestome sheath, Griffith et al. 1985) was properly preserved. The dimorphic exodermis (*e.g.*, in onion) also represents a difficult specimen, being composed of cells (long and short) with substantially varying permeability and being surrounded by tissues (epidermis and central cortex) exhibiting different permeability.

**Fig. 2.5** Plasmodesmata in radial wall of endodermis and pericycle

**A.** A plasmodesma (*PD*) in the outer portion of the radial endodermal wall. Margins of the Casparian band are indicated by arrowheads. **B** Plasmodesmata usually in the middle of walls of pericycle cells. Bars: 0.5  $\mu\text{m}$



To improve structural preservation, a fast penetrant as a component of the primary fixative mixture was especially helpful. For a combination of formaldehyde and glutaraldehyde, it was surmised that the former quickly penetrated and temporarily stabilized cellular structures that were subsequently more permanently immobilized by glutaraldehyde (Karnovsky 1965). Acrolein in conjunction with glutaraldehyde enhanced the fixation even further, apparently due to the higher reactivity and faster penetration of the former (Zee and O'Brien 1970, Mersey and McCully 1978). During fixation in osmium tetroxide, a low concentration of the fixative (0.5%) coupled with an extended incubation (12-24 h) alleviated the undesired binding of osmium to the wall, which otherwise would probably make it more impermeable (Mersey and McCully 1978). The quality of fixation (preservation) could only be maintained through adequate resin infiltration. Either prolonged incubation in the complete resin (Holloway and Wattendroff 1987) or in the incomplete resin until the final change of infiltration (Hayes et al. 1985) usually improves infiltration. These minor modifications, however, were definitely not sufficient to infiltrate the exodermis/epidermis and endodermis (data not shown). Best results were obtained by infiltrating with resin without accelerator for an initial 4 d, followed by infiltration with resin plus accelerator for an additional 4 d. The initial infiltration process was accelerated by propylene oxide. This solvent can quickly remove dehydrating chemicals from the tissue, and offers better compatibility between the resin and the sample (Luft 1961). During the second period of infiltration, the tissues were penetrated essentially by only the small molecules of accelerator (MW 89).

The protocol outlined above was used to achieve good preservation of onion root epidermal, exodermal and endodermal protoplasts. It should also be suitable for related materials that have low wall permeability.

### **2.5.2 Plasmodesmata**

The present study has yielded a clear picture for the plasmodesmatal connections in onion roots. In young zones, plasmodesmata were present in all directions between all adjacent

cells, all the way from the epidermis to the stelar parenchyma. Moreover, all living cells were capable of synthesizing wound pit callose, which is an active response to injury (in this case, sectioning). The TBO staining procedure was useful for a gross determination of the cell wall-specific distribution of primary pit fields (and, thus, plasmodesmata), which served as a helpful guide for closer observations in the TEM.

Earlier investigators have experimentally demonstrated the existence of a symplastic transport pathway across the root cortex in maize (Ginsburg and Ginsburg 1970a, b) and *Pisum sativum* (Dick and ap Rees 1975). These observations gained support from the findings with TEM on maize (Wang et al. 1995) and onion (the present study). Also, our results are in accord with the previous postulation that the endodermis does not represent a symplastic barrier at any stage of its development (Clarkson et al. 1971, Scott and Peterson 1979, Warmbrodt 1985a, b, Warmbrodt 1986a, Wang et al. 1995). Assuming that the expansion of the plasmodesmatal diameter (Fig. 2.2A) is not an artifact, then this would have two implications. (1) The expanded plasmodesmata could accommodate the increased symplastic transport since the substances delivered through the cortical apoplast are blocked by the Casparian bands and converge into the symplast (see Peterson and Cholewa 1998). (2) The expansion could compensate, at least partially, for the reduced transmembrane transport of certain substances across the post-State I endodermis due to wall modifications. The cytoplasmic annulus of the plasmodesmata is the most likely channel for symplastic transport (Ding et al. 1992) and the neck region might not be limiting since the neck constriction is probably not present *in vivo* (Radford et al. 1998).

Major changes in the symplastic network were found in the exodermis following deposition of suberin lamellae in the long cells. These cells were no longer able to respond to wounding by forming pit callose (Table 2.1, Fig. 2.1G). This negative response correlated with the severance of plasmodesmata by suberin lamellae (Fig. 2.2G). A similar effect of suberin lamellae on the plasmodesmatal continuity was documented at the ultrastructural level for *Citrus* (Walker et al. 1984) and *Hoya* (Olesen 1978), both with a dimorphic exodermis.

Whether or not this is a general pattern for the dimorphic exodermis remains to be answered by examination of more species.

Suberin lamellae are generally considered to be impermeable to ions. Direct evidence for this was obtained at the ultrastructural level in a leaf bundle sheath (Evert et al. 1985). This could also be the case for the root suberin lamellae (Storey and Walker 1987). It has been shown that the exodermal Casparian bands constitute an apoplastic barrier to fluorescent dyes (Peterson et al. 1978) and ions (Peterson 1987). Thus in the old zone, radial transport of ions between the epidermis and central cortex can only possibly occur through the symplast of short cells (Walker et al. 1984, Storey and Walker 1987).

### **2.5.3 Short cells**

The exodermal short cells (without suberin lamellae) were appropriately called “passage cells” (Kroemer 1903, von Guttenberg 1968, Kamula et al. 1994, Peterson and Enstone 1996). Although they occupied only 13% of the exodermal surface area in onion, 98% of the epidermal cells were in contact somewhere along their lengths with a short cell (Barrowclough and Peterson 1994). These (exodermal) passage cells, being the sole site of radial communication between epidermis and central cortex (see above), appear to be physiologically more important than their counterparts in the endodermis. This is because in the latter, symplastic movement could take place not only through the (endodermal) passage cells, but also through the non-passage cells. At the periphery of the root, ions taken up by the epidermis can be moved into the short cells as described in *Citrus* (Walker et al. 1984, Storey and Walker 1987). Short cells could also absorb water and ions initially from the soil since most epidermal cells normally die off, leaving only the short cells’ outer tangential plasmalemma accessible to the soil solution (Walker et al. 1984, Barrowclough and Peterson 1994, Kamula et al. 1994). The richness of their cytoplasm is consistent with the active involvement of short cells in uptake and transport processes. In certain instances, the outer tangential membrane surface area was expanded by developing wall ingrowths (Wilson and Robards 1980). Water would also be expected to enter the



root preferentially through the short cells, as these are lacking the hydrophobic, suberin coats of the long cells.

## **2.6 Conclusion**

Using an improved TEM technique to preserve the protoplasts of suberized cells, this study established that all cell layers in onion roots are connected by plasmodesmata. The exodermal long cells are symplastically isolated in old zones, but the epidermis remains symplastically bridged to the central cortex by the exodermal short cells. This makes possible the inward and outward symplastic transport (of ions and photosynthates, respectively) across the root. Symplastic communication can also take place along individual cell layers (except for the long cells of the mature exodermis) through their plasmodesmata.

## Chapter 3

# Plasmodesmatal frequencies in onion roots: implications for solute transport pathways

### 3.1 Abstract

The plasmodesmatal frequencies between all cell types were analyzed in onion roots with a mature exodermis. In the inward direction, the cell/tissue interfaces studied were: epidermis-exodermal short cells-central cortex-central cortex-endodermis-pericycle-stelar parenchyma. For each, data were collected from 60 walls using a transmission electron microscope. The numbers of plasmodesmata (PD) per  $\mu\text{m}^2$  wall surface ( $F_w$ ) were 0.21, 1.03, 1.59, 0.58, 0.70 and 0.12, respectively. Two other expressions of frequency, namely PD/mm root length ( $F_n$ ) and PD/ $\mu\text{m}^2$  tissue interface ( $F_t$ ) were also used.  $F_n$  was considered the most instructive for comparing the potential capacity of symplastic transport across individual interfaces since they were organized in concentric cylinders. At the interfaces of exodermis-central cortex, central cortex-endodermis and endodermis-pericycle, the frequencies were rather high and constant ( $F_n = 4.05 \times 10^5$ ,  $5.13 \times 10^5$ , and  $5.64 \times 10^5$ , respectively). The number was much lower at the epidermis-exodermis interface ( $F_n = 8.96 \times 10^4$ ) and even lower at the pericycle-stelar parenchyma interface ( $F_n = 1.25 \times 10^4$ ). Therefore, across the interface of epidermis-short cells, a transmembrane transport pathway was expected to occur in addition to a possible symplastic pathway. At the interface of pericycle-stelar parenchyma, little symplastic transport would be anticipated; rather, ions might be transferred directly from the pericycle to the xylem vessels. The

second part of the study was concerned with the plasmodesmatal frequencies associated with the phloem. The highest frequency was detected at the interface of metaphloem sieve element and companion cell ( $F_w = 0.42$ ). The frequencies on other interfaces were much lower, yet constant (around 0.10). Thus, symplastic transport was possible for the translocated photosynthate from metaphloem sieve elements to the companion cells and further to other parenchyma cells. In the pericycle cells, a high frequency of plasmodesmata was observed on their radial walls ( $F_w = 0.75$ ), which could permit lateral circulation of solutes, thus facilitating ion and photosynthate delivery into and out of the stele, respectively.

**Keywords:** *Allium cepa* L.; phloem unloading; plasmodesmata; plasmodesmatal frequency; root; symplastic transport; transmission electron microscopy

**Abbreviations:** ANOVA analysis of variance; PD plasmodesmata; TEM transmission electron microscopy

### 3.2 Introduction

There is evidence that suggests the presence of a symplastic transport pathway in the root although its extent has not been defined clearly. More direct evidence was obtained with ion precipitation techniques (Läuchli et al. 1974a, b, Stelzer et al. 1975). These experiments, however, do not elucidate the relative efficiency of individual tissue/cell layers for symplastic transport. Plasmodesmatal frequency analysis could help predict the direction and efficiency of symplastic flows. To date, only very few species have been examined and measurements were made only for selected interfaces (Robards et al. 1973, Robards and Jackson 1976, Warmbrodt 1985a, b, 1986a, b, Kurkova 1989, Wang et al. 1995). Therefore, a survey of plasmodesmatal distribution across the root is necessary. Species like onion (*Allium cepa* L.) deserve special attention as the exodermis consists of long and short cells (*i.e.*, dimorphic exodermis). Earlier observations have made clear that the exodermal long cells in the old zone are symplastically isolated by suberin lamellae (Chapter 2). Accordingly, the short cells must play a paramount role in the ionic and water relations of the root. A closer examination

of their plasmodesmatal distribution will provide further insight into their performance in root function.

The pathway of xylem loading has been a matter of controversy. Are the vessels loaded by the stelar parenchyma (cells intervening between the xylem and phloem strands) or by the pericycle or by both? Most authors have assumed that ions are transferred from the cortex to the stelar parenchyma (by way of the pericycle) and are then transferred into vessels (see Clarkson 1993). Some experiments indicated that these parenchyma cells are capable of actively accumulating ions from the cortex in maize (Läuchli et al. 1971a, b; Läuchli et al. 1974a, b). A proton pump was described in the stelar parenchyma of onion roots (Clarkson and Hanson 1986). Another study on barley roots has suggested that the pericycle might play a major role in xylem loading (Vakhmistrov et al. 1972). Since the pericycle-stelar parenchyma interface has a much lower plasmodesmatal frequency than the pericycle-endodermis interface, the majority of ions would proceed from pericycle directly to the xylem vessels, rather than being transported through the stelar parenchyma (Vakhmistrov et al. 1972). In onion roots, the relative significance of these two tissues (stelar parenchyma and pericycle) at this critical point of the radial transport path remains to be seen.

Phloem unloading in the old zone is required by living cells (mainly of the cortex). Unlike in the root tip (Dick and ap Rees 1975, Oparka et al. 1994, Zhu et al. 1998a), these cells apparently do not form a significant sink. Yet, they need a continuous food supply for respiration and biosynthesis. Results obtained from physiological (Giaquinta et al. 1983) and structural studies (Warmbrodt 1985a, b, 1986a, b) are in favor of a symplastic pathway of photosynthate distribution from the phloem. It remains to be seen if such a possibility occurs in onion roots. An intensive observation of plasmodesmatal distribution associated with the phloem will help resolve this matter.

There are several ways of expressing plasmodesmatal frequencies. The number of plasmodesmata per  $\mu\text{m}^2$  wall surface is the basic and the most commonly used value (as in

the studies cited above). This is usually obtained from ultrathin sections, following the formula of Gunning (in Robards 1976):

$$F_w = N/(L \cdot (T + 1.5D/2)) \quad (1)$$

where, L - the length of a given cell wall, N - the number of PD along the wall, T - the thickness of sections, and D - the diameter of plasmodesmata. L, T and D are all in  $\mu\text{m}$ . The values of  $F_w$  will be most useful when a comparison is to be made among cell interfaces to predict their relative capacity for symplastic transfer. Thus, this expression is applicable to the phloem region of the root, where the paths concerned are very short and in all directions. For tissues external to the phloem, the numbers of plasmodesmata on the entire surfaces over a unit root length ( $F_n$ , See § 3.3.2 and 3.3.3) would be more meaningful. This is because all tissues (except for the central cortex) are organized into concentric cylinders and the surface area traversed by all inward-moving materials decreases gradually (Fig. 3.1). A third expression, the number of plasmodesmata per  $\mu\text{m}^2$  tissue surface, was employed for the purpose of comparing the present results to related literature data.

### **3.3 Materials and methods**

#### **3.3.1 Transmission electron microscopy**

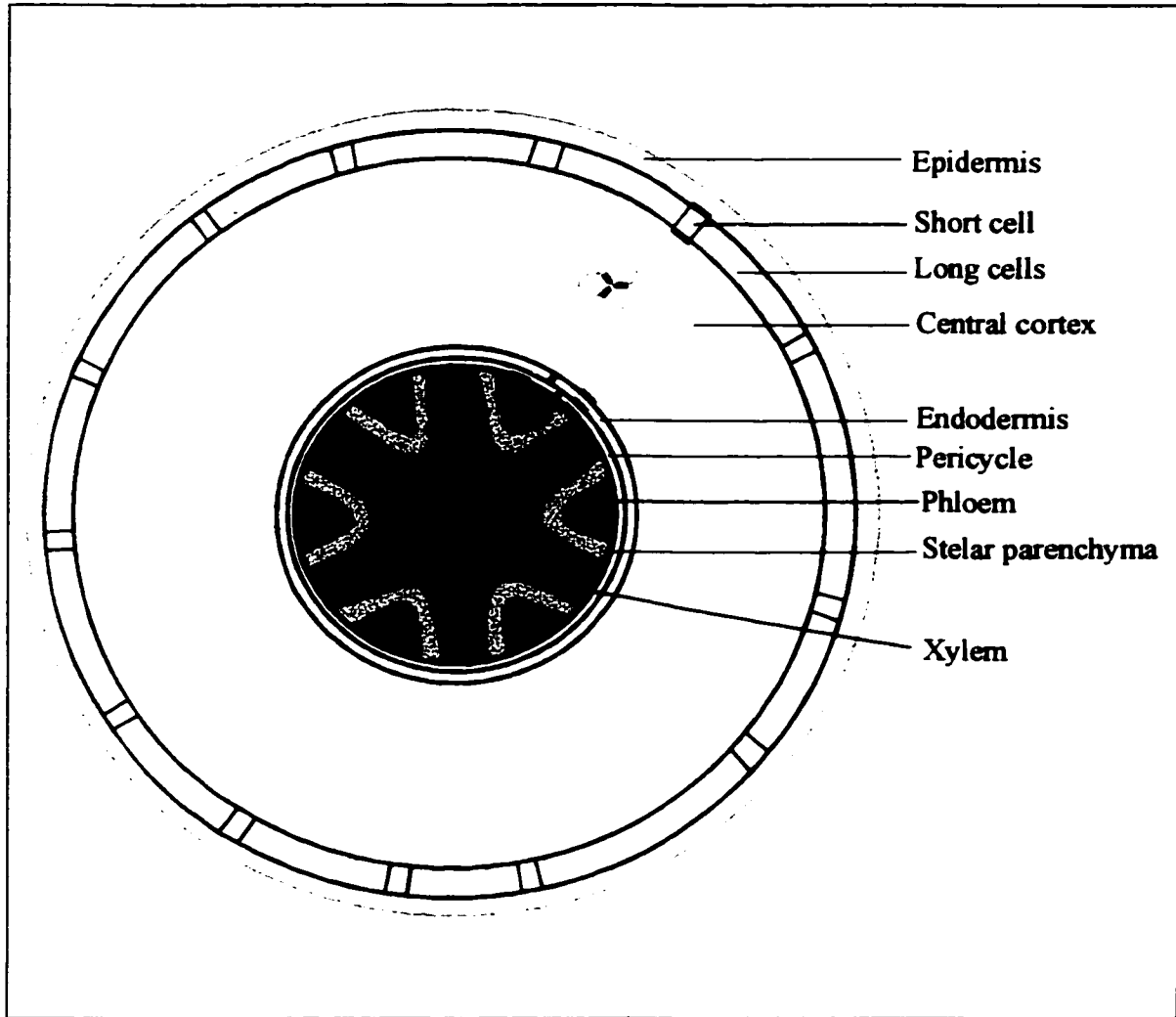
Bulbs of onions (*Allium cepa* L. cv. Ebenezer) were planted in moist vermiculite as described previously (see § 2.3.1). At 7 to 14 days, root segments 100 mm from the root tip were processed for transmission electron microscopy. The thickness of sections (T) was set at  $8 \times 10^{-2} \mu\text{m}$  on the microtome (as described in Chapter 2).

#### **3.3.2 Calculation of plasmodesmatal frequencies along the inward path (from the epidermis to the stelar parenchyma)**

All three expressions of frequencies were carried out for this region of the root. To calculate  $F_w$ , the diameters of plasmodesmata (D, in  $\mu\text{m}$ ) were measured from TEM negatives for

**Fig. 3.1** Diagram of a cross section of onion root showing cell and tissue interfaces studied for plasmodesmatal frequencies

For the measurement of plasmodesmatal numbers per  $\mu\text{m}^2$  wall surface ( $F_w$ ), cell walls are coloured pink. For plasmodesmatal numbers per mm root length ( $F_n$ ), tissue interfaces are drawn in blue.



individual interfaces. To obtain N and L for each interface, 60 walls were randomly collected from 5-30 non-serial ultrathin sections (which were cut from 5-10 root segments). On each wall, N was counted directly in the microscope. Then the wall was digitized (at 2,600 ×) by the program Analysis 2.0 (Soft-Imaging Service GmbH) and its length (L) was subsequently measured with another program, Northern Exposure (Empix Imaging, Inc.).

A second expression,  $F_n$ , was the total number of plasmodesmata in each interface (Fig. 3.1) over a root length of 1 mm ( $= 10^3 \mu\text{m}$ ), calculated from:

$$F_n = 10^3 \cdot 2\pi R \cdot F_w \quad (2)$$

where, R - the radius (in  $\mu\text{m}$ ) of the cylinder into which each tissue interface fits. Values of R were measured directly from fluorescence microscope colour slides of cross sections prepared previously (Chapter 2). The interfaces included: (1) epidermis-exodermis, (2) exodermis-central cortex, (3) central cortex-endodermis, (4) endodermis-pericycle, and (5) pericycle-stele proper (Fig. 3.1). It should be noted that this approach is not suitable for the central cortex, because intercellular spaces had developed in this region and cells were not arranged in concentric cylinders.

Clearly, formula 2 was not readily applicable to interfaces 1 and 2 (above) since functional plasmodesmata occurred only in the tangential walls of short cells and not of long cells (see Chapter 2). The “functional area” of the exodermis (*i.e.*, occupied by short cells) was 13.4% (measured from color slides of paradermal sections prepared previously (see Chapter 2). Then,

$$F_n = 13.4\% \cdot 10^3 \cdot 2\pi R \cdot F_w \quad (2-1)$$

For interface 5, modification to formula 2 is also necessary. Based on the assumption that the centripetal symplastic transport (if any) from the pericycle to the stele is only through the stelar parenchyma, then:

$$F_n = A_{sp} \cdot F_w \quad (2-2)$$

where  $A_{sp}$  is the outer tangential area ( $\mu\text{m}^2$ ) of the stelar parenchyma (pericycle-stelar parenchyma) over a 1 mm root length. It was calculated that  $A_{sp} = 1.04 \times 10^5$ .



Finally, the number of plasmodesmata per  $\mu\text{m}^2$  tissue interface of entire cylinders ( $F_t$ ) was obtained using:

$$F_t = F_n / (10^3 \cdot 2\pi R) \quad (3)$$

where  $10^3 \cdot 2\pi R$  is the area ( $\mu\text{m}^2$ ) of a given tissue interface over 1 mm root length. This calculation was performed for the interfaces of epidermis-exodermis, exodermis-central cortex, and pericycle-stele proper. For the interfaces of central cortex-endodermis and endodermis-pericycle,  $F_t = F_w$ . This expression of plasmodesmatal frequencies was taken for comparing the data of the present study with those in the literature expressed in this way. Values of  $F_t$  were not estimated for the central cortex for the reason stated above. All data for these calculations were displayed in Table 3.1.

### **3.3.3 Calculation of plasmodesmatal frequencies associated with the phloem**

The interfaces investigated are listed in Table 3.2 (see also Fig. 3.1). The values of  $F_w$  were calculated following the same procedure as in § 3.2.2. At the interface of phloem-pericycle, the total number of plasmodesmata over a 1 mm root length ( $F_n$ ) was also estimated; this value was used to compare the potential capability of transporting photosynthates of different cell layers all the way from the phloem to the epidermis (see Results and Discussion).

Plasmodesmatal frequencies ( $F_w$ ) on the radial walls of the endodermis and pericycle were obtained (Table 3.2) to assess their possible involvement in symplastic communication in the tangential direction.

### **3.3.4 Statistics**

Analysis of variance (ANOVA) was carried out at  $\alpha = 0.05$  for the values of  $F_w$  for the phloem region and some other interfaces (see Results). The procedure was performed

**Table 3.1 Plasmodesmatal frequencies along the radial files of onion root tissues**

<sup>a</sup>  $F_w$ , PD/ $\mu\text{m}^2$  wall surface;  $F_n$ , PD/mm root length;  $F_t$ , PD/ $\mu\text{m}^2$  tissue interface

<sup>b</sup> *CC* central cortex; *EN* endodermis; *EP* epidermis; *EX* exodermis; *PE* pericycle; *PR* stele proper (stele excluding pericycle); *SC* short cell; *SP* stelar parenchyma

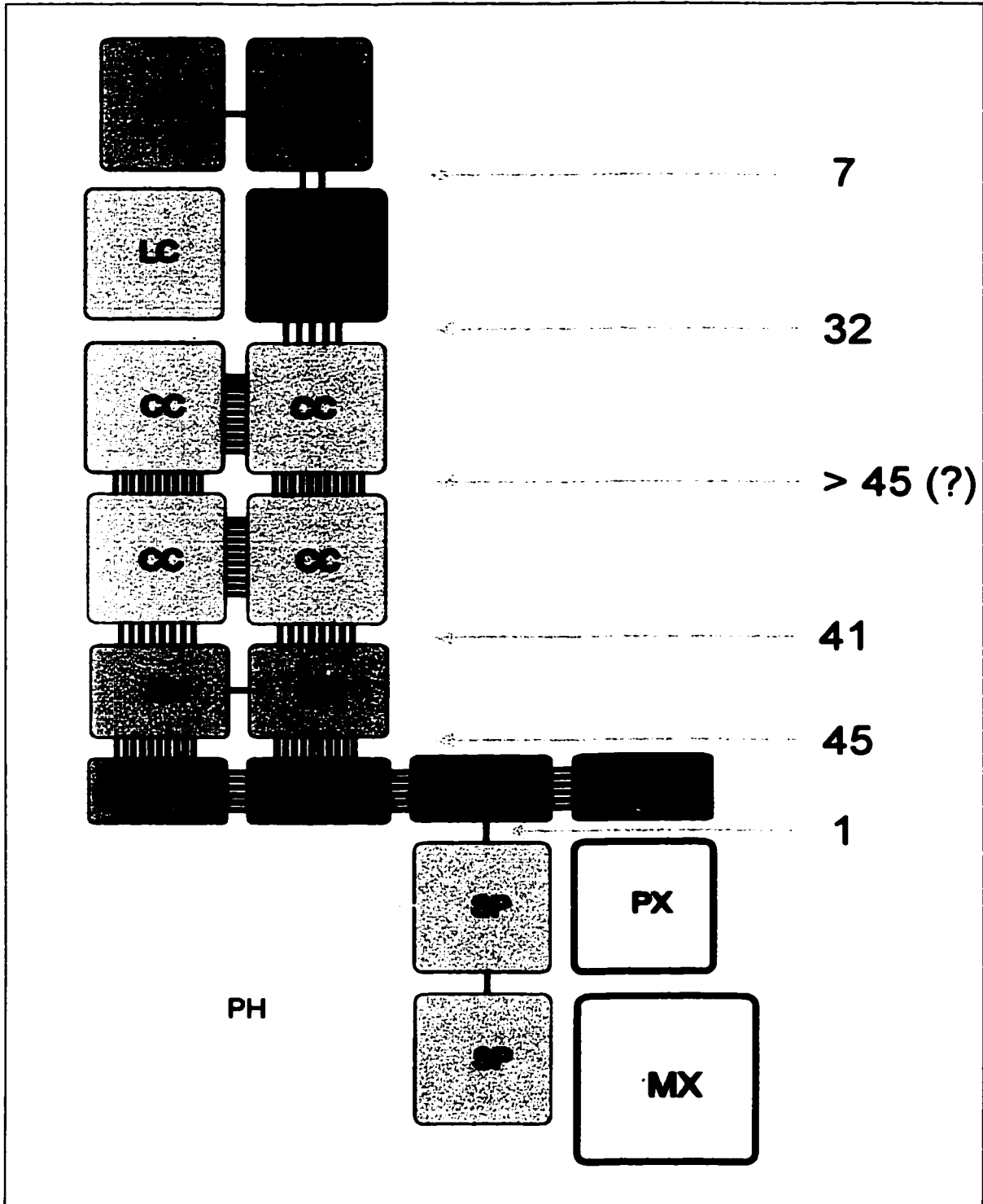
<sup>c</sup> n.a., not applicable

<sup>d</sup> The plasmodesmata on the pericycle-phloem interface are not included

	EP-EX <sup>b</sup>	EP-SC	EX-CC	SC-CC	CC-CC	CC-EN	EN-PE	PE-PR	PE-SP
F <sub>w</sub> <sup>a</sup>	n.a. <sup>c</sup>	0.21 ± 0.16	n.a.	1.03 ± 0.44	1.59 ± 0.43	0.58 ± 0.22	0.70 ± 0.19	n.a.	0.12 ± 0.09
F <sub>n</sub>	8.96 × 10 <sup>1</sup>		4.05 × 10 <sup>5</sup>		n.a.	5.13 × 10 <sup>5</sup>	5.64 × 10 <sup>5</sup>	<sup>d</sup> 1.25 × 10 <sup>4</sup>	
F <sub>t</sub>	2.77 × 10 <sup>2</sup>	n.a.	1.68 × 10 <sup>1</sup>	n.a.	n.a.	5.83 × 10 <sup>1</sup>	7.00 × 10 <sup>1</sup>	1.74 × 10 <sup>2</sup>	n.a.

**Fig. 3.2** Plasmodesmogram of onion roots: plasmodesmatal frequencies from the epidermis to the stele.

The frequencies of plasmodesmata ( $F_w$ , plasmodesmata per  $\mu\text{m}^2$  wall surface) are approximately represented by short lines that link neighboring cells. The more the lines, the higher the frequencies. The frequencies associated with the phloem are not shown in this diagram (but see Fig. 3.4). This diagram can also be used to show the overall pattern of plasmodesmatal frequencies expressed as  $F_n$  (plasmodesmata per mm root length). The numbers on the right side are the ratios of the values of  $F_n$ . For the central cortex (*CC*),  $F_n$  was not calculated, but the number of plasmodesmata available for the symplastic transport must be very high (assumed to be higher than 45 in the ratio list; see text). *EN* endodermis; *EP* epidermis; *LC* long cells; *MX* metaxylem vessels; *PE* pericycle; *PH* phloem; *PX* protoxylem vessels; *SC* short cells; *SP* stelar parenchyma



following Sokal and Rohlf (1981). ANOVA was not done for  $F_t$  and  $F_n$ , since these values are secondary in nature (*i.e.*, derived from the means of  $F_w$ ).

## **3.4 Results**

### **3.4.1 Plasmodesmatal frequencies along the path of ions**

Certain variations have been observed between all cell/tissue interfaces, with all three expressions of plasmodesmatal frequencies. Based on  $F_w$  (Table 3.1), the PD frequencies in tissue interfaces were in the following order: central cortex–central cortex > short cells–central cortex > endodermis–pericycle > central cortex–endodermis > epidermis–short cell > pericycle–stelar parenchyma. For  $F_n$ , the values were rather constant in the region from the exodermis up to the pericycle, in spite of the uncertainty about the central cortex (Table 3.1). [For this latter tissue, although it is theoretically possible to obtain the value, the estimate would be misleading if applied to the explanation of radial transport, due to the presence of intercellular spaces and the cells' irregular arrangement. Nevertheless, the abundance of plasmodesmata in the cell walls ( $F_w$ ) of the central cortex apparently renders it efficient for symplastic transport.] At the epidermis–exodermis interface, a very small number of plasmodesmata was obtained. At the pericycle–stelar parenchyma interface, the number was even smaller. When expressed in ratios, the overall view was more obvious (Fig. 3.2).

### **3.4.2 Plasmodesmatal frequencies associated with the phloem**

The root usually contained 6 phloem strands. In a cross section, each strand contained 1 or 2 protophloem sieve elements, 3–5 metaphloem sieve elements and their associated companion cells. At its outer tangential side, the phloem was in contact with the pericycle by 3–4 companion cells and 1 (rarely 2) protophloem sieve element (Fig. 3.3). On the

**Fig. 3.3** Structure of phloem and surrounding tissues

**A** An overview of the phloem and surrounding tissues. **B** Pericycle and surrounding tissues. The radial walls of pericycle cells are marked by asterisks. **C** Plasmodesmata between metaphloem sieve element (*MSE*) and companion cell (*C*). **D** Companion cells. **E** stelar parenchyma cells. *EMX* early metaxylem; *EN* endodermis; *ER* endoplasmic reticulum; *IEMX* immature early metaxylem; *MI* mitochondrion; *MSE* metaphloem sieve element; *PE* pericycle; *PSE* protophloem sieve element; *PX* protoxylem; *SP* stelar parenchyma. Bars: 50  $\mu\text{m}$  (**A**) and 0.5  $\mu\text{m}$  (the rest)

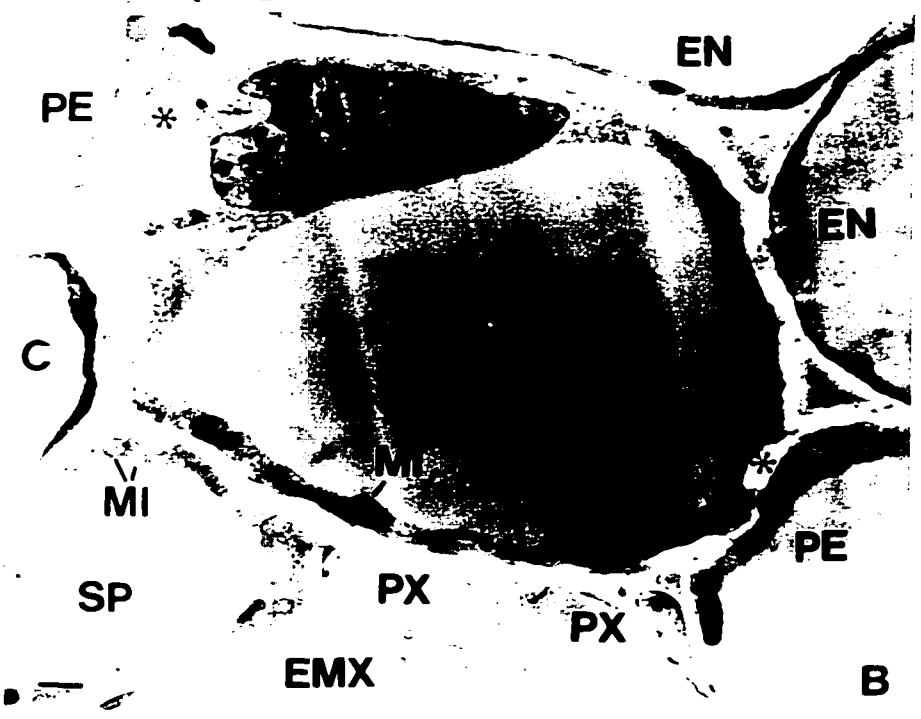
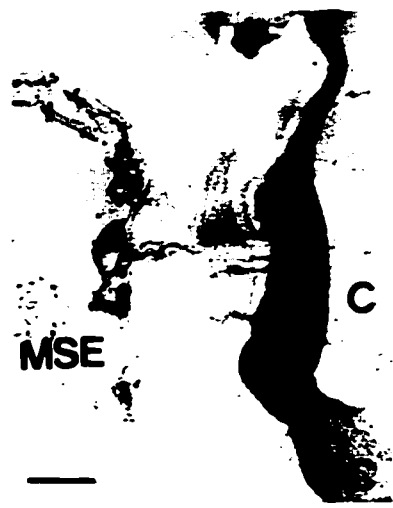
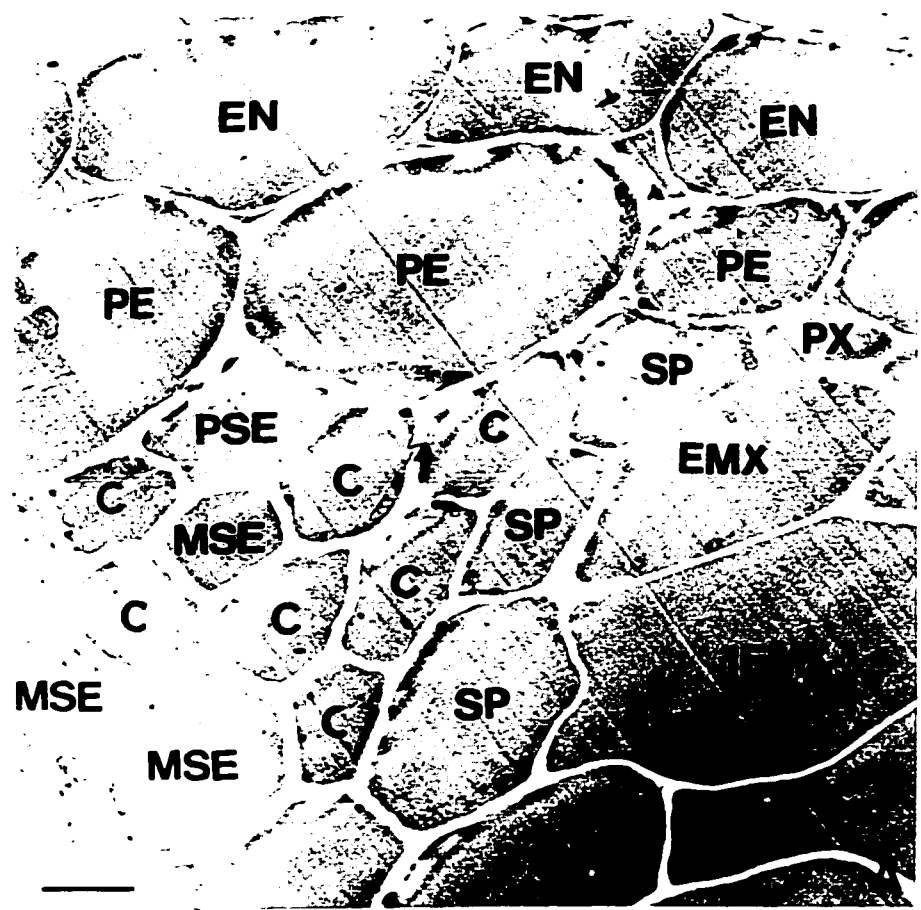




**Table 3.2** Plasmodesmatal frequencies associated with the phloem

The frequencies are expressed in  $F_w$ .

<sup>a</sup> *C* companion cell; *EN* endodermis; *MSE* metaphloem sieve element; *PE* pericycle; *PSE* protophloem sieve element; *SP* stelar parenchyma

	<sup>a</sup> EN	PE	SP	C	PSE	MSE
EN	0.06 ± 0.04					
PE	0.70 ± 0.19	0.75 ± 0.19				
SP		0.12 ± 0.09	0.11 ± 0.06			
C		0.16 ± 0.12	0.17 ± 0.10	0.11 ± 0.06		
PSE		0.08 ± 0.04		0.07 ± 0.06		
MSE				0.42 ± 0.16	0.13 ± 0.08	0.10 ± 0.05

flanks of the phloem, companion cells are symplastically connected to the stelar parenchyma. The metaphloem sieve elements were physically associated with neither the pericycle nor the stelar parenchyma. In this region, companion cells had the richest protoplasts of any cell, characterized by dense cytoplasm and numerous mitochondria. The cytoplasm of pericycle cells was similar to (or denser than) that of stelar parenchyma cells underneath. Those stelar parenchyma cells deep in the stele had very thin cytoplasm and were poor in organelles (Fig. 3.3).

A much higher PD frequency ( $F_w$ ) was observed between the metaphloem sieve elements and the companion cells than at any interface (Table 3.2, Fig. 3.4), but the difference was not significant (ANOVA at  $\alpha = 0.05$ ). All other frequencies were not significantly different from each other. For the pericycle, frequencies ( $F_w$ ) on the outer tangential and the radial walls were not significantly different from each other, but each was significantly different from (higher than) that on the inner tangential walls. In the endodermis, the frequencies on the outer and inner tangential walls were not significantly different, but the frequency on the radial walls were significantly lower.

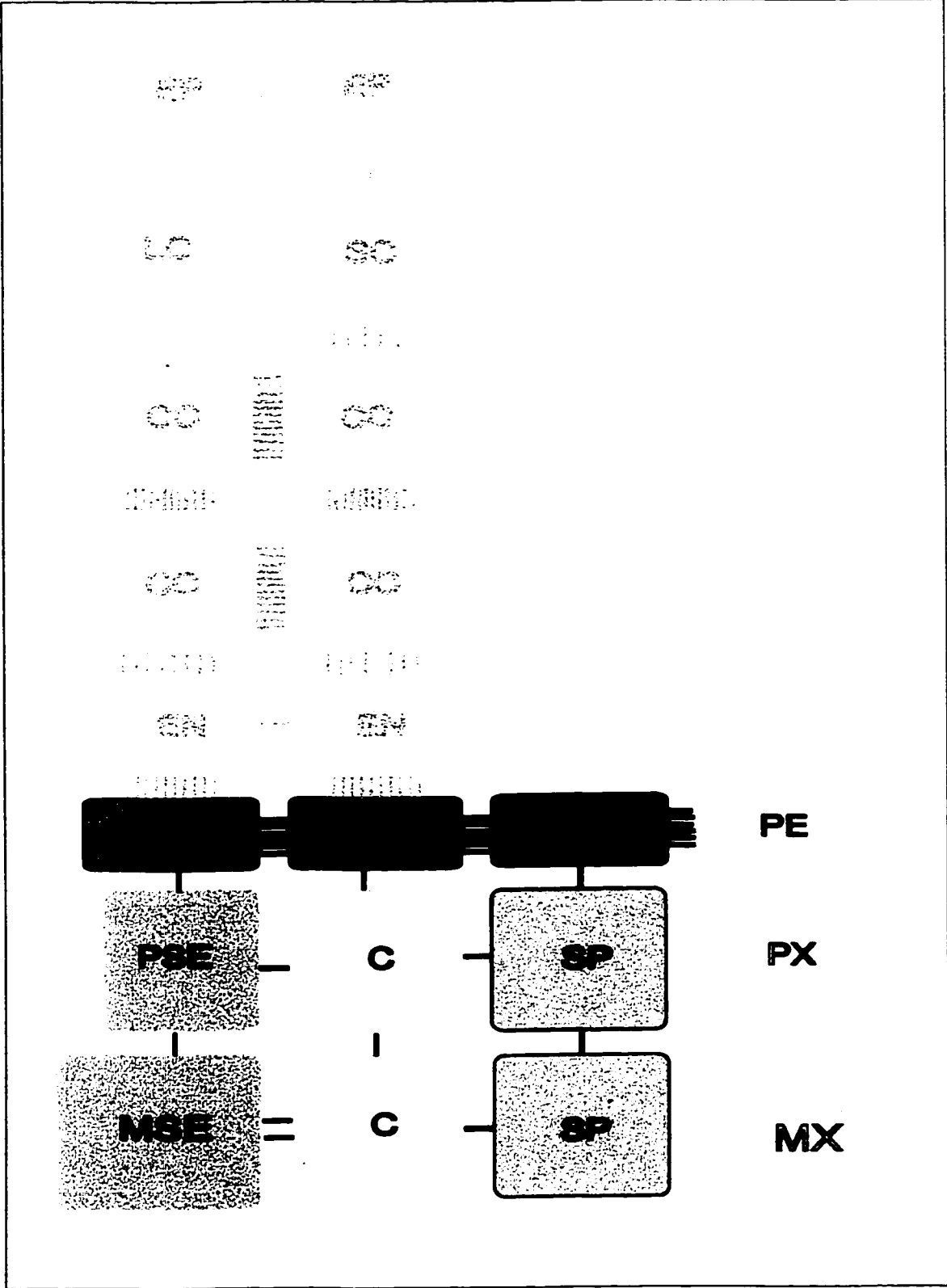
The total number of plasmodesmata at the phloem-pericycle interface was estimated. (This value will be used to discuss the outward transport of photosynthates from the phloem. See § 3.5.2) As seen in a cross section of the root, the phloem is connected to about half of the inner tangential surface of the pericycle. In this area, companion cells took 4/5 and protophloem sieve elements took 1/5. The values of  $F_n$  for the interfaces of the pericycle with the companion cells and with the protophloem sieve elements were estimated at  $4.61 \times 10^4$  and  $5.76 \times 10^3$ , respectively, totaling at  $5.19 \times 10^4$ .

### **3.5 Discussion**

The present study provided a complete assessment of the plasmodesmatal frequencies that are associated with both inward (for ions) and outward (for photosynthates) transport in onion roots. This is the first such comprehensive information for any root system.

**Fig. 3.4** Plasmodesmogram of onion roots: plasmodesmatal frequencies associated with the phloem

Tissues external to the pericycle and beside the phloem are drawn in grey. (For a complete list of abbreviations, see Fig. 3.2.) This diagram is based on the values of  $F_w$ . The more the lines, the higher the frequencies. *C* companion cell; *MSE* metaphloem sieve element; *PSE* protophloem sieve element



### 3.5.1 Plasmodesmatal frequencies: implications for ion transport

Symplastic transport is made possible in onion roots by the presence of plasmodesmata in all cell/tissue interfaces. It has long been demonstrated that a symplastic path occurs traversing the root cortex (Arisz 1956, Anderson and Reilly 1968, Ginsberg and Ginsberg 1970a, b, Jarvis and House 1970, Baker 1971, Clarkson and Sanderson 1974, van Iren and Boers-van de Sluijs 1980). This is most probably also true for the onion root cortex, since its plasmodesmatal frequency ( $F_w$ ) was rather high (Table 3.1). [In the literature, Scott et al. (1956) photographed surface views of isolated onion cortical cells in the light and scanning electron microscopes. From those micrographs, Tyree (1970) estimated the frequency in the cortex at  $F_w = 1.50 \text{ PD}/\mu\text{m}^2$ . The result of the present study by using cross sections in the TEM was actually the same as the literature data.] Similarly, this major, if not the only, pathway is most likely to occur near both the root surface (from short cells to central cortex) and deep in the root (from central cortex to endodermis to pericycle), as high and constant plasmodesmatal numbers ( $F_n$ ) were found on these interfaces (Table 3.1, Fig. 3.2).

It is interesting to note the differential associations of the exodermal cells with the epidermis and with the central cortex. In maize exodermis, the plasmodesmatal frequency on the outer tangential wall is half that on the inner tangential wall ( $F_t$ , 0.54 vs. 1.14 - Clarkson et al. 1987). In onion, taking the exodermis as a whole, the difference is much higher (*i.e.*, 5 times), although the frequencies are much lower (Table 3.1). An earlier estimation of plasmodesmatal frequency on the epidermis-exodermis interface ( $F_t \ll 0.10$  - Peterson et al. 1978) fits well with the present measurements ( $F_t = 0.03$ , Table 3.1). Note that the mature exodermis was symplastically connected with the neighbor tissues only through the short cells without suberin lamellae (Chapter 2), and the plasmodesmatal frequencies on the “functional” surfaces (of the outer and inner tangential walls) were 0.21 and 1.03, respectively ( $F_w$ , Table 3.1). Assuming that a constant flow of material is sustained from the soil solution to the cortex and the PD function close to their capacity, how could it be made possible? From the

short cells to the central cortex, symplastic movement is highly likely; this is supported by a high plasmodesmatal frequency (see above). From the epidermis to short cells, a combination of symplastic and trans-membrane mechanisms is indicated. In extreme situations, the short cells developed wall ingrowths in onion (Wilson and Robards 1980) and *Atriplex hastata* L. (Kramer et al. 1978), suggestive of enhanced transport across the outer tangential plasma membrane.

The plasmodesmatal frequencies of the endodermis (on the outer and inner tangential walls) have important implications for its function. It is generally believed that the Casparian bands divert apoplastic flows of solutes from the central cortex across the outer tangential plasma membrane (of the endodermis). Thus, a higher plasmodesmatal frequency ( $F_w$ ) is expected on the inner side than on the outer side to accommodate this situation. In barley (*Hordeum vulgare* L.), a difference of 0.75 : 0.37 ( $F_w$ ) was observed (Robards et al. 1973), but in onion, only a slight difference (not significant, at  $\alpha = 0.05$ ) was noticed (Table 3.1). An explanation for the discrepancy between these two species is that apoplastic transport through the central cortex, if any, is less significant in onion than in barley. This hypothesis is favored by the facts that: (1) Onion has an exodermis that is an apoplastic barrier (Peterson et al. 1978, Peterson 1987) and, thus, symplastic transport is initiated near the very periphery of the root (see next section). By contrast, barley roots lack an exodermis (Perumalla et al. 1990); as a result, the apoplast is accessible to ions up to the endodermis. (2) Onion root cortex has a much higher plasmodesmatal frequency ( $F_w = 1.59$ , Table 3.1) than barley (0.28 - Robards et al. 1973).

On the radial walls of the endodermis, the plasmodesmatal frequency was extremely low (Table 3.2). This result was in accord with those for barley (Helder and Boerma 1969, Kurkova et al. 1974). By contrast, Robards and Clarkson (1976) reported that all endodermal walls in barley had comparable frequencies and suspected that the low frequency at radial walls in the earlier reports was due to sampling problems. This criticism, however, is not valid for the present study because a large sample was collected (60 walls, total length = 354  $\mu\text{m}$ ). When compared to the pericycle radial walls (60 walls,

total length = 348  $\mu\text{m}$ ), the difference in their plasmodesmatal frequencies is obvious (Table 3.2). The location and construction of the endodermis indicate that this cell layer is mainly involved in radial transport and little tangential transport is necessitated, unlike the pericycle (next paragraph and §3.5.3).

The plasmodesmatal frequencies at the periphery of the stele are important in considering the relative significance of stelar parenchyma and pericycle in loading the xylem. The question as to which of the cell types plays a major role in loading the xylem vessels has not been settled (see § 3.2). The present study calls attention to the model proposed for barley roots by Vakhmistrov (Vakhmistrov et al. 1972, Vakhmistrov 1981). In brief, this model claims that ions will move through the pericycle to the xylem vessels. This argument is based on the fact that the pericycle and the stelar parenchyma are poorly connected by plasmodesmata, which is also true in onion (the present study). Furthermore, an immunofluorescence study of  $\text{H}^+$ -ATPase in barley roots showed that the pericycle had a higher signal than the stelar parenchyma (Samuels et al. 1992). In onion roots, pericycle cells usually have more active-looking protoplasts (based on cytoplasmic features) than stelar parenchyma cells (Fig. 3.3). Nevertheless, for onion roots, it would be inappropriate to rule out the stelar parenchyma's possible contribution to xylem-loading. There is evidence that an active step exists from the symplast to the xylem (for  $\text{Cl}^-$  - Hodges and Vaadia 1964). A pump has been reported in the stele (Clarkson and Hanson 1986). In both studies, the location of these activities was not clearly specified; it could be in the stelar parenchyma or the pericycle or both. It should be pointed out that, in the literature (e.g., Läuchli et al. 1971a, b, 1974a, b; De Boer 1999), the term "xylem parenchyma" has been used to include the stelar parenchyma and pericycle. An ultrastructural ATPase localization study would help resolve this matter.

### **3.5.2 On phloem unloading and post-phloem transport of photosynthates in the old zone**

A symplastic pathway for photosynthates, as for ions (see above), across the cortex has been commonly recognized (Dick and ap Rees 1975, Giaquinta et al. 1983, Fisher and Oparka



1996). Inside the phloem, it also seems to be a general rule that the companion cells are the principal receivers of the translocated photosynthates from the shoot (Warmbrodt 1985a, b). These ideas gain strong support from the present study (Tables 3.1 and 3.2). Yet, as to the initial post-companion cell transport pathway(s), variations have been observed among species. For instance, in barley (Warmbrodt 1985a), maize (Warmbrodt 1985b) and some other species (see Patrick and Offler 1996), the preferred path would be from the companion cells to the parenchyma cells and to the pericycle, following a decreasing gradient of plasmodesmatal frequency. A parallel solute gradient was detected in barley (Warmbrodt 1986a). Although onion shares certain similarities with barley (Warmbrodt 1985a) and maize (Warmbrodt 1985b) with respect to phloem construction, no such preference is expected in the former since the plasmodesmata distributed approximately evenly.

The pathway by which photosynthates are transported to the pericycle in onion is uncertain. The interfaces of phloem with the pericycle and with the stelar parenchyma have  $F_n = 5.19 \times 10^4$  and  $1.25 \times 10^4$  PD/mm root, respectively. The combined value is  $6.44 \times 10^4$ . This number is close to that at the exodermis-epidermis interface (Table 3.1). Assuming either all or a portion of these plasmodesmata are transferring photosynthates to the pericycle, a significant amount of transport is anticipated, all the way outward to the epidermis (see Introduction). In *Arabidopsis* roots, plasmodesmata between the phloem and the surrounding cells, however, were reported to be held in a physiologically “closed” state by an energy-dependent process under normal circumstances (Wright and Oparka 1997). Functional isolation of phloem is also reported in stems (Hayes et al. 1985, Aloni and Peterson 1990, van Bel and Kempers 1990, van Bel and van Rijen 1994). If this is true, the photosynthates will be released from the phloem only across the plasma membrane (mainly of the companion cells). Then, we need to look into the advantage of “blocking” (at the cost of energy) over removing these structures. It should be mentioned that the “symplastic isolation” was detected using fluorescent tracer dyes. The fluorescence techniques might not be sensitive enough to detect the dye movement as the transport across the interfaces under discussion was not significant. Furthermore, the reliability of these approaches remains to be further tested.

### 3.5.3 A further note on the pericycle

The pattern of plasmodesmatal frequency in pericycle cells points to a special role they might play in solute delivery. Their possible role in the radial transport of ions (*i.e.*, xylem-loading) was discussed in § 3.5.1. Earlier, Vakhmistrov suggested that the pericycle could also act as an “annular collector/disperser” (Vakhmistrov et al. 1972, Vakhmistrov 1981). This hypothesis is illustrated in Figs. 3.5 and 3.6. The idea was based on the high plasmodesmatal frequency in the radial walls of pericycle cells. In brief, substances received from the endodermis tend to move laterally (inside the pericycle), toward those pericycle cells that abut the xylem vessels where transpiration stream starts (*i.e.*, the “annular collector” role). At the same time, the pericycle functions as an “annular disperser” in the outward transport of photosynthates (Kurkova et al. 1974, Vakhmistrov 1981). Physically, only those pericycle cells that are connected with the phloem (and, to a lesser extent, probably also those connected with the stelar parenchyma) are able to receive substances from the phloem. A portion of the photosynthates could be delivered directly to the adjacent endodermal cells. The rest would tend to equilibrate across the pericyclic radial walls *via* the plasmodesmata, reaching the xylem-associated pericycle cells, then move to the endodermal cells. A comparison between the endodermis (§ 3.5.1) and the pericycle will help understand how these two layers are designed to perform different functions.

These brilliant ideas about the pericycle function deserve to be better known. The present results on onion roots are in favor of the “annular collector/disperser” model. This model could be widely applicable since the structure and spatial relationship of the pericycle is constant in essentially all species.

## 3.6 Conclusion

Analysis of plasmodesmatal frequencies in onion roots indicated that a constant symplastic transport of ions is possible from the exodermal short cells up to the pericycle. Across the interface of epidermis and short cells, less symplastic transport is anticipated. Symplastic

transport from the pericycle to the stelar parenchyma would be even less significant. For the transport of photosynthates, phloem unloading would most probably occur at the interfaces of companion cells to the stelar parenchyma and to the pericycle cells. In the pericycle, the distribution pattern of plasmodesmata in the tangential walls and in the radial walls has important implications for transport. This cell layer might play a role in loading the protoxylem vessels. Considerable circulation (of ions and photosynthates) is possible in the tangential direction of the tissue; this will potentially facilitate both inward and outward transport.

**Fig. 3.5** Pericycle as “annular collector” for ions

Adapted from Vakhmistrov et al. (1972). The radial walls of pericycle cells are drawn with broken lines to indicate the high frequency of plasmodesmata. Possible routes are labeled with letters and intensities of symplastic ion transport (between living cells, routes A through D) are represented with arrows of different sizes (corresponding to the postulated flows). Overall ion flows across other interfaces (routes E through G) are also indicated. See text for a discussion of the various flows.

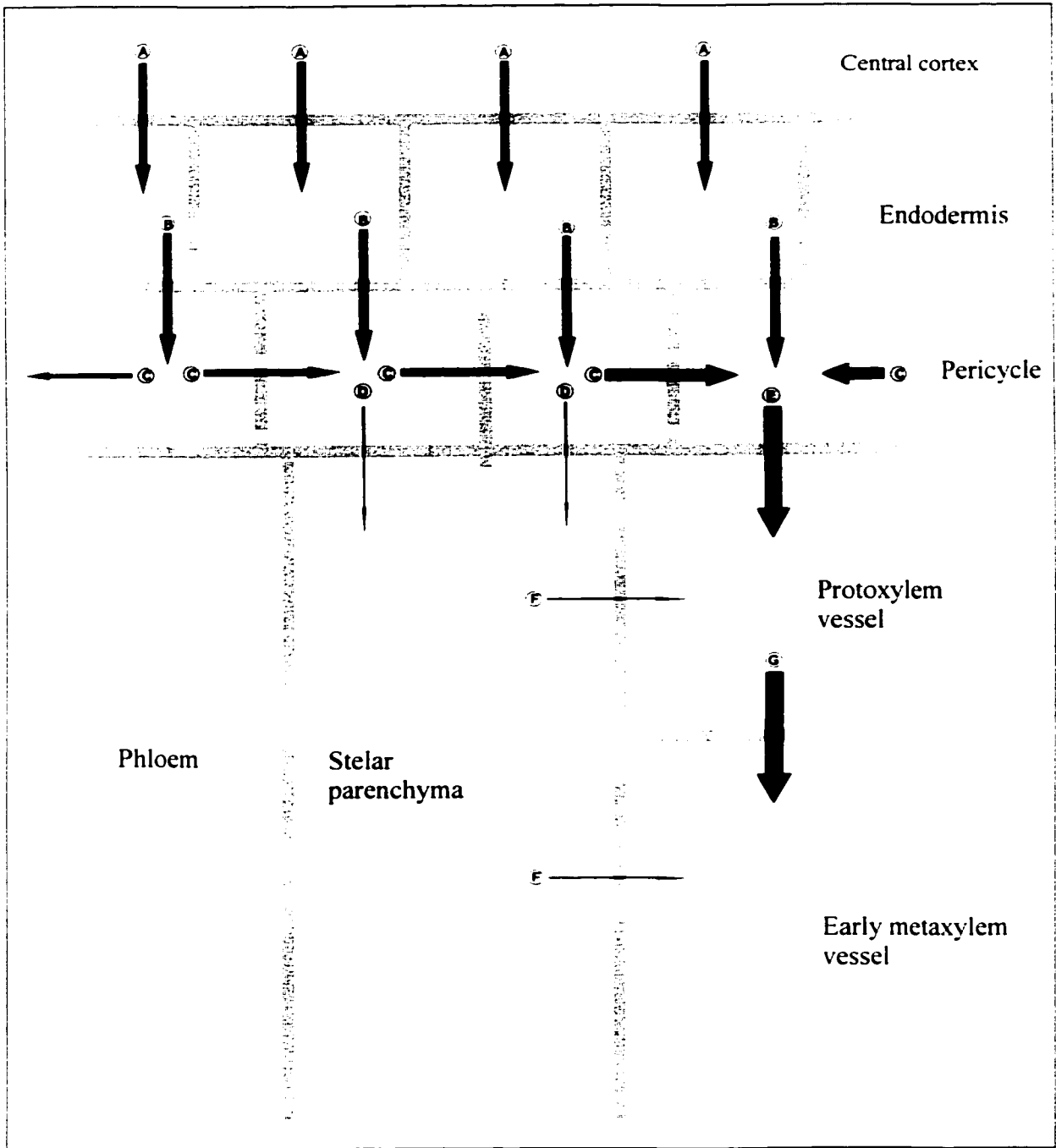
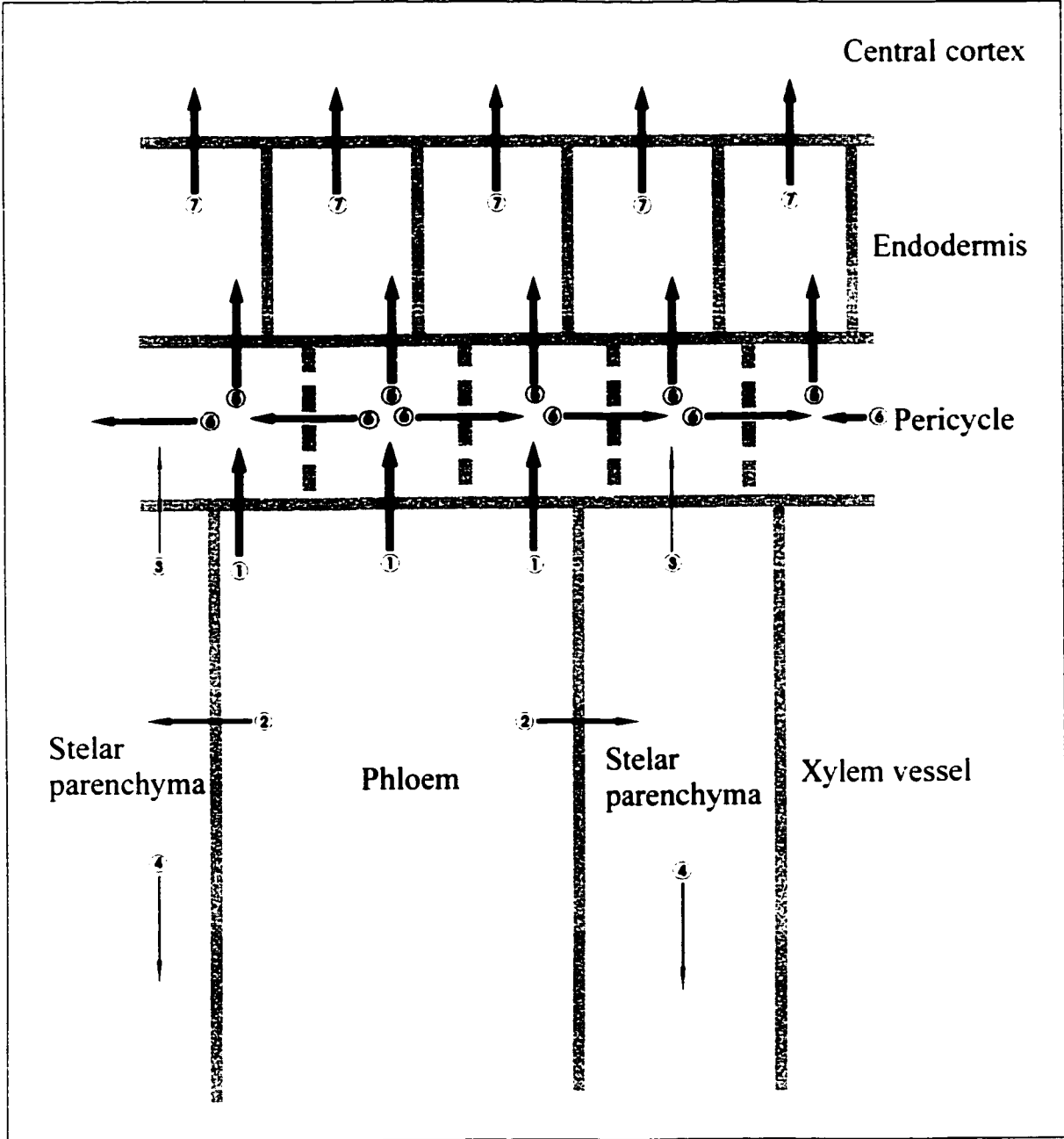


**Fig. 3.6** Pericycle as “annular disperser” for photosynthates

Adapted from Vakhmistrov et al. (1972). The radial walls of pericycle cells are drawn with broken lines to indicate the high frequency of plasmodesmata. Possible routes are labeled with numbers and intensities of symplastic phloem-unloading and/or post-phloem transport are represented with arrows of different sizes. See text for a discussion of various flows.



## Chapter 4

# **Plasmodesmata in symplastic transport in onion roots: an ultrastructural ion localization study**

### **4.1 Abstract**

This study was designed to test the functionality of plasmodesmata for ion transport in onion (*Allium cepa* L.) roots. Plants were grown either in moist vermiculite, pure water, or 1 mM CaSO<sub>4</sub>. In the latter two culture systems, roots were transferred to 5 mM NaCl for 2, 5, and 60 (or 120) min prior to sampling. Segments were collected at various distances from the root tip and fixed in a buffered mixture of OsO<sub>4</sub>, silver acetate, and picric acid. Specimens were then processed for embedding in Spurr's resin. Ultrathin sections were examined without post-staining. In roots grown in vermiculite, AgCl precipitates were formed in all parenchyma cells and mature xylem vessels, with varying densities. Plasmodesmata were also sites of AgCl precipitate formation. When roots grown in pure water or CaSO<sub>4</sub> were subjected to a short-term (2 or 5 min) treatment in NaCl, precipitates were observed essentially in the outer tissue layers of the root. Precipitates were detected in the plasmodesmata that linked these layers; this is evidence for the symplastic transport of chloride. Across the interface of the epidermis and exodermal short cells, transmembrane transport also occurred. In Cl<sup>-</sup>-depleted roots (*i.e.*, grown in pure water, as a control), the phloem was able to deliver ions from the shoot to the root tissues by way of the symplast; this process could be enhanced by calcium. Stellar parenchyma might play a role during the outward transfer of ions.



**Keywords:** ion precipitation; onion (*Allium cepa* L.); phloem; plasmodesmata; symplastic transport; stelar parenchyma

## 4.2 Introduction

It is well known that plasmodesmata are intercellular links that serve in symplastic transport, and that the lack of plasmodesmata is an indication of symplastic isolation. On the other hand, the presence of plasmodesmata is not always indicative of functional symplastic communication. This is not surprising as plasmodesmata are regulated in concert with the physiological status of the plant. For example, in the shoot apex of *Betula pubescens* Ehrh. at low temperatures, callöse was deposited at the neck regions of plasmodesmata, leading to symplastic isolation, and this was believed necessary for induction of dormancy (Rinne and van der Schoot 1998). During early morphogenesis in *Solanum nigrum* and *Molinia caerulea*, plasmodesmata at certain locations were plugged by an osmiophilic material, and this was postulated to contribute to the establishment of symplastic domains (Ehlers et al. 1999). In *Arabidopsis thaliana* L. roots, the epidermal cells were symplastically uncoupled at late stages of root development (Duckett et al. 1994). In zones behind the phloem unloading region (approx. 1 mm from the root tip, Duckett et al. 1994) of *Arabidopsis* roots, plasmodesmata at the root phloem-pericycle interface are physiologically closed (Wright and Oparka 1997). In onion, roots exhibit a considerable structural heterogeneity and their component tissues are linked together with varying plasmodesmatal frequencies (Chapters 2 and 3). The present study is intended to test the functionality of plasmodesmata in symplastic transport of ions.

Choosing a proper technique to fulfill the purpose can be a challenge. Among the methods available, fluorescence techniques have been the most popular in unraveling symplastic relationships, but they have several limitations. Cells deep within tissues cannot be visualized. The dyes are unable to visualize individual plasmodesmata. All tracer dyes are much larger than nutrient ions and none is physiologically required by plants. Therefore, ultrastructural ion localization techniques would be preferred. In principle, an

ion in a cellular structure can be precipitated in place with a heavy metal ion during fixation, and the precipitate is visualized in the electron microscope. Among the ions tested,  $\text{Cl}^-$  (to be precipitated by  $\text{Ag}^+$ ) has been the most extensively investigated (see van Steveninck and van Steveninck 1978). As for all localization methods, specificity and relocation have been of the utmost concern. The Ag-Cl precipitation technique has been improved to alleviate these disadvantages for chemical fixation, and its validity has been confirmed by a number of approaches (van Steveninck and van Steveninck 1978). Stelzer et al. (1978) further refined the procedure by including picric acid to enhance tissue preservation. In the present study, additional adjustments were made to the procedure to deal with the low permeability of the epidermis, exodermis, and endodermis of onion roots (see Chapter 2). Chlorine is an essential nutrient element for plants and its transport essentially follows a symplastic pathway (Läuchli et al. 1971a, b; Läuchli 1972; Tyree et al. 1974, Stelzer et al. 1975). Therefore, by incubating the root system in a dilute NaCl solution, this technique could be used to test the function of plasmodesmata. Another procedure (precipitation of  $\text{Tl}^+$  by  $\text{I}^-$ , van Iren and van der Spiegel 1975) was also tried, but was unsuccessful, and the results are not presented.

## **4.3 Materials and methods**

### **4.3.1 Growth conditions and treatments**

Bulbs of onion (*Allium cepa* L. cv. Ebenezer) were grown in different media and several experiments were performed on the roots.

(1) Onions were grown in moist vermiculite under greenhouse conditions as described previously (Chapter 2) for the entire period of the experiment.

(2) As in (1), but at 14 days after planting, the root system was gently removed from the medium and briefly rinsed in pure water (prepared in an UHQ II system, Elga Ltd., Bucks, England). This was followed by immersion in 5 mM NaCl for 10 and 120 min (under continuous aeration) prior to further processing. Additional illumination during the

daytime was provided by two, 100-W, white bulbs about 100 mm above the leaves. (The same aeration and lighting conditions were provided for all hydroponic cultures below).

These two experiments were designed to check whether or not  $\text{Cl}^-$  could be detected in roots grown in vermiculite, and if any differences in  $\text{Cl}^-$  distribution occurred between treatments for different periods of time.

(3) Onions were grown in pure water at room temperature. The water was replaced every other day, during a 2-week period.

(4) As in (3), but, after 14 days, onions were transferred to 5 mM NaCl for 2, 5, and 120 min.

Experiment 3 was included to deplete the chloride from root tissues and experiment 4 was intended to show if inward movement could be detected over time.

(5) Onions were grown the same way as in (3), except that 1 mM  $\text{CaSO}_4$  was added.

(6) As in (5), but root systems were then treated in 5 mM NaCl for 2 and 5 min, respectively.

The last two experiments were designed to examine (a) if calcium could alleviate nutrient deficiency and (b) if inward ion movement can be detected by using short-time treatments.

### **4.3.2 Chloride precipitation for the TEM**

The procedure used to detect  $\text{Cl}^-$  in the TEM was modified from Stelzer et al. (1978) and Ma and Peterson (2000). Briefly, root segments from all treatments (above) were fixed for 20 h in a mixture containing 0.5%  $\text{OsO}_4$ , 0.5% silver acetate, 0.1% picric acid, and 25 mM cacodylate acetate buffer (pH 7.2). Dehydration was achieved in acetone. To the 30% and

40% steps, 0.1 M nitric acid was added (to remove nonspecific precipitates). Tissues were infiltrated and embedded in Spurr's resin (Spurr 1969) through an extended protocol (Chapter 2). Sections were cut at 80 nm with glass knives on a Reichert-Young Ultracut E microtome (Wien) and observed in a Philips CM 10 microscope.

## **4.4 Results**

The results will be presented in order of the experiments. Unless otherwise specified, observations on AgCl precipitation were made on tissues 100 mm from the root tip.

### **4.4.1 Plants grown in vermiculite (experiment 1)**

At the time of sampling, the roots were about 200 mm long and 1.2 mm thick. No laterals or hairs had developed. At 40 mm from the tip, both endodermal cells and exodermal long cells had developed Casparian bands but not suberin lamellae. At 100 mm from the tip, all exodermal long cells and very few endodermal cells had developed suberin lamellae.

Cl<sup>-</sup> was detected in all tissues. In the extracellular wall layer (terminology of Peterson et al. 1978) of the epidermis, large silver-chloride precipitates were frequently observed (Fig. 4.1A). In the outer tangential walls of epidermal cells, tiny precipitates were frequently present. At 40 mm from the tip, some epidermal radial walls contained tiny precipitates. In other examples, crystals were absent from radial walls or were restricted to the outer portion of the radial walls. In all specimens, there were precipitates along the outer tangential plasma membrane (Fig. 4.1A, B). Very few small crystals were found in the cytoplasm. In the central vacuole, precipitates were usually on the inner side of the tonoplast, rarely seen dispersed in the central vacuole (Fig. 4.1A, B). Nuclei usually had very few or no crystals. At the epidermis-short cell interface, precipitates were visible in both the plasmodesmata (Fig. 4.1B) and in the walls (Fig. 4.1C).

**Fig. 4.1** AgCl precipitation in onion roots grown in vermiculite

Sections 100 mm from the root tip. **A** Outer tangential and radial walls of epidermal cells. Precipitates in the extracellular wall layer (small arrowheads), along the plasma membrane (arrows) and the tonoplast (large arrowheads). **B** Tiny precipitates along the plasma membrane (arrows) and in the vacuole (asterisk).  $\text{Cl}^-$  is also in the plasmodesmata (arrowhead) between the epidermal cell (*EP*) and the exodermal short cell (*SC*). **C** Precipitates (arrowheads) in the wall between epidermal cell and short cell. Large precipitates in epidermal cell. **D** Precipitates in plasmodesmata between central cortical cells. **E** Precipitates in plasmodesmata between central cortical cell (*CC*) and endodermal cell (*EN*). Chloride is accumulated in the cytoplasm beside the plasmodesmata. **F** Precipitates in plasmodesmata in the radial walls of pericycle cells. **G** Precipitates in the protoxylem vessel (*PX*). A few precipitates in the stellar parenchyma cell (*SP*). Immature early metaxylem vessel (*IEMX*) does not contain precipitates. Bars: 0.5  $\mu\text{m}$



At 40 mm from the root tip, the exodermis and epidermis had similar patterns of precipitate distribution. At 100 mm from the tip, the exodermal short cells always contained chloride. Crystals were also found in the plasmodesmata at the short cell-central cortex interface. The long cells were free of precipitates.

In tissues internal to the exodermis, no significant differences in precipitate distribution were found between 40 mm and 100 mm from the tip. Crystals were observed along the membranes (plasma membrane and tonoplast), in plasmodesmata, and cytoplasm. In the central cortex, accumulation of crystals was frequently found in the cytoplasm and/or on the plasma membrane (at the outer tangential side of the cells) beside the plasmodesmata (Fig. 4.1 D, E). Intercellular spaces sometimes contained large precipitates. There were very few crystals in the endodermis, pericycle, stelar parenchyma, and phloem.  $\text{Cl}^-$  was detected in the plasmodesmata in the radial walls of pericycle cells (Fig. 4.1F). In mature xylem vessels crystals were scattered all over the lumina, but were rarely seen in immature xylem vessels (Fig. 4.1G)

#### **4.4.2 Plants in vermiculite with an additional incubation in NaCl (experiment 2)**

Incubation in NaCl for 10 min did not change the overall precipitation pattern. But this treatment remarkably increased the density of precipitates in all tissues, particularly obvious in the epidermis (Fig. 4.2A, B) and central cortex. After a long-term treatment (120 min), precipitation was not further increased over the short-time treatment.

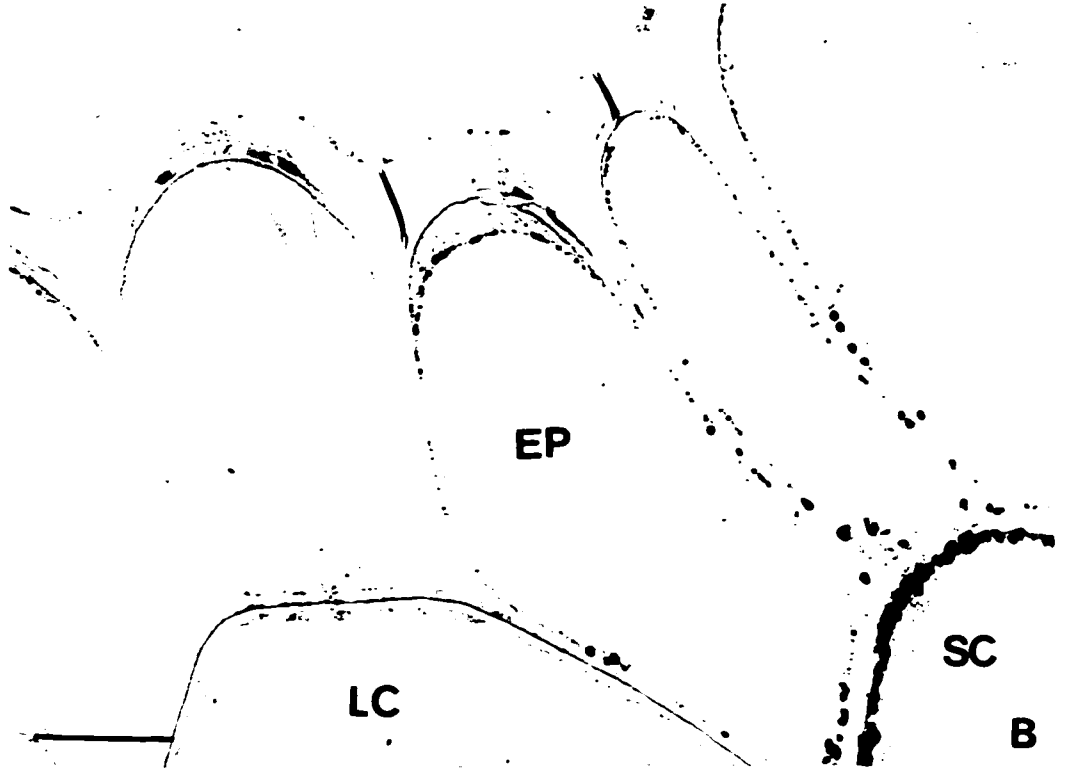
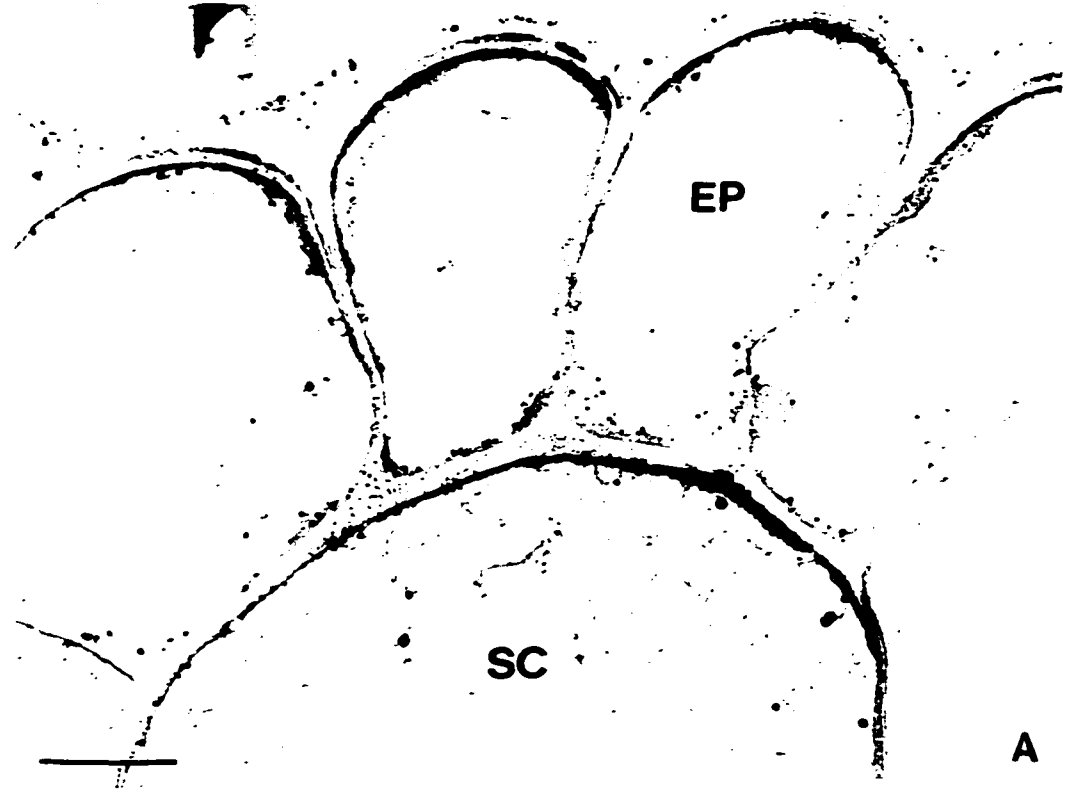
#### **4.4.3 In pure water (experiment 3)**

The roots were only about 50 mm long after 14 days in culture. But their diameters were larger than those of vermiculite-grown roots (1.5 mm vs. 1.2 mm). Short laterals (up to 1.0 mm) appeared close to the tip. Both endodermis and exodermis matured at about 10 mm from the root tip. Observations were carried out on tissues 40 mm from the root tip.

**Fig. 4.2 Chloride in roots grown in vermiculite and later treated in NaCl**

Epidermis and exodermis. **A** 5 mM NaCl, 10 min. Section 40 mm from the root tip. Precipitation of AgCl in epidermal radial walls, in the wall between epidermis (*EP*) and short cell (*SC*), and in vacuoles. **B** NaCl, 2 h. Section 100 mm from the root tip. Precipitates along the plasma membranes and tonoplasts of epidermal cells (*EP*). Heavy precipitation in short cell (*SC*). The long cell (*LC*) is free of chloride. Bars: 5  $\mu$ m





(Structurally, this zone is equivalent to zones over 100 mm from the root tip grown in experiment 1). Little precipitation was observed in the root tissues in general. If any, the precipitates were essentially formed along the plasma membrane of parenchyma cells. A few precipitates were sometimes found in plasmodesmata.

#### **4.4.4 Cultured in pure water, and later treated with NaCl (experiment 4)**

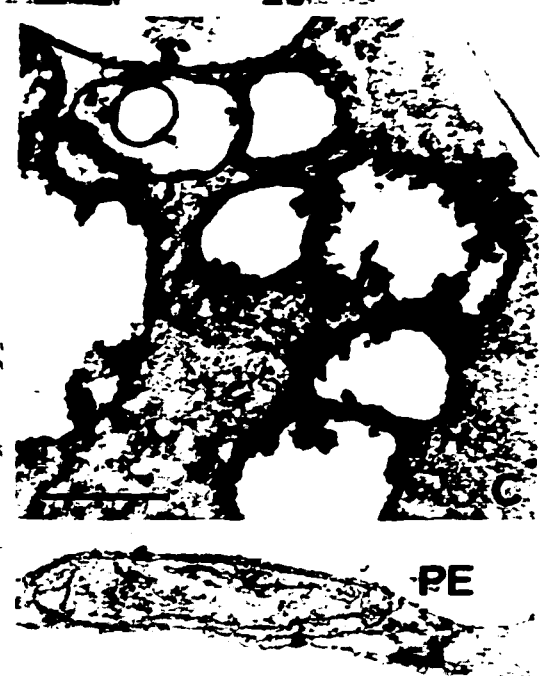
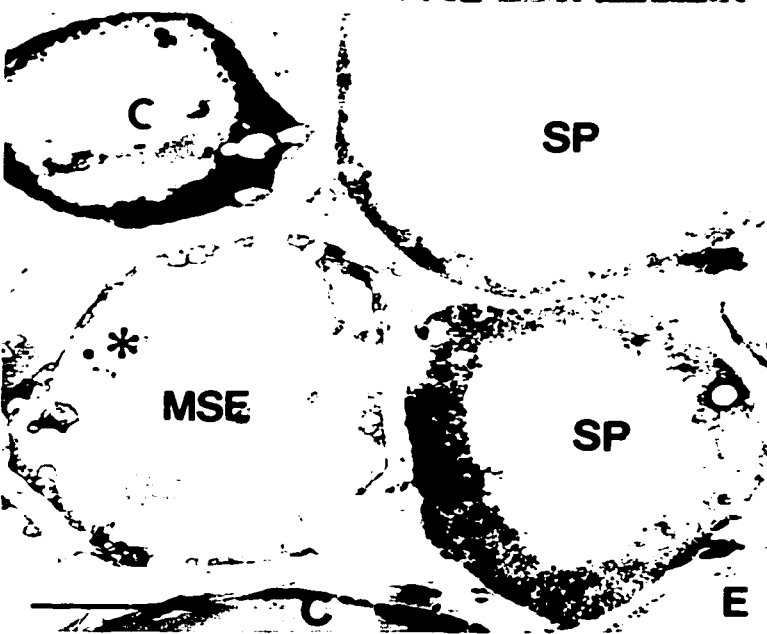
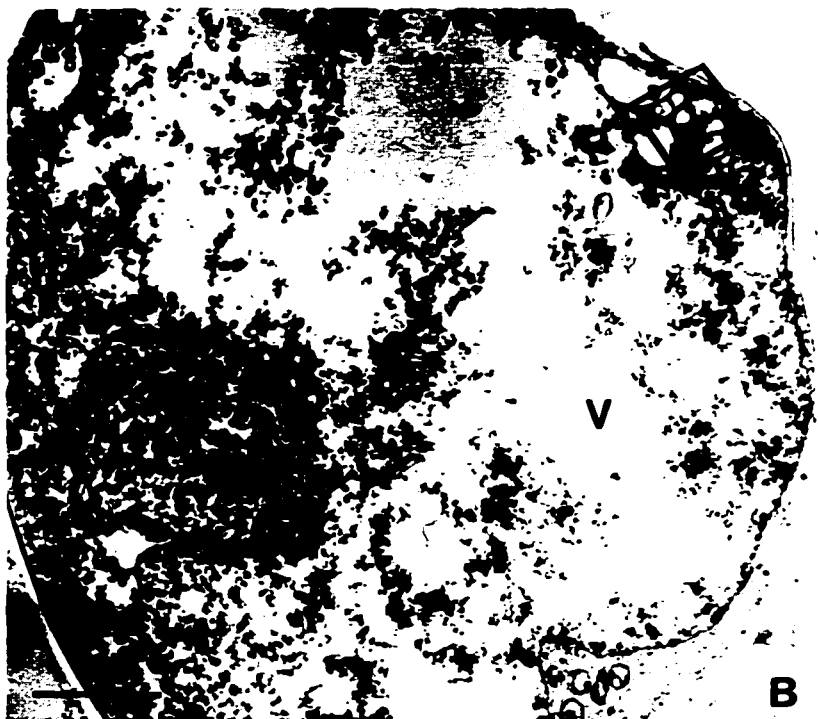
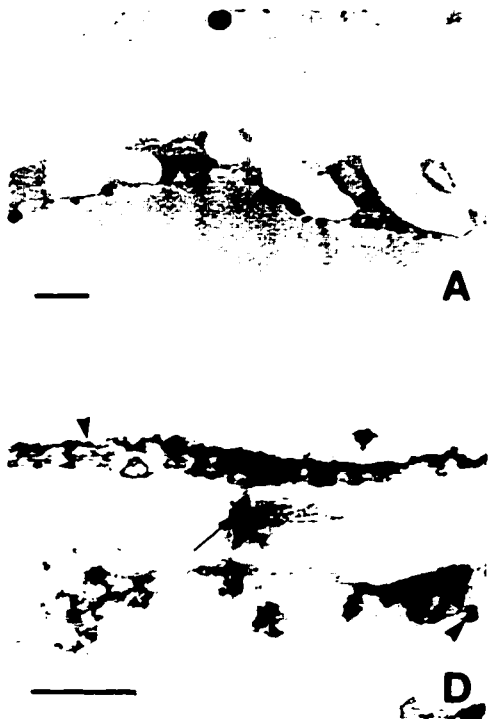
It is interesting to note that, in some roots, epidermal cells developed wall ingrowths associated with their outer tangential walls, thus becoming transfer cells. Precipitates were formed along the tonoplasts of such cells (Fig. 4.3A). Some short cells contained matrix substances and  $\text{Cl}^-$  accumulated in the vacuoles (Fig. 4.3B). Vesicles that contained  $\text{Cl}^-$  were observed in the cytoplasm (Fig. 4.3 B, C). Very few precipitates were found in the outer central cortex (Fig. 4.3D). Stellar parenchyma cells that were in contact with both companion cells and pericycle cells were densely cytoplasmic (Fig. 4.3E). Some precipitation was observed in these parenchyma and companion cells. In the 5-min treatment, the outer half of the cortex exhibited some precipitation. In tissues of both 2 and 5 min treatments, the inner cortex, endodermis, pericycle, companion cells, and stellar parenchyma cells had a few precipitates, a result similar to those of experiment 3. Some precipitation was also observed in sieve elements (Fig. 4.3E). Precipitates were also detected in the plasmodesmata between sieve elements and companion cells, and between stellar parenchyma and pericycle cells (Fig. 4.3F, G). In longer treatments, all tissues contained chloride, a situation comparable to that of the experiment 1.

#### **4.4.5 In $\text{CaSO}_4$ solution (experiment 5)**

The roots grew normally and attained the same length as those in the vermiculite culture (experiment 1), but their diameters were smaller (0.7 mm vs. 1.2 mm). No laterals or hairs developed. All tissues had  $\text{AgCl}$  precipitates. More precipitates were observed than in roots grown in pure water (experiment 3). For example, precipitates in the

**Fig. 4.3 Chloride in roots grown in pure water and later treated in NaCl**

**A** In pure water, NaCl 1h, 100 mm from the root tip. Epidermal transfer cell. AgCl precipitates along the tonoplast. **B** In pure water, NaCl 2 min, 40 mm from the root tip. Short cell. Matrix substances in the vacuole. Chloride is detected in the vacuole. **C** Enlarged from the box in **B**. Vesicles in the cytoplasm that contain AgCl. **D** Same condition as in **B**. Precipitates in the plasmodesma (arrow) between central cortical cells of the first and second layers. A few precipitates along the tonoplasts (arrowheads). **E** In pure water, then NaCl 5 min, 40 mm from the root tip. Precipitates in stelar parenchyma cells (*SP*), companion cells (*C*), and metaphloem sieve element (*MSE*, precipitates indicated by an asterisk). Companion cells and stelar parenchyma cells contain dense cytoplasms. **F** NaCl 1 h, 40 mm from the root tip. Precipitates in plasmodesma between sieve element (*SE*) and companion cell (*C*). **G** Same conditions as in **E**. Precipitates in the stelar parenchyma cell (*SP*) and in the plasmodesma between stelar parenchyma cell and pericycle cell (*PE*). Bars: 5  $\mu\text{m}$  (**B** and **E**) and 0.5  $\mu\text{m}$  (the rest)



plasmodesmata between the companion cell and stelar parenchyma cell, and between the sieve element and companion cell are shown in Fig. 4.4A, B.

#### **4.4.6 Grown in $\text{CaSO}_4$ solution, and later incubated in NaCl solution (experiment 6)**

In the 2-min treatment, short cells accumulated a large amount of chloride in their cytoplasm and vacuoles (Fig. 4.4C, D). The vacuoles contained dense matrix substances. Numerous tiny precipitates were formed in the outer tangential walls of short cells (Fig. 4.4C). In the long-term treatment (60 min), there was a general increase in the density of precipitation in all tissues.

### **4.5 Discussion**

In the present study, the movement pathway(s) of  $\text{Cl}^-$  was thoroughly examined. The Ag-Cl precipitation procedure has been applied to barley roots and precipitation was observed in a few cell interfaces (Stelzer et al. 1975). Now in onion roots, this technique was used to study chloride transport in all tissues under different conditions.

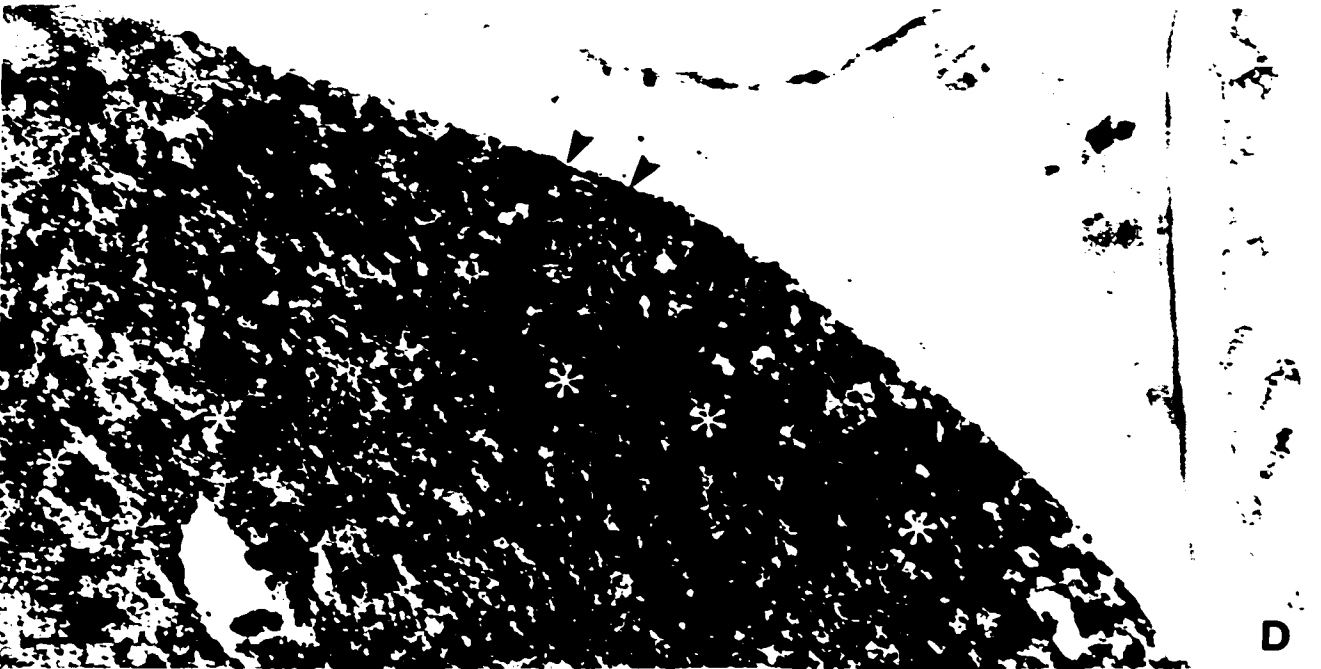
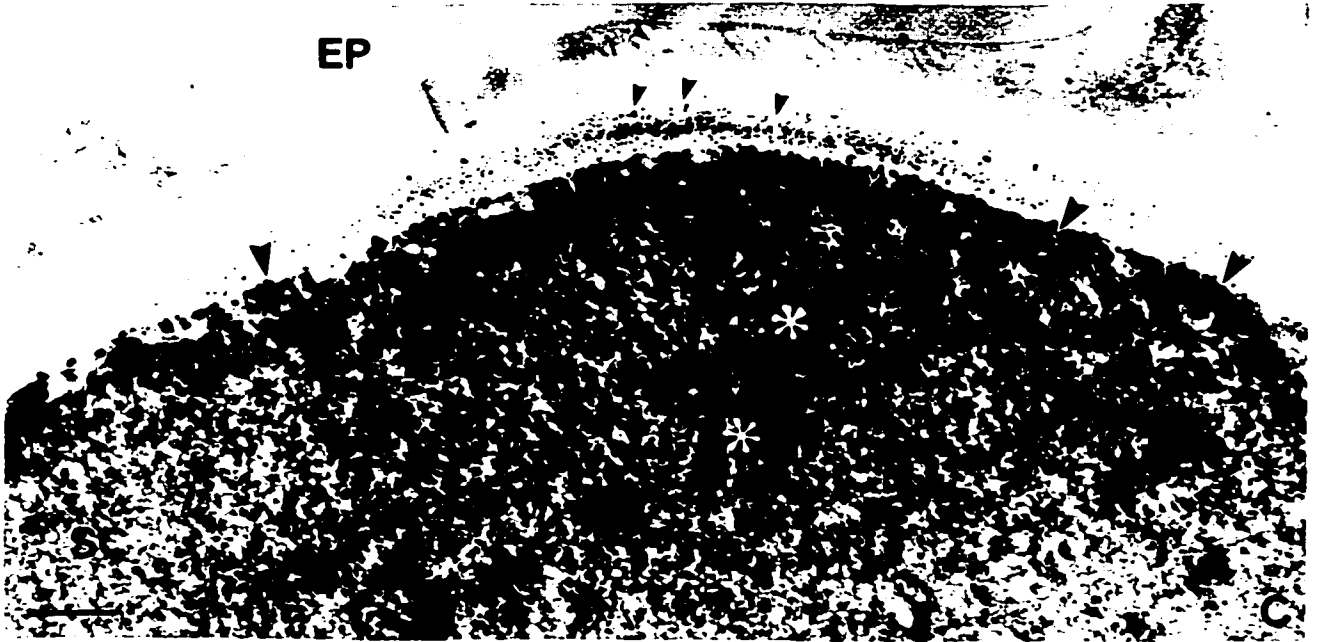
#### **4.5.1 The plasmodesmata are functional in the radial transfer of ions toward the stele**

The results provided direct evidence for plasmodesmatal functioning in transferring chloride ions. It was also shown that the symplast is the dominant route for chloride transport, as all plasmodesmata along the radial direction exhibited AgCl precipitation (see Fig. 4.1D, E), while in cell walls (except those of the epidermis and exodermis) very little precipitation was observed. This conclusion is in agreement with that for maize (Läuchli et al. 1971a, b).

When vermiculite-grown roots were allowed to absorb  $\text{Cl}^-$  for 10 min, the ions seemed to have traversed all the root tissues and joined the transpiration stream, since prolonged

**Fig. 4.4** Roots grown in pure water or  $\text{CaSO}_4$  solution and later treated in NaCl

**A** Grown in pure water, then NaCl 5 min, 40 mm from the root tip. Precipitates in the plasmodesmata between companion cell (*C*) and stelar parenchyma (*SP*). **B** Grown in pure water, then NaCl 1 h, 40 mm from the root tip. Precipitates in the plasmodesmata between sieve element (*SE*) and companion cell (*C*). **C** and **D** Grown in 1 mM  $\text{CaSO}_4$ , then NaCl 2 min, 100 mm from the root tip. Large precipitates in the cytoplasm of the short cell (large arrowheads). Some AgCl in the vacuole (white asterisks) which contained dense matrix substances. In **C**, numerous tiny precipitates (small arrowheads) in the wall between epidermal cells (*EP*) and short cell (*SC*). Bars: 0.5  $\mu\text{m}$



incubation did not further increase precipitation (experiment 2). This result is in accordance with the previous conclusion that symplastic transport (10 mm/h) is faster than diffusion (Epstein 1971). Among all experiments, the optimum growth conditions were provided by vermiculite culture. Although the  $\text{Cl}^-$  content of vermiculite was not measured, it did supply a sufficient amount of chloride to the roots, as the plants grew normally (experiment 1).

The vacuoles are spatially related to the symplast. In experiments with prolonged  $\text{Cl}^-$  supply (*i.e.*, in vermiculite and in long-term treatment with NaCl), vacuoles always had AgCl precipitates (Fig. 4.1A), while in  $\text{Cl}^-$ -depleted roots (*i.e.*, in pure water, experiment 3), vacuoles had no or very few precipitates. It was inferred from these results that vacuoles are an exchangeable pool of ions, *i.e.*, ions are being accumulated (from the cytoplasm) and released (to the cytoplasm) under high and low external concentrations, respectively. Thus, this observation confirmed the earlier postulations based on incubation experiments (Hodges and Vaadia 1964, Anderson et al. 1974) and disproved others (*e.g.*, by Lüttge and Laties 1966). It is also interesting to note that the dense matrix substances in the vacuoles of short cells (Figs. 4.3B, C and 4.4C, D) might be an adaptation to enhance accumulation of ions during nutrient deficiency.

The transport of  $\text{Cl}^-$  from the epidermal cells to the exodermal short cells is especially interesting. It is known that in old zones, the symplastic connection of the epidermis to the central cortex is provided by short cells (Chapter 2). Now, it has been proved that the plasmodesmata in this interface are functional (Fig. 4.1B). But, the available plasmodesmata are apparently not sufficient to meet the plant's nutritional requirements and thus an additional transmembrane pathway was predicted (Chapter 3). In the present study, chloride ions were also observed in the outer tangential walls of short cells (Figs. 4.2A and 4.4C, D). These observations indicated that ions are transported in both the symplastic and apoplastic pathways across the epidermis-short cells interface.



## 4.5.2 The function of the pericycle and stelar parenchyma

The pericycle could play a role in loading the xylem vessels. Initially, this idea was based on the fact that the plasmodesmatal frequency on the inner tangential walls (in contact with the stelar parenchyma cells) is much lower than on the outer tangential walls (in contact with the endodermis) in barley (Vakhmistrov et al. 1972). This was also found to be the case in onion roots (Chapter 3). In the ion precipitation experiments,  $\text{Cl}^-$  was detected in both tissues. This result indicates that both could load the xylem, but does not imply that they contribute equally. In other studies, it was found that stelar parenchyma cells were able to accumulate ions, which was taken as strong evidence for their active role in xylem-loading (Läuchli et al. 1971a, b). It should be pointed out that a strict distinction between the pericycle and stelar parenchyma was not made in almost all previous studies, *e.g.*, the one by Läuchli et al. (1974a) and, frequently, both tissues were collectively termed “xylem parenchyma” (see also § 3.5.1).

Under the nutrient-depletion condition (*i.e.*, culture in pure water), there was a higher  $\text{Cl}^-$  concentration in the stelar parenchyma (Fig. 4.3E) than in the pericycle (and in all tissues to the outside). It is interesting to note that the stelar parenchyma cells have a much denser cytoplasm than those in vermiculite-grown plants (see Fig. 4.3E and Fig. 3.3E). It is likely that ions are being transferred from the phloem to the stelar parenchyma under this growth condition. The ions could be reallocated from the shoot along the phloem as  $\text{Cl}^-$  is phloem-mobile (Ziegler and Lüttge 1967, Ziegler 1975). Once they reach the central cortex, the ions could be transported outward in the symplast (*cf.* Chapter 3). The alleviation of nutrient deficiency by the  $\text{Ca}^{+2}$  was at least partly due to its activity in accelerating nutrient reallocation (experiment 5). When roots from the pure-water culture were treated with NaCl for a short time (2 or 5 min, experiment 4), a precipitation-free zone, albeit faint, was observed in the central cortex, indicating the existence of the bi-directional movement of  $\text{Cl}^-$  (*i.e.*, both inward and outward) in this particular situation.

### 4.5.3 Function of the various vessel members

Observations from the present study suggest that the protoxylem vessels play a significant role in contributing ions to the transpiration stream. There were always some precipitates in these cells (Fig. 4.1G). This phenomenon was previously documented in barley roots (Clarkson and Sanderson 1974). In zones where both proto- and meta-xylem vessels are mature, ions could move from the former to the latter. In the pits between vessels, there were always some AgCl precipitates (not shown). It is commonly held that the bulk of the upward flow of xylem sap occurs in the metaxylem vessels, and little attention had been paid to the protoxylem vessels in the literature (see Robards and Jackson 1976). These latter cells might be particularly important in the root tip where metaxylem vessels have not yet fully differentiated. The ions in protoxylem vessels are apparently transferred in from the adjacent pericycle and/or stelar parenchyma cells.

What do the immature vessel members do? There is some evidence that they are capable of accumulating ions which will later (*i.e.*, at maturity of the vessel members) be released to supply the transpiration stream (*e.g.*,  $K^+$ , McCully 1994). In the present study, chloride ions were rarely seen in these cells, in sharp contrast to their relatively heavy precipitation in mature vessel members (Fig. 4.1G). As had been pointed out earlier, reallocation of ions had possibly occurred during the processing for TEM (see § 4.2). Yet, it is unlikely that ions, if any, were removed from the immature vessels, but retained in the mature ones. Therefore, ion accumulation in immature vessels, if any, is probably both ion-species- and plant-species-specific.

## Chapter 5

# **Development and ultrastructure of cell wall modifications in the endodermis and exodermis of onion roots**

### **5.1 Abstract**

The cytological events of wall modification in the endodermis and exodermis of onion roots were examined with the transmission electron microscope. In the endodermis, Casparian bands, suberin lamellae and tertiary walls developed in succession. During band initiation, the establishment of plasma membrane-wall binding was ahead of the deposition of hydrophobic components into the wall. A few dictyosomes were in the periphery of the developing bands. At the Casparian band, the bound plasma membrane was separated from the band at the frontier of the extending lamellae and continuous suberin lamellae were laid down over the band. More dictyosomes and ER profiles appeared during suberin lamellae and tertiary wall formation. Both suberin lamellae and tertiary walls commenced along tangential walls. Along each, wall formation was first observed in the primary pit fields, but none of the wall modifications interrupted the symplastic connections of the endodermis. In the exodermis, suberin lamellae were formed in long cells and all their plasmodesmata were severed. Suberin lamellae first appeared on the outer tangential walls and then on the inner tangential walls. Dictyosomes and ER were prominent during the wall formation, indicating that these membrane systems may be involved in suberin lamella development. Casparian bands were not positively detected, and tertiary walls did not develop.

## 5.2 Introduction

Major wall modifications take place in certain cell layers of the root during morphogenesis. Virtually all plants develop Casparian bands in their endodermis and may also form suberin lamellae (Clarkson and Robards 1975). Many plants also have a hypodermis that is characterized by the formation of suberin lamellae (Kroemer 1903). Now it is known that a Casparian band is frequently formed in the hypodermis, which is then termed an "exodermis" (Perumalla et al. 1990, Peterson and Perumalla 1990). These wall modifications consist principally of depositions of suberin and lignin (Schreiber et al. 1999). The endodermal Casparian band, sitting in the central part of the anticlinal walls, is homogeneously dense as observed in the transmission electron microscope (TEM). But the exodermal Casparian band has not been identified from its electron density. In both cell layers, the suberin lamellae exhibit alternating electron-dense and -lucent components. This has been interpreted as due to the presence of polar and nonpolar suberins, respectively (Schmidt and Schönherr 1982). Recent analysis of isolated Casparian bands and suberin lamellae from several species has established that both wall modifications are chemically complicated, consisting of suberin, lignin, proteins and carbohydrates (Schreiber et al. 1999). In the exodermis of *Monstera deliciosa*, waxes have also been detected (Schreiber et al. 1999).

Casparian bands and suberin lamellae are apoplastic barriers for ions due to the presence of hydrophobic substances, especially suberins (see Peterson and Cholewa 1998, Schreiber et al. 1999). The two sets of bands and lamellae, situated near the periphery of the root and of the stele, respectively, thus could be viewed as the initial and final filtration systems. Yet, the relationship of suberin lamellae to symplastic transport (*i.e.*, through plasmodesmata) is more complicated. In the leaf bundle sheath of grass leaves (O'Brien and Carr 1970, O'Brien and Kuo 1975) and root endodermis (Clarkson and Robards 1975), suberin is absent from the sites of plasmodesmata, thus the symplastic continuity of these cell layers remains intact. The same is true for the exodermis of maize (Clarkson et al. 1987, Wang et al. 1995), a species with a uniform exodermis (*i.e.*, all cells elongate, like

those in an endodermis - von Guttenberg 1968). However, in the dimorphic exodermis (with long and short cells) of citrus (Walker et al. 1984) and onion (Chapter 2), the suberin lamellae were deposited in the long cells and all their plasmodesmata were severed by these wall materials. Thus, the exodermis is symplastically linked to its neighbor tissues only through the short cells.

Casparian bands and suberin lamellae, however, are poorly understood in their structural development. Around the 1970's, some TEM work was carried out on the root endodermis, but was concerned primarily with its structure at maturity, rather than development. To date, the study on the endodermis of *Ranunculus acris* L. by Scott and Peterson (1979) remains the most detailed set of observations that focused on both structure and ontogenesis. There are several uncertainties about the endodermis and exodermis. (1) For the Casparian band, how is the tight plasma membrane-wall binding related to the initial suberin deposition? A recent study on maize exodermis using light and fluorescence microscopy showed that the plasma membrane-wall binding is established prior to the detectable deposition of suberin (Enstone and Peterson 1997). Ultrastructural information is lacking. (2) How are organelles (especially the ER and dictyosomes) involved in the formation of the bands and lamellae? In the endodermis of *Ranunculus*, ER and dictyosomes were frequently observed (Scott and Peterson 1979). It remains to be seen if same phenomena occur in other species. For the exodermis, no information is available for any species. (3) How is the suberin lamella formation related to other structures, including the Casparian band (and the associated plasma membrane) and plasmodesmata? The present study has focused on the ultrastructure of the onion root endodermis and exodermis to stress these issues. Throughout the chapter, "suberin" is used in a loose sense, meaning hydrophobic components of Casparian bands and suberin lamellae, since cytochemical techniques for suberin have not been devised at the ultrastructural level.

## **5.3 Materials and methods**

Bulbs of onions (*Allium cepa* L. cv. Ebenezer) were cultured in moist vermiculite (see Chapter 2). Roots were harvested 7 to 14 days after planting. To visualize the Casparian bands and suberin lamellae in cell walls using the fluorescence microscope, free-hand cross-sections at various distances from the root tip were examined directly under UV light in a Carl Zeiss Axiophot microscope (equipped with an Osram HBO 100W mercury lamp and epifluorescence optics). The filter set consisted of exciter filter G365, chromatic beam splitter FT395 and barrier filter LP420. Both wall modifications exhibited a bluish white autofluorescence. More specific methods were also employed to detect the bands (Brundrett et al 1988) and the lamellae (Brundrett et al 1991). For TEM, root segments 1 mm long were excised 50, 100, and 200 mm from the root tip. These regions were referred to as young, old and very old, respectively. The developmental stages of tissues in each zone were examined as in Chapter 2. All samples were processed following the procedure outlined previously (Chapter 2).

## **5.4 Results**

### **5.4.1 Casparian bands in the endodermis**

The pro-endodermis was characterized by unmodified, primary radial walls (Fig. 5.1A). The earliest visible sign of Casparian band development was the establishment of the close association of a small region of the plasma membrane to the radial wall (Fig. 5.1B). This happened along the central portion of the radial walls. The bound membrane was straight, while the membrane along the rest of the wall was slightly wavy. At this stage, no detectable alteration (increase) in the wall's electron density had taken place (Fig. 5.1B, C). These processes were usually simultaneous on both sides of the radial walls. Concomitant with, or immediately following, the inward and outward extension of the tight membrane-wall connection area, electron-dense material was incrustated into the wall, thus forming the Casparian band (Fig. 5.1D-F). The bound plasma membrane exhibited

**Fig. 5.1** Casparian band formation in the endodermis of onion roots

**A** Radial walls of proendodermal cells. The plasma membrane is not tightly associated to the wall. **B** A small area of the plasma membrane (marked between arrowheads) has become tightly associated with the radial wall. No electron dense wall material is detected along the binding region. **C** The binding area (arrowheads) has extended. **D** The wall of the binding region is slightly electron denser (arrowheads) than the non-binding region of the radial walls. **E** Well-established Casparian band occupying the middle half of the radial wall. The plasma membrane is tightly associated to the wall and the band contains electron dense material. **F** Dictyosomes (*DI*) are in the cytoplasm beside the band (asterisk). **G** Band plasmolysis of endodermal cells, caused by processing for TEM. The band is marked between arrowheads. **H** Normal plasmolysis in endodermal cells. The band is delimited by arrowheads. *ER* endoplasmic reticulum; *MI* mitochondrion; *PM* plasma membrane. Bars: 0.5  $\mu\text{m}$





more intense staining than the non-bound region. Both band plasmolysis (Fig. 5.1G) and normal plasmolysis (Fig. 5.1H) were observed, which resulted from sample processing for TEM. At the ultimate developmental stage, the bands rarely exceeded the middle half of the anticlinal walls.

At the initial stage of band formation, no ultrastructural changes were observed in the endodermal protoplasts (Fig. 5.1 A-D). During band extension, however, the ER profiles increased and a few dictyosomes were detected near the bands (Fig. 5.1E, F).

## **5.4.2 Suberin lamellae in the endodermis**

### **5.4.2.1 Along the tangential walls**

Suberin lamella formation started earlier along the outer tangential walls than along the inner tangential walls. And along each, the lamellae were initiated earlier at the primary pit fields (beside plasmodesmata, Fig. 5.2A, B) than elsewhere (Fig 5.2C, D). The early lamellae were fine, electron-dense wall material (Fig. 5.2A, D). Shortly after, suberin lamellae were found in both tangential walls (Fig 5.2E, F). The suberin lamellae were thicker in the primary pit fields than elsewhere (Fig. 5.2G). During suberin lamella deposition, dictyosomes and ER profiles were observed, and their population was larger than in previous stages (Fig. 5.2A-G). Sometimes, large invaginations of plasma membrane were observed, which were filled with vesicles.

### **5.4.2.2 Along the radial walls**

The suberin lamellae extended from the tangential walls toward the radial wall (Fig. 5.3A), until reaching edge of the Casparian band (Fig. 5.3B, C). Invaginations of plasma membrane were usually formed (Fig. 5.3B, C). Then, near the frontiers of the extending suberin lamellae, the bound plasma membrane was gradually separated from the band (Fig. 5.3 C, D) and a thin layer of wall material was finally laid down between the membrane and the band (Fig. 5.3E, F, G). During this process, there was an indication that vesicles of dictyosome- or ER-origin merged with the plasma membrane (Fig. 5.3D). In the space

**Fig. 5.2** Suberin lamella development along the outer and inner tangential walls of the endodermis

**A** Suberin lamellae (arrowheads) first appeared in the pit fields, as thin wall pieces beside plasmodesmata (*PD*). Dictyosomes (*DI*) and endoplasmic reticulum (*ER*) are observed in the vicinity of the new wall. **B** Further development of suberin lamellae (arrowheads) in the pit fields. Arrows point to the plasma membrane. Plasmodesmata are indicated by large arrowheads. **C** and **D** Inner and outer tangential walls of an endodermal cell. **C** Suberin lamellae have not initiated. Vesicles (arrowheads) are observed in the periplasmic space. Plasma membrane is marked by arrows. **D** Suberin lamellae appear as thin pieces (arrowheads) between the plasma membrane (arrows) and the primary wall (*PW*). **E** and **F** Inner and outer tangential walls of another endodermal cell. Early stage of suberin lamella development (arrowheads) along both walls, but more prominent along the outer tangential wall (**F**). Plasma membrane is marked by arrows, suberin lamellae by arrowheads. **G** Late stage of suberin lamella development. The lamellae in the pit fields (asterisks) are thicker than those elsewhere (arrowheads). Plasmodesmata (*PD*) remain intact. Bars: 0.5  $\mu\text{m}$

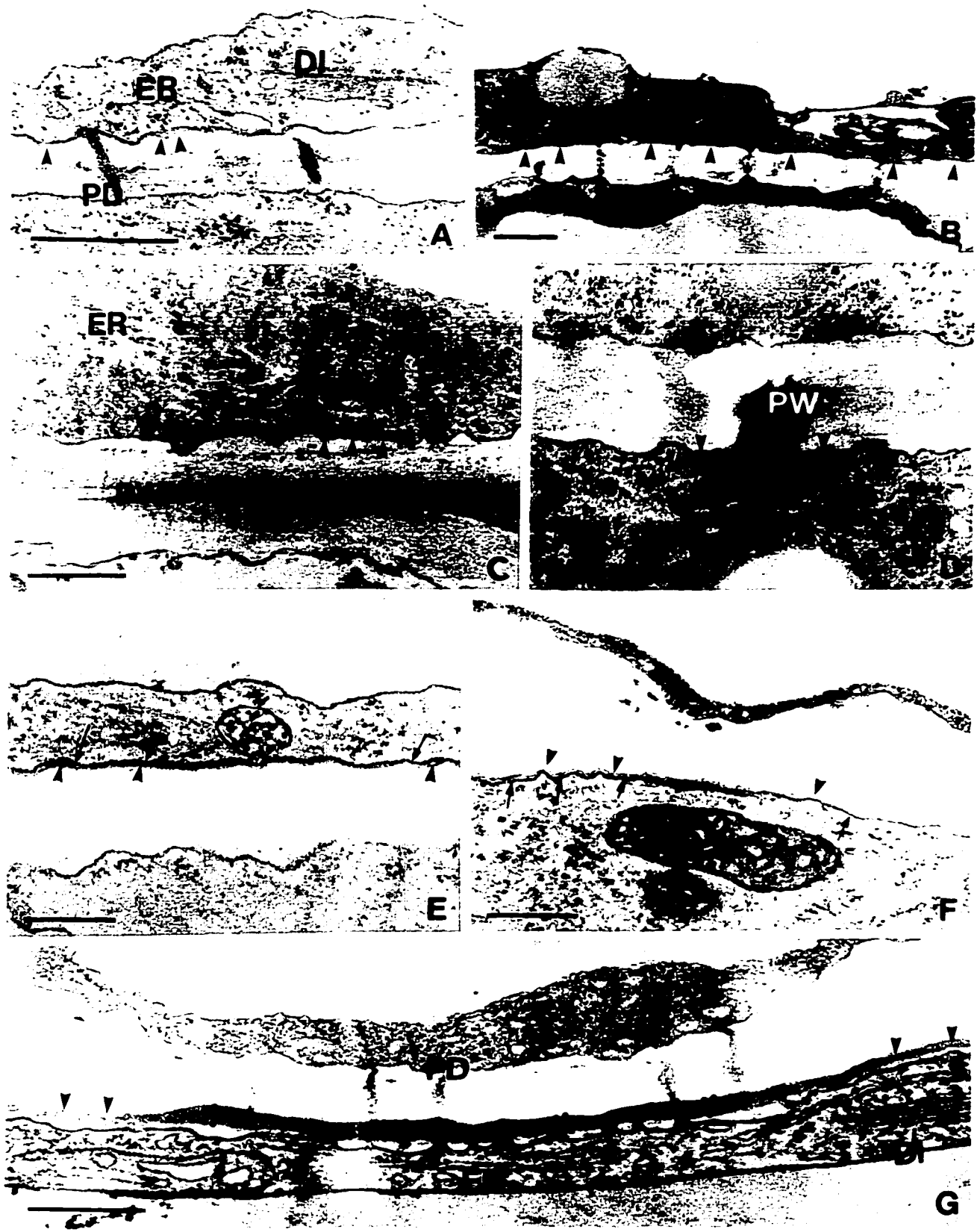


**Fig. 5.3** Suberin lamella formation over the Casparian band in the endodermis

**A** Radial wall and a portion of tangential walls of endodermis. Suberin lamellae (arrowheads) are formed along the tangential wall and progressing along the radial wall. The approximate edge of the extending suberin lamellae is pointed to by a large arrowhead. The margins of the band (asterisk) are marked by arrows. **B** Suberin lamellae reached the Casparian band (asterisk). The edges of the suberin lamellae are labeled by large arrowheads. Invagination (filled with vesicles) of plasma membrane is seen at the band's edge in the cell to the left. **C** Similar to **B**, but invaginations of plasma membrane are formed at both edges of the band. **D** At the band (asterisk), the plasma membrane (*PM*) is separated from the wall and suberin lamellae are laid down. This is obvious at the advancing edge (arrow) of the suberin lamellae. There is an accumulation of electron dense substances (marked between large arrowheads). **E** and **F** Details of suberin lamellae at the band. This portion of the lamellae is much thinner than those elsewhere. The plasma membrane is separated from the wall and numerous vesicles (*VE*) are in the periplasmic space. **G** Suberin lamellae (arrowheads) are complete around an endodermal cell. The band is marked by an asterisk. *DI* dictyosome; *ER* endoplasmic reticulum. Bars: 0.5  $\mu\text{m}$



between the plasma membrane and the suberin lamellae near the band, a large collection of vesicles was frequently found (Fig 5.3E). At both the inner and outer ends of the newly formed suberin lamellae (*i.e.*, over the band), accumulation of suberin material was frequently observed (Fig. 5.3 E, F). Subsequently, suberin lamellae were deposited continuously all around the endodermal cells, and the electron-dense and -lucent components alternated. The lamellae attained a maximum thickness of about 40 nm.

### **5.4.3 Tertiary walls in the endodermis**

The tertiary wall was deposited immediately after suberin lamella development was accomplished. The early tertiary wall was a thin sheet at the primary pit fields (Fig. 5.4A, B). Some dictyosomes were observed near the wall (Fig. 5.4B). Apparently, dictyosome-derived vesicles were in association with, and even merged with, the plasma membrane (Fig. 5.4 A, B). At the mature state of state III, tertiary walls were slightly thinner in the primary pit fields than elsewhere (Fig. 5.4C). Plasmodesmata were preserved intact through all stages (Fig. 5.4A, C). At the state III development, the Casparian bands were still recognizable (Fig. 5.4D).

### **5.4.4 Suberin lamellae in the exodermis**

A Casparian band of typical construction (as in the endodermis) was not observed in the transmission electron microscope. The exodermal radial walls were very thin (about 70 nm, compared to 200 nm of the endodermal radial walls) and it was hard to tell if any alterations had occurred in their electron density. Yet, the process of suberin lamella development was observed. Suberin lamella formed only in long cells in the root zones observed (50 and 100 mm from the root tip) for the exodermis. The suberin lamellae started earlier at the outer tangential side than at the inner tangential side (Fig. 5.5A, B). The first material deposited was in the form of darkly-stained, thin pieces ((Fig. 5.5B). They were in close association with the plasma membrane and thus could be better visualized at sites of slight plasmolysis. Shortly after, a continuous wall layer was formed

**Fig. 5.4** Tertiary wall formation in the endodermis

**A** Tertiary wall is first deposited in the pit field (arrowheads), beside plasmodesmata (*PD*). There is an indication that exocytosis occurred (large arrowhead). Suberin lamellae are indicated by asterisks. **B** Early tertiary wall (small arrowheads) along the tangential wall. Suberin lamellae are indicated by asterisks. Large arrowheads point to sites of exocytosis. **C** Tertiary wall at the mature stage. The lamellae at the pit field (arrowheads) are thick and display a multilayered structure. **D** All wall modifications in the tangential wall. The Casparian band (asterisk) has clear edges (small arrowheads). The suberin lamellae at the band are labeled by large arrowheads. Accumulation of hydrophobic substances near the band's edge is apparent (white arrow). *DI* dictyosome; *ER* endoplasmic reticulum; *PL* plastid; *SL* suberin lamellae; *TW* tertiary wall; *VE* vesicle. Bars: 0.5  $\mu\text{m}$

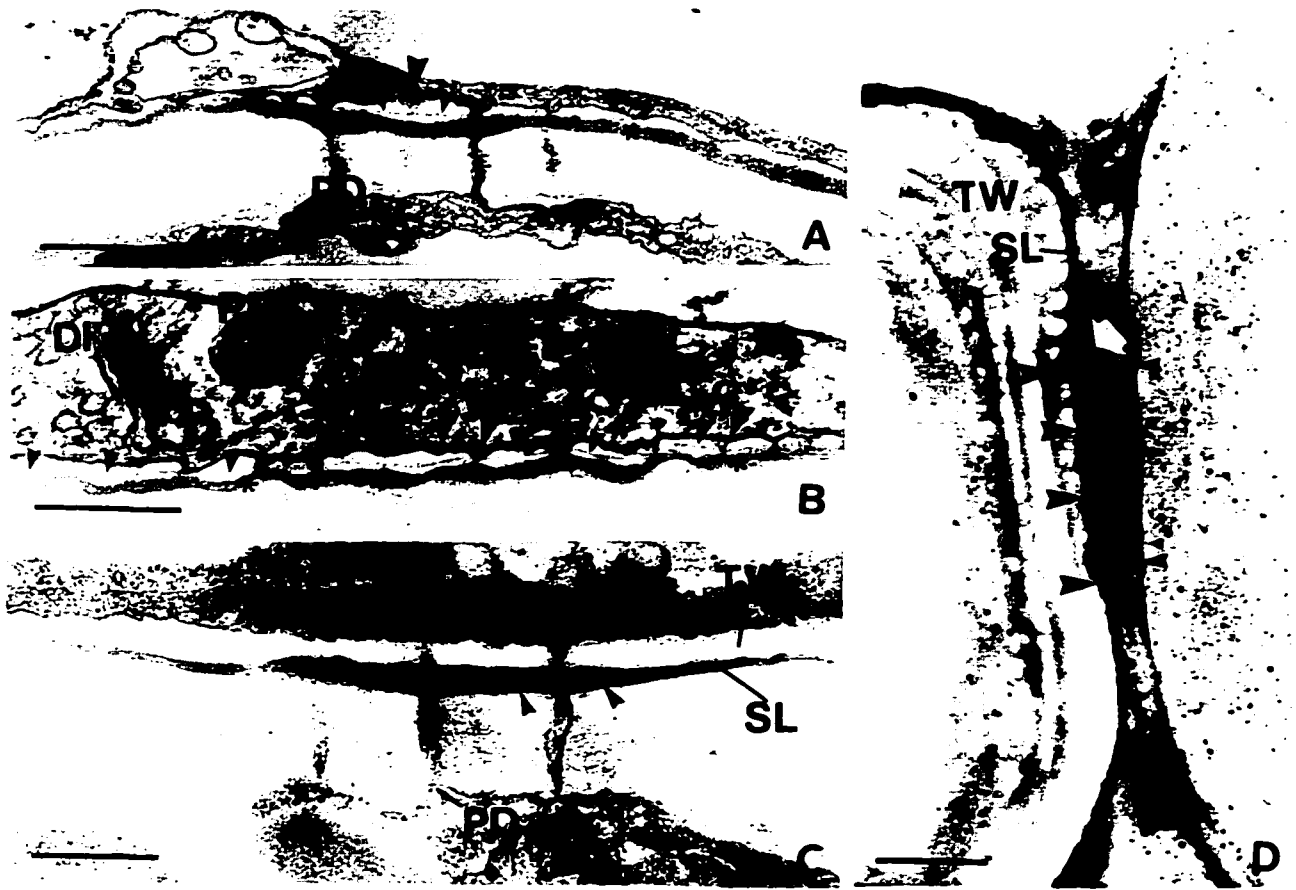




**Fig. 5.5** Suberin lamella deposition in the exodermal long cells (early stage)

**A** and **B** Inner and outer tangential walls, respectively, of an exodermal long cell. **A** Suberin lamellae are not initiated yet. Vesicle (*VE*)-filled invagination of plasma membrane. **B** Suberin lamellae are just visible (arrowheads). **C** and **D** Inner and outer tangential walls, respectively, of another exodermal long cell that is at a later stage of wall modification. Along both walls, suberin lamellae are visible, but are more prominent along the outer tangential wall (**D**). Suberin lamellae are indicated by small arrowheads and plasma membrane by arrows. ER is connected to the plasma membrane (large arrowhead, **C**). **E** Dictyosomes (*DI*) and ER in cytoplasm during suberin lamella formation. **F** Dictyosome in association with ER (at the sites of arrows), and vesicles originated from the latter are connected to the plasma membrane (at the sites of arrowheads). **G** Vesicles originated from ER and or dictyosome (asterisk) are in connection with plasma membrane (arrow). Plastids (*PL*) are darkly stained. *SL* suberin lamellae. Bars: 0.5  $\mu\text{m}$

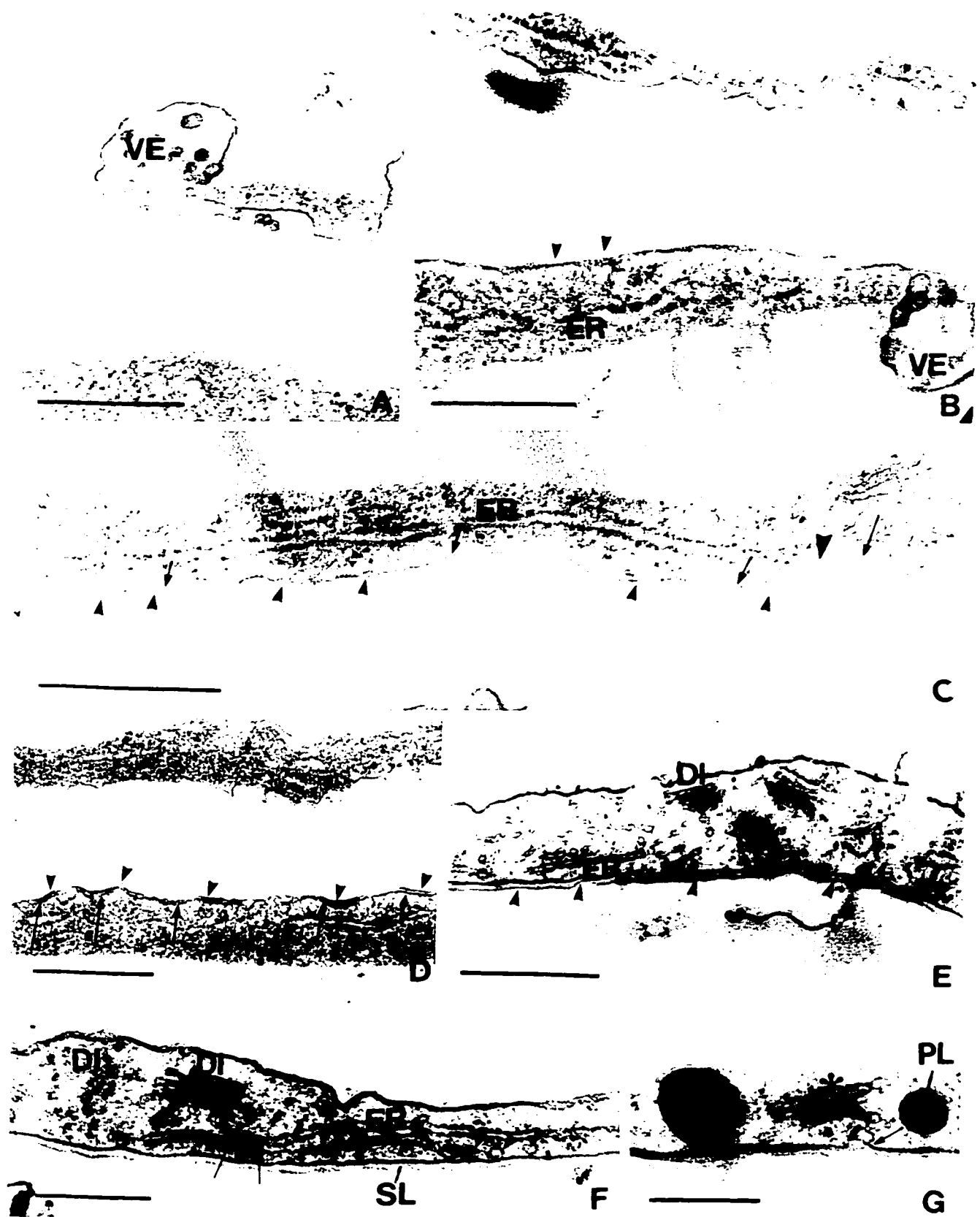


(Fig. 5.5 C, D). During the mid-phase of suberin lamella formation, the long cells appeared metabolically active. Numerous dictyosomes and ER profiles were evenly distributed in the cytoplasm (Fig. 5.5E, F). A continuity of dictyosomes to ER was observed (Fig. 5.5F). Close contact of ER- or dictyosome-derived vesicles to the plasma membrane was common (Fig 5.5 F, G). Plasma membrane invaginations frequently appeared; these were usually full of vesicles (spherical and/or elongate) containing electron-dense material (Fig. 5.5A, B, Fig. 5.6A). Such invaginations were particularly evident near the primary pit fields. Plastids were heavily osmiophilic (Fig. 5.5G), a feature that was not observed in other cell types.

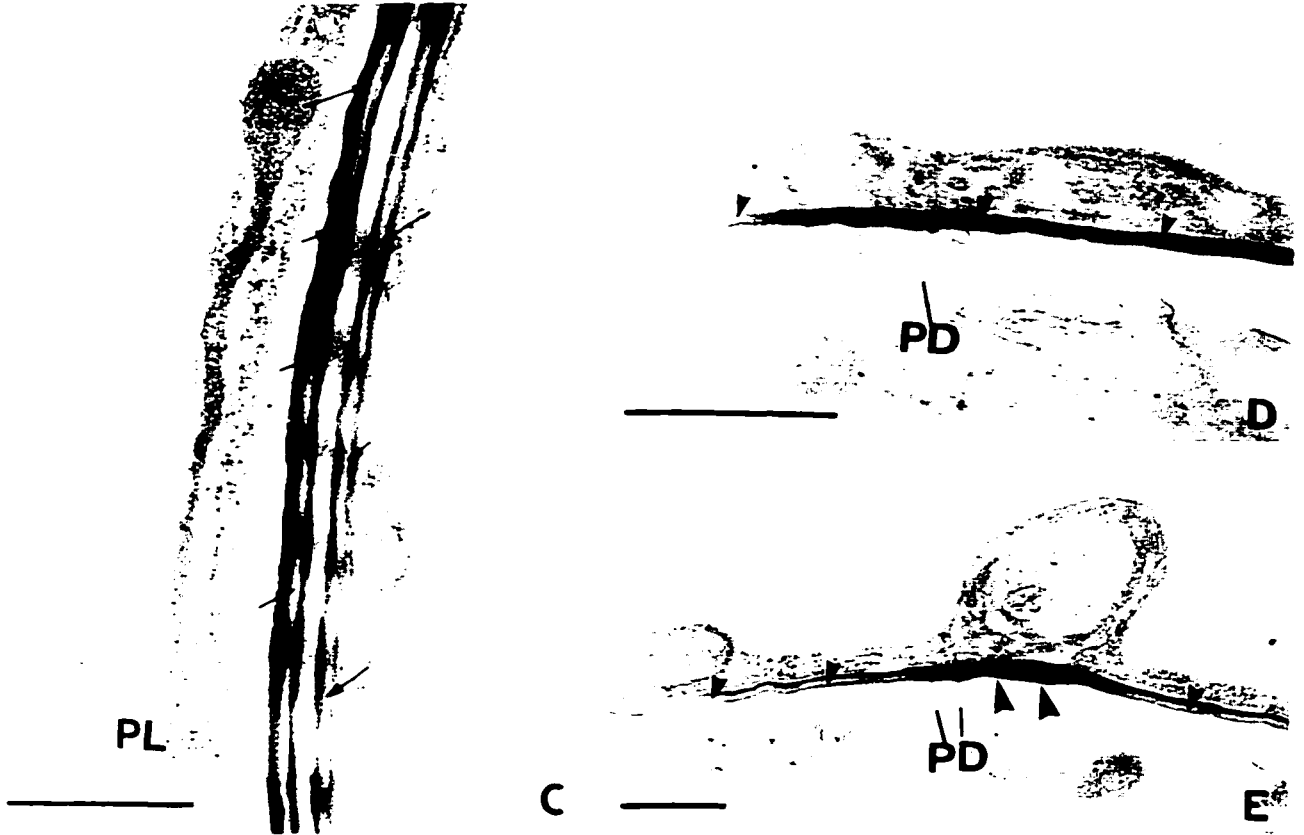
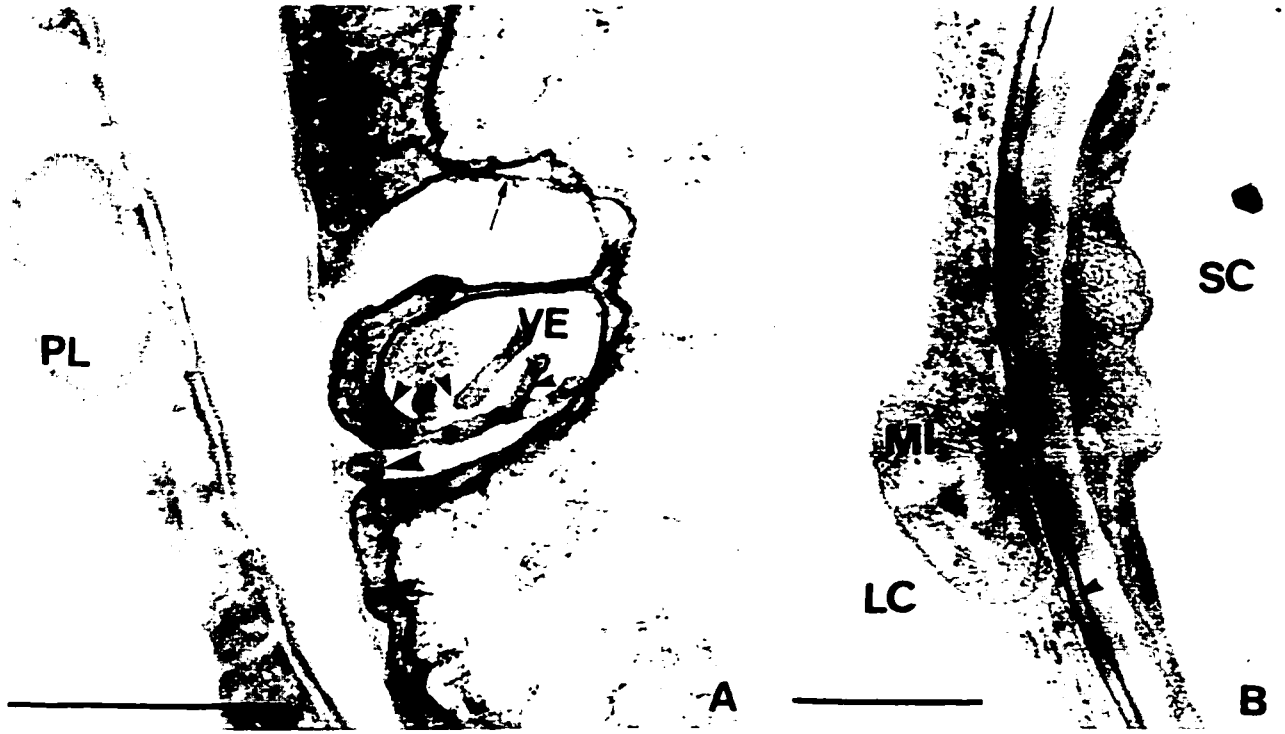
At 100 mm from the root tip, suberin lamellae were completed in all long cells. The structure of suberin lamellae was generally sandwich-like (Fig. 5.6B), with two electron-dense layers enveloping a much thicker electron-lucent layer. Careful examination revealed that much finer layers were present near both sides of the new wall (Fig. 5.6B, C). Over the plasmodesmata, the suberin lamellae were usually thicker and displayed a multi-layered structure (Fig. 5.6E). The structure of the cytoplasm was simplified and the number of organelles decreased (Fig. 5.6C, D, E). The suberin lamellae completely severed the plasmodesmata (Fig. 5.6D, E). The protoplast of long cells degenerated soon after the completion of suberin formation. No tertiary cellulosic walls were detected in this study.

## **5.5 Discussion**

The endodermis and exodermis share certain similarities in their wall modifications. In both cell layers, suberin lamellae were formed. A Casparian band, however, was detected with TEM in the endodermis and not in the exodermis. In a previous study of the project, the ultrastructure of the endo- and exo-dermal cell walls at their mature states were described. In the present contribution, the cellular events in both cell layers exhibited some variations at different stages of wall formation.

**Fig. 5.6 Suberin lamella deposition in the exodermal long cells (late stage)**

**A** Suberin lamella formation along the radial wall. Invagination of plasma membrane and included vesicles (*VE*). Arrows point to the plasma membrane that exhibits a lipid bilayer. Vesicles are also enveloped by bilayered membrane (small arrowheads). The vesicle (large arrowhead) lying beside the suberin lamellae does not have a membrane. **B** Suberin lamellae (arrowheads) in long cell (*LC*) and not in short cell (*SC*). **C** Suberin lamellae (arrows) along tangential walls of two adjacent long cells. The lamellae display a multilayered structure. **D** Suberin lamellae (arrowheads) along the tangential wall of a long cell. Plasmodesmata (*PD*) are severed. **E** Suberin lamellae (arrowheads) are thick and exhibit a multilayered structure at the pit field. The damaged plasmodesmata (*PD*) are diminishing. *MI* mitochondrion; *PL* plastid. Bars: 0.5  $\mu\text{m}$



### 5.5.1 Casparian bands and suberin lamellae in the endodermis

It seems that the establishment of the special plasma membrane-wall relationship preceded the commencement of hydrophobic molecules being incrustated into the wall to form the Casparian bands (Fig. 5.1A-C). A similar sequence of events was reported in the maize exodermal Casparian band development, at the light microscopic level (Enstone and Peterson 1997). If these observations are correct, they will have several implications. (1) The build-up of the membrane-wall connection represents a recognition process between the two cell components, which determines the site, and then triggers the machinery, of suberin incrustation into the primary wall. (2) The linkage of the membrane and the wall may be due to the presence of proteins in them (Clarkson and Robards 1975, Oparka 1994). In any case, it is not due to the interactions between the hydrophobic components of the wall and of the membrane as postulated by Bonnett (1968). Polypeptides unique to Casparian bands have been isolated from pea (*Pisum sativum* L.) roots (Karahara and Shibaoka 1992). A high protein content has also been detected in the Casparian bands from some other species (Schreiber et al. 1999). These proteins probably play a role during Casparian band formation. The mechanism remains to be illustrated.

During Casparian band formation in onion roots, monomers of hydrophobic substances could be delivered to sites directly across the plasma membrane. Occasionally, dictyosomes were observed in the vicinity of the developing bands, but they were so infrequent that it is not clear whether or not these organelles serve as vehicles for the monomers. In *Ranunculus*, a much larger population of dictyosomes was observed, strongly suggestive of their involvement in Casparian band formation (Scott and Peterson 1979). In addition, the cytoplasm is thicker and other organelles (ribosomes, mitochondria, plastids, and lipid bodies) are more numerous than in onion. In this respect, onion is closer to *Convolvulus arvensis* (Bonnett 1968), barley (Robards et al. 1973), and maize (Haas and Carothers 1975), characterized by thin cytoplasm and few organelles.

Suberin lamella deposition is probably brought about by a mechanism different from that for Casparian bands. In *Ranunculus acris* L., dictyosomes were less frequently observed during suberin lamella deposition than during band (and tertiary wall) formation (Scott and Peterson 1979). By contrast, in onion, dictyosomes and ER profiles were present more frequently during lamella formation than in early stages (although quantification was not attempted). This continued until the tertiary wall was laid down. In both stages, there is some indication that vesicles derived from dictyosomes or ER are moved to, and merged with the plasma membrane (e.g., Figs. 5.3D, 5.4B). In fully mature cells, these organelles were rarely found. The discrepancy between species in their ultrastructural dynamics discussed above points to the different extent to which cellular structures (especially the membrane systems) are involved. In the present study, it is also interesting to note that both suberin lamellae and tertiary walls are first started in the primary pit fields and then the rest of the walls. It is not clear what is the mechanism that underlies this phenomenon.

It is worth mentioning that suberin lamella formation can only commence when Casparian bands have fully developed. The bands of onion roots occupied the middle 1/3 - 1/2 of the radial walls (Fig. 5.1E) and no further extension was ever observed in later stages (Fig. 5.4D). Ultrastructural studies of other species have produced similar results (e.g., Scott and Peterson 1979, Verdaguer and Molinas 1997). In an earlier study on onion roots with fluorescence microscopy, it was claimed that, with the development of suberin lamellae, the band expanded through the radial wall, eventually filling its entire span (Barnabas and Peterson 1992). Apparently, the fluorescence techniques are not sensitive enough to differentiate the bands and the developing lamellae in the radial walls. Consequently, the fluorescing radial walls could have been mistakenly interpreted as having wall-length Casparian bands. A similar result was reported in *Cucurbita pepo* L., based on light microscopic observations (Harrison-Murray and Clarkson 1973). But, a later study on this latter species failed to confirm this observation (see Fig. 2d, in Warmbrodt 1986a). It is concluded the Casparian bands and suberin lamellae are formed in succession and that the bands do not extend during the lamella development.

### 5.5.2 Wall modification in the exodermis

A Casparian band was not positively detected in the exodermis by the electron microscope. This result is in agreement with the findings in *Citrus* roots (Walker et al. 1984). In an ultrastructural study on the roots of *Zostera capensis* Setchell, a Casparian band was declared to be detected in the exodermis (Barnabas and Arnott 1987), but this was not clearly illustrated in the published micrographs. So, it remains a challenge to identify the exodermal bands at the ultrastructural level in the extremely thin walls (§ 5.4.4). This sounds surprising since the bands have been detected by several techniques in onion and other plants at the light microscopic level (see § 1.2.4.4). It has also been demonstrated that exodermal Casparian band is an apoplastic barrier for fluorescent dyes (Peterson et al. 1978),  $\text{SO}_4^{-2}$  (Peterson 1987), and  $\text{Ca}^{+2}$  (Cholewa, personal communication). It is surmised that the exodermal Casparian band is structurally different from the endodermal one. (This, in turn, could be due to the differences in their chemical compositions. See Schreiber et al. 1999). Future TEM work on exodermal Casparian bands will benefit from suitable probes for suberins and lignins.

Nevertheless, the exodermis exhibited certain similarities to the endodermis in suberin lamella formation. In both cell layers, ER, plasma membrane invaginations, and membrane-bound vesicles occurred at the early stages of suberin deposition. Similar results were obtained for suberin lamella development in the grass mestome sheath (Eleftheriou and Tsekos 1979) and in potato cortex following wounding (Thomson et al. 1995). In the present study, dynamic changes in the activity of the vesicles were observed: this observation confirmed that the vesicles were derived from dictyosomes or ER and are destined for the plasma membrane, pointing to the exocytotic nature of suberin lamella (and also tertiary wall, in the endodermis) deposition. On the other hand, some dissimilarities were obvious between the exodermis and endodermis in onion root. In the former, dictyosomes and ER, separately (Fig. 5.5C, E) or in a co-ordinated mode (Fig. 5.5F), apparently contributed more intensively to the synthesis, delivery, and deposition of hydrophobic molecules than in the latter.



### 5.5.3 The relationships of suberin lamellae to other cellular structures

The fate of the Casparian band-bound plasma membrane in the endodermis has been a concern at the time of suberin lamella formation. The connection is so tight that the bound membrane is generally inseparable from the band (as demonstrated by displaying band plasmolysis when treated by a hypertonic solution). In barley roots, it was reported that the bound membrane was covered by the developing suberin lamellae (Robards et al. 1973). The evidence is that a dark-staining lamellar structure was present over the original Casparian band region, which was interpreted to be the remnant of the bound membrane. Similar membrane changes were reported during endodermal dedifferentiation for lateral root initiation (Bonnett 1969, Karas and McCully 1973), only the new wall material was cellulosic rather than of suberin. To accomplish this, a sequence of events must take place (Fig 5.7). (1) The endodermal plasma membrane has to be cut through at both outer and inner tangential margins of the Casparian bands. (2) Over the band region, the precursor molecules of suberin lamellae are delivered to place directly, rather than across the plasma membrane, at least during the initial period. (Whereas the suberin lamellae over the non-Casparian band region are formed by exocytosis - presumably.) (3) Then, the plasma membrane internal to the suberin lamellae in the area above the original Casparian bands must be formed either by *de novo* assembly or by extension of the plasma membrane from the non-Casparian band region. In *Quercus suber* L. (Verdaguer and Molinas 1997), the suberin lamellae in the Casparian band region can be either extremely thin or absent. But the fate of the bound plasma membrane was not illustrated. In onion, the results clearly showed that the endodermal cells are able to separate the bound plasma membrane from the band (by an as yet unknown mechanism) to make way for the release of suberin precursors (Fig. 5.8). Actually, the membrane could be separated by force (*e.g.*, during the processing for TEM. Fig. 5.1H). In *Ranunculus*, electron-dense (membrane-like) platelets were observed in mature suberin lamellae, which was interpreted as originating from the paramural and multivesicular bodies (presumably the vehicle for suberin precursors - Scott

**Fig. 5.7** Schematic reconstruction of suberin lamella formation in the endodermis as illustrated in the literature

**A** Endodermis with a Casparian band (dark portion of the radial wall). **B** Formation of suberin lamellae (blue line) along the tangential walls. **C** The edge of the extending suberin lamellae has reached the edges of the Casparian band. **D** Suberin lamellae are formed over the Casparian band and the bound-plasma membrane is buried in the wall. **E** The plasma membrane is cut off at the band's edges (arrows). **F** *de novo* formation of plasma membrane (yellow line).

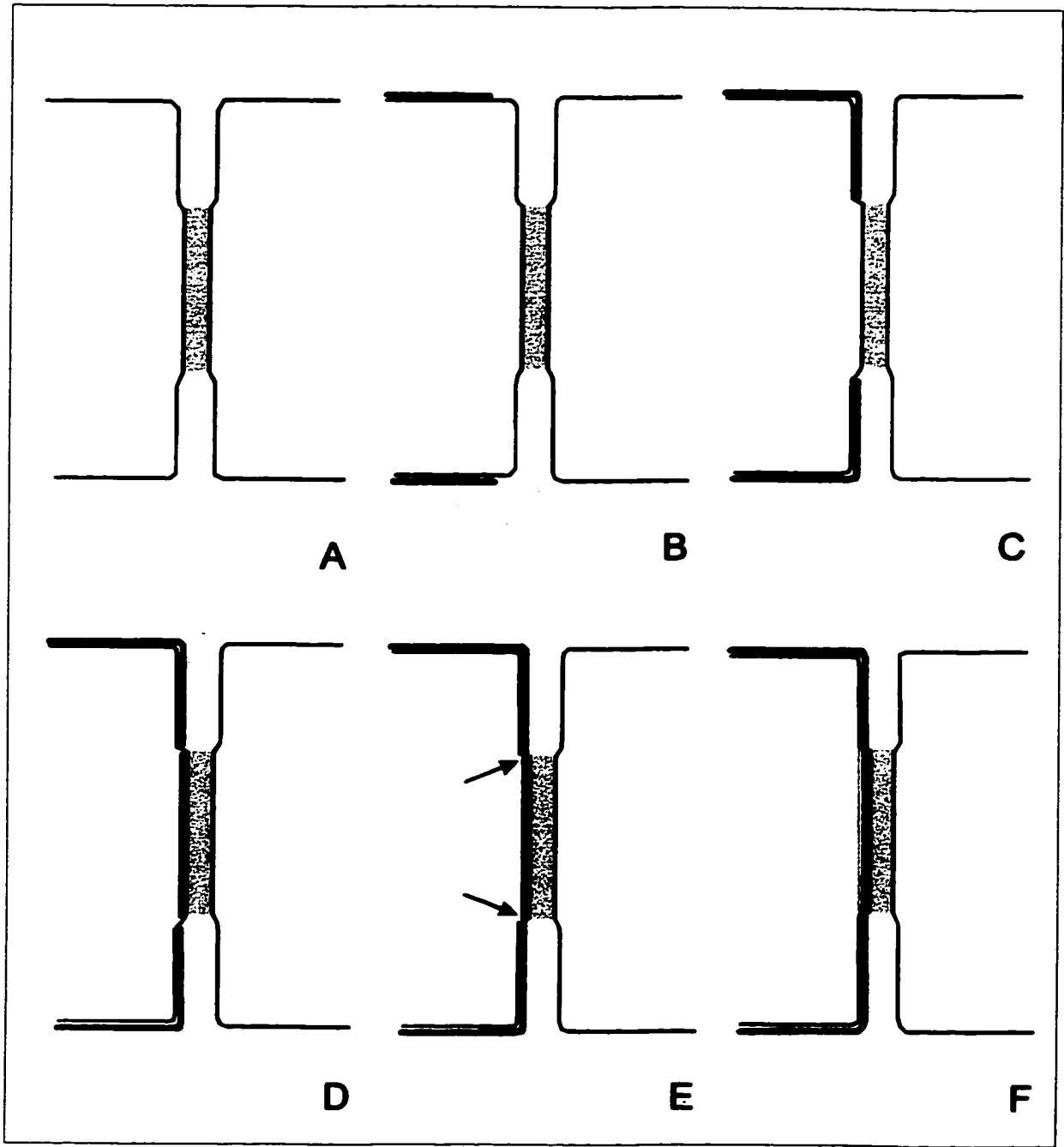
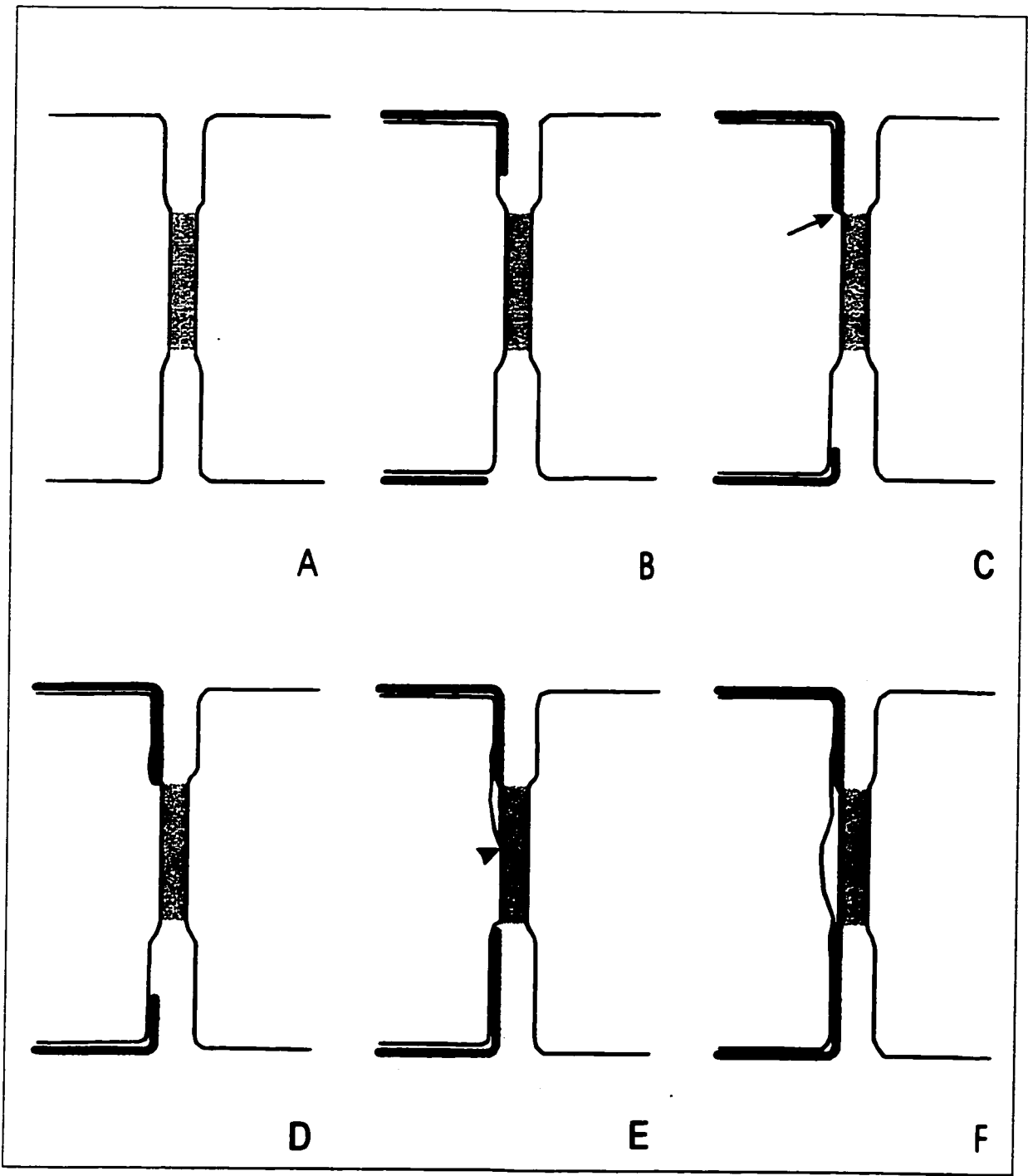


**Fig. 5.8** Schematic representation of suberin lamella formation in the endodermis of onion roots

**A** Endodermis with a Casparian band. **B** Suberin lamellae (red) of the outer tangential wall are initiated earlier than those of the inner tangential wall. **C** The suberin lamellae of the outer tangential wall first reached the edge of the band (arrow). The extension of the lamellae appears to be hindered due to the tight binding of the plasma membrane to the band. **D** Hydrophobic substances accumulate at the band's margin. **E** The bound plasma membrane is separated from the band and suberin lamella deposition (between the wall and plasma membrane) has been resumed. The edge of the lamellae is marked by an arrowhead. At the inner side, the suberin lamellae have reached the band's edge. **F** Hydrophobic substances are being accumulated at the band's inner edge. The previously bound plasma membrane is separated from the band (at the inner side) and suberin lamella deposition is resumed. Suberin lamellae have been formed over the band. During the process, the plasma membrane is not damaged.



and Peterson 1979). In the endodermis, wall modifications do not interrupt the plasmodesmatal continuity of the cell layer (Chapter 2). This is true for some wounded tissues (*e.g.*, in *Prunus persica*; Biggs and Stobbs 1986). Comparable events were observed in the exodermal cells of maize, a species with a uniform exodermis (Wang et al. 1995). By contrast, in the dimorphic exodermis, all plasmodesmatal connections of the long cells were severed by the developing suberin lamellae, as in citrus (Walker et al. 1984) and in onion (see also Chapter 2). The protoplasts of long cell will degenerate afterwards (Chapter 2). These results could well explain why a tertiary wall could be deposited in the endodermis (in general) and the uniform exodermis (as in maize), and not in the dimorphic exodermis (in onion).

## Chapter 6

### **General discussion**

The present study has been focused on revealing the structure of onion roots in relation to their function, with special reference to the symplastic relationships in the zone with a mature exodermis. Never before has a complete assessment of the distribution of plasmodesmata been done in the root of any species. Neither has an examination of plasmodesmatal functionality in all cell types been performed. Previous studies in very few species (and on limited cell interfaces) did not permit a generalization of symplastic transport patterns (see Introduction). Onion roots, despite their advantages as a model system in studying transport physiology, represent one of the most complicated examples, by having a dimorphic exodermis and various wall modifications.

#### **6.1 Root development, transport, and wall modifications**

The function of plasmodesmata in the root varies along its length. In the meristem and its early derivatives, plasmodesmata could serve as canals for signaling that would control pattern formation (Zhu et al. 1998a). Behind the apical meristem, phloem unloading of photosynthates (at the newly differentiated protophloem sieve elements) and post-phloem transport take place (Duckett et al. 1994). At this level of the root axis, however, xylem vessels have not yet matured and thus inward transport of ions is insignificant. With the development of xylem vessels, ion transport increases from the culture medium to the stele, and these ions will eventually contribute to the transpiration stream. At certain distances from the root tip, wall modifications (Casparian bands, suberin lamellae, and tertiary walls) occur in the endodermis (Clarkson and Robards 1975) and exodermis

(Perumalla and Peterson 1986, Wang et al. 1995). Casparian bands will block the apoplastic movement of ions (Clarkson and Robards 1975, Peterson 1987, Peterson and Cholewa 1998), but not the symplastic transport (Clarkson et al. 1971, Walker et al. 1984). In the endodermis (Clarkson and Robards 1975) and the uniform exodermis (Wang et al. 1995), the symplastic continuity is preserved through all stages. In a dimorphic exodermis, however, once suberin lamellae are developed, the symplastic connections are lost. This happens first in all long cells (Walker et al. 1984, Ma and Peterson 2000) and later also in some short cells (Kamula et al. 1994). In all cells, suberin lamellae are generally assumed to be impermeable to ions. Therefore, the differences between roots with a uniform exodermis and those with a dimorphic exodermis are obvious at maturity. In the former, symplastic transport is likely to be the only pathway available at the outer tangential walls of the exodermis. In the latter, both symplastic and transmembrane transport are possible, but the functional area is markedly reduced.

## **6.2 The distribution of plasmodesmata in the old zone of the root**

### **6.2.1 In the inward direction**

It is clear that, since the distribution of plasmodesmata exhibited such a high variation across the root (Chapters 2 and 3), the component tissues are not contributing equally to the overall function of the root. It is commonly known that a symplastic pathway exists in the root, but this basically refers to the region of the cortex (Ginsburg and Ginsburg 1970a, b; Dick and ap Rees 1975). The plasmodesmatal frequency data of the present study have more specifically indicated that the bulk of symplastic transport in onion roots could occur from the exodermal short cells up to the pericycle. The low frequency at the interface of epidermis-short cells might imply that the plasma membranes at this interface exercise a further control (*i.e.*, selectivity) over the solutes, immediately following their entry into the epidermis and before joining the main stream of the symplast. At the innermost side of the flow, the frequency was so low at the pericycle-stelar parenchyma interface that a



significant symplastic transport is not anticipated. Therefore, the pericycle, for practical purpose, is most probably the inner end of the radial symplast. Solutes in the pericycle (received from the endodermis) would be transferred into the apoplast where some would diffuse into the lumina of the protoxylem vessels, and then the metaxylem vessels, where differentiated (§ 4.5.3). At the same time, the pericycle might also act as an “annular collector and disperser” for ions and photosynthates, respectively, as proposed for barley by Vakhmistrov et al. (1972). This model highlights the significance of the pericycle in contributing to both inward and outward transport by facilitating solute circulation across the plasmodesmata on the radial walls (Chapter 3). Unfortunately, the possible functions of the pericycle in transport have been largely ignored and Vakhmistrov’s hypothesis has not received the attention it deserves. Rather, attention has been focused on the stelar parenchyma (*e.g.*, Läuchli et al. 1971 a, b, 1974a, b). Some recent research has been done on barley roots, but the results are not in agreement to each other. Ion channels have been studied in the protoplasts isolated from the stelar parenchyma (Wegner and Raschke 1994, de Boer 1999), which is in favor of a passive pathway for xylem loading by the stelar parenchyma. Another study showed that the plasma membrane  $H^+$ -ATPase was more intensely expressed in the pericycle than in the stelar parenchyma (Samuels et al. 1992); this implied that the pericycle might play a role in secreting ions into the xylem. Regrettably, since the authors intended to emphasize the significance of the stelar parenchyma, they provided an alternative explanation for the pericycle that exhibited potential for renewed meristematic activity. But when checking the published micrographs carefully, it was obvious that the labeling along the pericycle is uniform. This is unlikely due to the “renewed meristematic activity” (for lateral root initiation, in this case) that is usually localized to cells facing the protoxylem poles (Luxová 1990). For onion, while our observations on plasmodesmatal frequency and cell structure are suggestive of a significant role that the pericycle might play, the results are not conclusive (Chapter 3). Earlier, a proton-pump was described in the stelar parenchyma of onion roots. Care is needed, however, when looking at the terminology used in the literature (*e.g.*, Drew et al. 1990, de Boer 1999), confusion frequently arises (see Chapter 3). Either “xylem parenchyma” was frequently substituted for “stelar parenchyma” or they were used interchangeably, or

“xylem parenchyma” was used to refer to the collective of stelar parenchyma and pericycle. Maybe variations really occur among species that use different mechanisms and pathways for xylem loading. Or, the seemingly conflicting results are largely due to the confusion in terminology.

The present state of our knowledge of both pericycle and stelar parenchyma is still rudimentary. While the plasmodesmatal data are valuable in predicting the symplastic flow, it can only be tested by properly designed experiments in the future. Although the progress in the studies of protoplasts originating from stelar parenchyma sounds exciting, the validity of this approach is open to debate. It has not yet been determined if the protoplasts *in vitro* function the same way as the cells do *in vivo*. For the near future, a clarification in the terminology and distinction in the function of the pericycle and stelar parenchyma are definitely needed. An ultrastructural localization study of ATPase activity could help clarify the relative contributions of pericycle and stelar parenchyma in loading the vessels with ions.

### **6.2.2 Plasmodesmatal frequency: implications for phloem unloading and post-phloem transport**

The symplastic connections associated with the phloem have been qualitatively (Chapter 2) and quantitatively (Chapter 3) analyzed. The phloem is composed of protophloem sieve element(s), metaphloem sieve elements and companion cells. All cells are interconnected by plasmodesmata. To the outside, the protophloem sieve elements and companion cells are linked to the pericycle. To the flanks, companion cells are bridged to the stelar parenchyma cells. The highest plasmodesmatal frequency was observed between the metaphloem sieve element and the companion cell. All other interfaces exhibited very low, yet constant, frequencies. This relationship indicated that phloem unloading (of photosynthates) took place at the companion cells and post-phloem transport happened approximately equally among different cell types, if the symplastic pathway was in operation. This result is a novel contribution to phloem function. The frequency data are not totally parallel to those obtained

for other species. For instance, in both barley (Warmbrodt 1985a, 1986b) and maize (Warmbrodt 1985b, 1987), the stelar parenchyma cells probably play an important role in the initial post-phloem steps as they share a relatively high plasmodesmatal frequency with the companion cells. In both species, the frequency data were in good accordance with the solute concentration gradients. Although the solute concentrations could not be taken as equal to those of the photosynthates, they do provide a clue for the direction of photosynthate movement. It will be useful to test whether or not this parallelism occurs in onion.

### **6.3 Plasmodesmata in ion transport**

The ultrastructural ion localization technique proved useful in examining the functionality of plasmodesmata. In vermiculite- or water-grown roots, AgCl precipitates in individual plasmodesmata and other cell structures can be observed with high resolution. With short-time treatments (2 and 5 min) on pure water-grown roots, the “frontier” of Cl<sup>-</sup> movement, albeit not a sharp line, could be seen grossly at the first outermost central cortical cell layer and a few more layers deeper, respectively. In all long-time treatments, a “frontier” was not observed; rather, all cells had comparable densities of precipitate. This is proof of the movement of ions through plasmodesmata (and cell walls and membranes, to a lesser extent, where applicable. See Chapter 4). By using fluorescence microscopy, an apoplastic “diffusion ring” was observed in the roots of onion and some other species (Aloni et al. 1998). Therefore, different ions can diffuse either in the symplast or in the apoplast (or in both).

The present study confirmed the results from earlier experiments concerning chloride transport. Chlorine is an essential element, and it has long been known from physiological tests that it is principally transported in the symplast of onion roots (Hodges and Vaadia 1964) and of several other systems. But the latter experiments usually can only provide an overall idea about the transport in a complex system, whose structural heterogeneity was largely overlooked. Now it is clear that all plasmodesmata are functioning in transferring Cl<sup>-</sup>. With sufficient chloride supply (grown in vermiculite or in NaCl solution), inward

transport was observed through the plasmodesmata, until reaching the xylem vessels. When cultured in pure water, the growth of the root system was significantly retarded. In this situation, little AgCl precipitation was observed in tissues external to the stele. The detected Cl<sup>-</sup> is probably retained during the depletion period. But it is more likely that ions in the shoot were relocated by the phloem and finally delivered to all root tissues through plasmodesmata (Chapter 4). Cl<sup>-</sup> is one of the phloem-mobile elements (Ziegler 1975) and its precipitation in companion cells and sieve elements points to their involvement in chloride reallocation. In the epidermis, wall ingrowths were formed in the outer tangential side (*i.e.*, transfer cells), which is apparently a response to nutrient deficiency (Chapter 4). When cultured in a CaSO<sub>4</sub> solution, the root system grew much better than in pure water. The distribution pattern of Cl<sup>-</sup> was essentially the same as in the Cl<sup>-</sup>-amended cultures. This is explained as benefited from the function of Ca<sup>+2</sup>.

## **6.4 Wall modifications in the endodermis and exodermis**

The endodermis and exodermis in onion roots have different mechanisms for wall modification. In the former, Casparian bands, suberin lamellae and tertiary walls develop in succession. In the latter, Casparian bands were detected by light and fluorescence microscopy (Chapter 2), but not by the TEM (Chapter 5). Suberin lamellae were formed mainly in the exodermal long cells; short cells developed suberin lamellae in very old root zones (Kamula et al. 1994). No tertiary wall was ever observed in the exodermis in the present study. This is conceivable taking into account the different relationships of the suberin lamellae to the plasmodesmata in the endodermis and exodermis. In the former, suberin lamellae do not interrupt the symplastic connections, which made possible further wall development (*i.e.*, tertiary walls), while in the latter, all plasmodesmata are severed by suberin lamellae that would terminate the development of these cells. The process of suberin deposition exhibited some dissimilarity in these two cell layers (Chapter 5). In the onion exodermis, the membrane systems (ER and dictyosomes) are more intensely involved during suberin lamella formation than during Casparian band development. In *Ranunculus*, the relationship is somewhat reversed (Scott and Peterson 1979). To better understand the cellular processes of how

precursor molecules are delivered to a specific place to accomplish the wall modifications. probes suitable for ultrastructural studies have to be developed.

In the endodermis, the relation of the developing suberin lamellae to the existing Casparian bands has been established. It was observed that the deposition of the suberin lamellae over the bands was preceded by, or concomitant with, the separation of the plasma membrane from the band. A similar conclusion was drawn for *Ranunculus*, but the process was not clearly elucidated (Scott and Peterson 1979). The results of the present study sharply contrast with the previous postulation that suberin lamellae are laid down over the membrane (Figs. 5.7, 5.8). During the endodermal activation prior to lateral-primordium initiation, it was also reported that new wall material (presumably cellulose) was deposited over the membrane (Bonnett 1969, Karas and McCully 1973). The latter mechanism is unlikely since the published micrographs showed neither definitely the structures involved nor the process of the new wall formation. The present observations indicated that plant cells would produce the lamellae in better physiological and economical ways, as for all biological phenomena.

The present ultrastructural study provided detailed information of wall modification in the exodermis (Chapter 4). Using TEM, the presence of Casparian bands was not positively identified. As discovered by light and fluorescence microscopy, the principal hydrophobic component of exodermal Casparian bands is suberin and lignin (Brundrett et al. 1988). But this is not indicative of an identical chemistry between the exodermal and endodermal bands. Preliminary results suggested that the exodermal bands were structurally different from their endodermal counterparts. On the contrary, major stages of the suberin lamella formation had been recognized in the TEM. The earliest material laid down was electron dense (as in the endodermis). This is followed by the formation of alternate electron-dense and -lucent lamellae. Dictyosomes and ER are extensively involved in the construction of the new wall. Future work will include developing a suberin antibody to probe where suberin precursors are synthesized and how they are delivered to specific sites.

## 6.5 Conclusions

The variance of the distribution of plasmodesmata in onion roots is obvious. In young zones, all cells are interconnected by plasmodesmata, in all directions. In old zones, suberin lamellae developed in the exodermal long cells and severed all their plasmodesmatal connections. Therefore, the epidermis is symplastically linked to the central cortex only through the exodermal short cells that lack suberin lamellae. Analysis of plasmodesmatal frequencies indicates that a constant symplastic flow of ions is possible from the short cells up to the pericycle, and little symplastic transport is anticipated from the epidermis to short cells and even less from the pericycle to the stelar parenchyma. In the phloem, symplastic unloading could occur at the companion cells to surrounding parenchyma cells. On the radial walls of pericycle cells, a high plasmodesmatal frequency is present, which implies a considerable solute circulation in the tangential direction across this layer. This feature makes the pericycle an important tissue in promoting inward and outward movement of solutes.

All plasmodesmata are functional in transferring  $\text{Cl}^-$  from the medium to the stele, as tested by an ultrastructural ion precipitation technique. There is also an indication that transmembrane transport occurs across the epidermis-short cell interface. Under ion-deficiency conditions, the phloem could reallocate ions from the shoot to the root tissues by a symplastic pathway. This process is enhanced by  $\text{Ca}^{+2}$ .

The endodermis and exodermis exhibit certain similarities and dissimilarities in their wall modifications. In the endodermis, the development of Casparian bands is followed by deposition of suberin lamellae. The latter first appear in the primary pit fields along the tangential walls. At the band region, the bound plasma membrane is detached from the wall and, then, hydrophobic substances are laid down. Tertiary walls are formed afterwards. Plasmodesmata are preserved through all stages. In the exodermis, a Casparian band has been detected by fluorescence microscopy, but not by transmission electron microscopy. Suberin lamellae develop only in the long cells in the samples examined (100 mm from the root tip).

Dictyosomes and ER are intensively involved in wall development. Also, the severance of plasmodesmata by the developing suberin lamellae is unique to the exodermis.

## References

- Aloni R, Enstone DE, Peterson CA (1998)** Indirect evidence for bulk water flow in root cortical cell walls of three dicotyledonous species. *Planta* 207: 1-7
- Aloni R, Peterson CA (1990)** The functional significance of phloem anastomoses in stems of *Dahlia pinnata* Cav. *Planta* 182: 583-580
- Anderson WP, Goodwin L, Hay RKM (1974)** Evidence for vacuole involvement in xylem ion supply in the excised primary roots of two species, *Zea mays* and *Allium cepa*. In: Kolek J, ed, Structure and Function of Primary Root Tissues. Veda, Publishing House of the Slovak Academy of Sciences, Bratislava. pp 379-388
- Anderson WP, Reilly EJ (1968)** A study of the exudation of excised maize roots after removal of the epidermis and outer cortex. *J Exp Bot* 19: 19-30
- Arisz WH (1956)** Significance of the symplasm theory for transport across the root. *Protoplasma* 46: 1-62
- Badelt K, White RG, Overall RL, Vesik M (1994)** Ultrastructural specializations of the cell wall sleeve around plasmodesmata. *Am J Bot* 81: 1422-1427
- Baker DA (1971)** Barriers to radial diffusion of ions in maize roots. *Planta* 98: 285-293
- Barnabas AD, Arnott HJ (1987)** *Zostera capensis* Setchell: root structure in relation to function. *Aqu Bot* 27: 309-322
- Barnabas AD, Peterson CA (1992)** Development of Casparian bands and suberin lamellae in the endodermis of onion roots. *Can J Bot* 70: 2233-2237
- Barrowclough DE, Peterson CA (1994)** Effects of growing conditions and development of the underlying exodermis on the vitality of the onion root epidermis. *Physiol Plant* 92: 343-349
- Biggs AR, Stobbs LW (1986)** Fine structure of the suberized cell walls in the boundary zone and necrophylactic periderm in wounded peach bark. *Can J Bot* 64: 1606-1610
- Blackman LM, Overall RL (1998)** Immunolocalisation of the cytoskeleton of plasmodesmata of *Chara corallina*. *Plant J* 14: 733-741
- Bonnett HT Jr (1968)** The root endodermis: fine structure and function. *J Cell Biol* 37: 199-205
- Bonnett HT Jr (1969)** Cortical cell death during lateral root formation. *J Cell Biol* 40: 144-159
- Botha CEJ, Hartley BJ, Cross RHM (1993)** The ultrastructure and computer-enhanced digital image analysis of plasmodesmata at the Kranz mesophyll-bundle sheath interface of *Themeda triandra* var. *imberbis* (Retz) A. Camus in conventionally-fixed leaf blades. *Ann Bot* 72: 255-261
- Brundett MC, Enstone DE, Peterson CA (1988)** A berberine-aniline blue fluorescent staining procedure for suberin, lignin, and callose in plant tissues. *Protoplasma* 146: 133-142



- Brundrett MC, Kendrick B, Peterson CA** (1991) Efficient lipid staining in plant material with Sudan red 7B or Fluorol yellow 088 in polyethylene glycol-glycerol. *Biotech Histochem* 66: 111-116
- Campbell N, Thomson WW** (1975) Chloride localization in the leaf of *Tamarix*. *Protoplasma* 83: 1-14
- Carpita N, Sabularse D, Montezinos D, Delmer DP** (1979) Determination of the size of cell walls of living plant cells. *Science* 205: 1144-1147
- Carr DJ** (1976a) Plasmodesmata in growth and development. In: Gunning BES, Robards AW, eds. *Intercellular communication in plants: studies on plasmodesmata*. Springer-Verlag, Berlin. pp243-289
- Carr DJ** (1976b) Historical perspectives on plasmodesmata. In: Gunning BES, Robards AW, eds. *Intercellular communication in plants: studies on plasmodesmata*. Springer-Verlag, Berlin. pp 291-295
- Clarkson DT** (1993) Roots and the delivery of solutes to the xylem. *Phil Trans R Soc Lond B* 341: 5-17
- Clarkson DT, Hanson JB** (1986) Proton fluxes and the activity of a stelar proton pump in onion roots. *J Exp Bot* 37: 1136-1150
- Clarkson DT, Robards AW** (1975) The endodermis, its structural development and physiological role. In: Torrey JG, Clarkson DT, eds, *The development and function of roots*. Academic Press, London. pp 415-436
- Clarkson DT, Robards AW** (1975) The endodermis, its structural development and physiological role. In: Torrey JJ, Clarkson DT, eds, *The development and function of roots*. Academic Press, London. pp 415-436
- Clarkson DT, Robards AW, Sanderson J** (1971) The tertiary endodermis in barley roots: fine structure in relation to radial transport of ions and water. *Planta* 96: 292-305
- Clarkson DT, Robards AW, Stephens JE, Stark M** (1987) Suberin lamellae in the hypodermis of maize (*Zea mays*) roots: development and factors affecting the permeability of hypodermal layers. *Plant Cell Environ* 10: 83-93
- Clarkson DT, Sanderson J** (1974) The endodermis and its development in barley roots as related to radial migration of ions and water. In: Kolek J, ed, *Structure and function of primary root tissues*. Veda, Publishing House of the Slovak Academy of Sciences, Bratislava. pp 87-100
- Cleland RE, Fujiwari T, Lucas WJ** (1994) Plasmodesmal-mediated cell-to-cell transport in wheat roots is modulated by anaerobic stress. *Protoplasma* 178: 81-85
- Cote R, Thain JF, Fensom DS** (1987) Increase in electrical resistance of plasmodesmata of *Chara* induced by an applied pressure gradient across nodes. *Can J Bot* 40: 509-511
- Crafts AS, Broyer TC** (1938) Migration of salts and water into xylem of the roots of higher plants. *Am J Bot* 25: 529-535
- Crawford KM, Zambryski PC** (1999) Plasmodesmata signaling: many roles, sophisticated statutes. *Curr Opin Plant Biol* 2: 382-387
- De Boer AH** (1999) Potassium translocation into the root xylem. *Plant Biol* 1: 36-45
- de Rufz de Lavison J** (1910) Du mode de pénétration de quelques sels dans la plante vivante. Role de l'endoderme. *Rev Gén Bot* 22: 225-241
- Dick PS, ap Rees T** (1975) The pathway of sugar transport in roots of *Pisum sativum*. *J Exp Bot* 26: 305-314

- Ding B** (1998) Intercellular protein trafficking through plasmodesmata. *Plant Mol Biol* 38: 279-310
- Ding B, Itaya A, Woo Y-M** (1999) Plasmodesmata and cell-to-cell communication in plants. *Intl Rev Cytol* 190: 251-316
- Ding B, Kwon M-O, Warnberg L** (1996) Evidence that actin filaments are involved in controlling the permeability of plasmodesmata in tobacco mesophyll. *Plant J* 10: 157-164
- Ding B, Turgeon R, Parthasarathy MV** (1992) Substructure of freeze-substituted plasmodesmata. *Protoplasma* 169: 28-41
- Drake G, Carr DJ** (1978) Plasmodesmata, tropisms, and auxin transport. *J Exp Bot* 29: 1309-1318
- Drake G, Carr DJ** (1979) Symplastic transport of gibberellins: evidence from flux and inhibitor studies. *J Exp Bot* 30: 439-447
- Drew MC, Webb J, Saker LR** (1990) Regulation of  $K^+$  uptake and transport to the xylem in barley roots:  $K^+$  distribution determined by electron probe X-ray microanalysis of frozen-hydrated cells. *J Exp Bot* 41: 815-825
- Duckett CM, Oparka KJ, Prior DAM, Dolan L, Roberts K** (1994) Dye-coupling in the root epidermis of *Arabidopsis* is progressively reduced during development. *Development* 120: 3247-3255
- Dunlop J, Bowling DJ** (1971a) The movement of ions to the xylem exudate of maize roots. I. Profiles of membrane potential and vacuolar potassium activity across the root. *J Exp Bot* 22: 434-444
- Dunlop J, Bowling DJ** (1971b) The movement of ions to the xylem exudate of maize roots. II. A comparison of the electrical potential and electrochemical potentials of ions in the exudate and in the root cells. *J Exp Bot* 22: 445-452
- Dunlop J, Bowling DJ** (1971c) The movement of ions to the xylem exudate of maize roots. III. The locations of the electrical and electrochemical potential between the exudate and the medium. *J Exp Bot* 22: 453-464
- DuPont FM, Leonard RT** (1977) The use of lanthanum to study the functional development of the Casparian strip in corn roots. *Protoplasma* 91: 315-323
- Ehlers K, Binding H, Kollmann R** (1999) The formation of symplastic domains by plugging of plasmodesmata: a general event in plant morphogenesis? *Protoplasma* 209: 181-192
- Ehlers K, Kollmann R** (1996) Formation of branched plasmodesmata in regenerating *Solanum nigrum*-protoplasts. *Planta* 199: 126-138
- Eleftheriou EP, Tsekos I** (1979) Development of mestome sheath cells in leaves of *Aegilops comosa* var. *thessalica*. *Protoplasma* 100: 139-153
- Enstone DE, Peterson CA** (1997) Suberin deposition and band plasmolysis in the corn (*Zea mays* L.) root exodermis. *Can J Bot* 75: 1188-1199
- Epel BL, Bandurski RS** (1990) Tissue to tissue symplastic communication in the shoots of etiolated corn seedlings. *Physiol Plant* 79: 604-609

- Epstein E** (1971) Lateral and longitudinal transport of ions in the root of *Zea mays*. *Plant Physiol* 47(suppl.): 26
- Erwee MG, Goodwin PB** (1985) Symplast domains in extrastellar tissues of *Egeria densa* Planch. *Planta* 163: 9-19
- Erwee MG, Goodwin PB, van Bell PB** (1985) Cell-cell communication in the leaves of *Commelina cyanea* and other plants. *Plant Cell Environ* 8: 173-178
- Esau K** (1977) Anatomy of seed plants. 2nd. ed. John Wiley & Sons, New York. pp 215-242
- Evert RF, Botha CEJ, Mierzwa RJ** (1985) Free-space marker studies in the leaf of *Zea mays* L. *Protoplasma* 126: 62-73
- Fisher DB, Oparka KJ** (1996) Post-phloem transport: principles and problems. *J Exp Bot* 47: 1141-1154
- Frey-Wyssling A** (1969) The structure and biogenesis of native cellulose. *Fortschr Chem Org Naturst* 26: 1-30
- Gamalei YV, van Bel AJE, Pakhomova MV, Sjutkina AV** (1994) Effects of temperature on the conformation of the endoplasmic reticulum and on starch accumulation in leaves with the symplastic minor-vein configuration. *Planta* 194: 443-453
- Ghoshroy S, Lartey R, Sheng J, Citovsky V** (1997) Transport of proteins and nucleic acids through plasmodesmata. *Annu Rev Plant Physiol Plant Mol Biol* 48: 27-50
- Giaquinta RT, Lin W, Sadler NL, Franceschi VR** (1983) Pathway of phloem unloading of sucrose in corn roots. *Plant Physiol* 72: 362-367
- Ginsburg H, Ginsburg BZ** (1970a) Radial water and solute flows in roots of *Zea mays*. I. Water flow. *J Exp Bot* 21: 580-592
- Ginsburg H, Ginsburg BZ** (1970b) Radial water and solute flows in roots of *Zea mays*. II. Ion fluxes across root cortex. *J Exp Bot* 21: 593-604
- Gisel A, Barella S, Hempel FH, Zambryski PC** (1999) Temporal and spatial regulation of symplastic trafficking during development in *Arabidopsis thaliana* apices. *Development* 126: 1879-1889
- Goodwin PB** (1983) Molecular size limit for movement in the symplast of the *Elodea* leaf. *Planta* 157: 124-130
- Grabski S, de Feijter AW, Schindler M** (1993) Endoplasmic reticulum forms a dynamic continuum for lipid diffusion between contiguous soybean root cells. *Plant Cell* 5: 25-38
- Griffith M, Huner NPA, Espelie KE, Kolattukudy PE** (1985) Lipid polymers accumulate in the epidermis and mestome sheath cell walls during low temperature development of winter rye leaves. *Protoplasma* 125: 53-64
- Gunning BES** (1978) Age-related and origin-related control of the numbers of plasmodesmata on cell walls of developing *Azolla* roots. *Planta* 143: 181-190
- Gunning BES, Hughes JE** (1976) Quantitative assessment of symplastic transport of pre-nectar into the trichomes of *Abutilon* nectaries. *Aust J Plant Physiol* 3: 619-637

- Gunning BES, Overall RL** (1983) Plasmodesmata and cell-to-cell transport in plants. *BioSci* 33: 260-265
- Gunning BES, Pate JS** (1969) Transfer cells - plant cells with wall ingrowths, specialized in relation to short distance transport of solute - their occurrence, structure and development. *Protoplasma* 68: 107-133
- Haas DL, Carothers ZB** (1975) Some ultrastructural observations on endodermal cell development in *Zea mays* roots. *Am J Bot* 62: 336-348
- Haas DL, Carothers ZB, Robbins RR** (1976) Observations on the phi-thickenings and Casparian strips in *Pelargonium* roots. *Am J Bot* 63: 863-867
- Harrison-Murray RS, Clarkson DT** (1973) Relationships between structural development and the absorption of ions by the root system of *Cucurbita pepo*. *Planta* 114: 1-16
- Hayashi T, Marsden MPF, Delmer DP** (1987) Pea xyloglucan and cellulose. V. Xyloglucan-cellulose interaction *in vitro* and *in vivo*. *Plant Physiol* 83: 384-389
- Hayes PM, Offler CE, Patrick JW** (1985) Cellular structures, plasma membrane surface areas and plasmodesmatal frequencies of the stem of *Phaseolus vulgaris* L. in relation to radial photosynthate transfer. *Ann Bot* 56: 125-138
- Helder RJ, Boerma J** (1969) An electron microscopical study of the plasmodesmata in the roots of young barley seedlings. *Act Bot Neerl* 18: 99-107
- Hepler PK** (1982) Endoplasmic reticulum in the formation of the cell plate and plasmodesmata. *Protoplasma* 111: 121-133
- Hodges TK, Vaadia Y** (1964) Uptake and transport of radiochloride and tritiated water by various zones of onion roots of different chloride status. *Plant Physiol* 39: 104-108
- Holloway PJ, Wattendorf J** (1987) Cutinized and suberized cell wall. In: Vaughn KC, ed, CRC handbook of plant cytochemistry. Vol. 2. Other cytochemical staining procedures. CRC Press., Boca Raton, Florida. pp 1-35
- Huang CX, van Steveninck RFM** (1989) Longitudinal and transverse profiles of K<sup>+</sup> and Cl<sup>-</sup> concentration in 'low-' and 'high-salt' barley roots. *New Phytol* 112: 475-480
- Huisinga B, Knijff AMW** (1974) On the function of the Casparian strips in roots. *Acta Bot Neerl* 23: 171-175
- Javis P, House CR** (1970) Evidence for symplastic ion transport in maize roots. *J Exp Bot* 21: 83-90
- Jones MGK** (1976) The origin and development of plasmodesmata. In: Gunning BES, Robards AW, eds, Intercellular communication in plants: studies on plasmodesmata. Springer-Verlag, Berlin. pp 81-105
- Kamula SA, Peterson CA, Mayfield CI** (1994) The plasmalemma surface area exposed to the soil solution is markedly reduced by maturation of the exodermis and death of the epidermis in onion roots. *Plant Cell Environ* 17: 1183-1193
- Kamula SA, Peterson CA, Mayfield CI** (1995) Impact of the exodermis on infection of roots by *Fusarium culmorum*. In: Baluška F, Ciamporova M, Gašpariková O, Barlow PW, eds, Structure and function of roots. Kluwer Academic Publishers, the Netherlands. pp 271-276

- Karahara I, Shibaoka H** (1992) Isolation of Casparian strips from pea roots. *Plant Cell Physiol* 33: 555-561
- Karas I, McCully ME** (1973) Further studies of the histology of lateral root development in *Zea mays*. *Protoplasma* 77: 243-269
- Karnovsky MJ** (1965) A formaldehyde-glutaraldehyde fixative of high osmolarity for use in electron microscopy. *J Cell Biol* 27: 137A-138A
- Kempers R, Prior DAM, van Bel AJE, Oparka KJ** (1993) Plasmodesmata between sieve element and companion cell of extrafascicular stem phloem of *Cucurbita maxima* permit passage of 3 kDa fluorescent probes. *Plant J* 4: 567-575
- Kempers R, van Bel AJE** (1997) Symplastic connections between sieve element and companion cell in the stem phloem of *Vicia faba* L. have a molecular exclusion limit of at least 10 kD. *Planta* 201: 195-201
- Kikuyama M, Hara Y, Shimada K** (1992) Intercellular transport of macromolecules in *Nitella*. *Plant Cell Physiol* 33: 413-417
- Kramer D** (1981) Structure and function in absorption and transport of nutrients. In: Brouwer R, Gašpariková O, Kolek J, Loughman BC, eds, *Structure and function of plant roots*. Martinus Nijhoff/Dr. W. Junk Publishers, The Hague. pp 303-307
- Kramer D, Anderson WP, Preston J** (1978) Transfer cells in the root epidermis of *Atriplex hastata* L. as a response to salinity: a comparative cytological and X-ray microprobe investigation. *Aust J Plant Physiol* 5: 739-747
- Kroemer K** (1903) Wurzelhaube, Hypodermis und Endodermis der Angiospermenwurzel. *Bibliotheca Bot* 12: 1-159
- Kurkova EB** (1989) Three-dimensional distribution of plasmodesmata in the rhizodermis of *Trianea bogotensis* Karst. In: Loughman BC, Gašpariková O, Kolek J eds, *Structural and functional aspects of transport in roots*. Kluwer Academic Publishers, The Netherlands. pp 57-59
- Kurkova JB, Vakhmistrov DB, Solovev VA** (1974) Ultrastructure of some cells in the barley root as related to transport of substances. In: Kolek J, ed, *Structure and function of primary root tissues*. Veda. Publishing House of the Slovak Academy of Sciences, Bratislava. pp 75-86
- Kwiatkowska M** (1991) Autoradiographic studies on the role of plasmodesmata in the transport of gibberellin. *Planta* 183: 294-299
- Landsberg E-C** (1986) Function of rhizodermal transfer cells in the Fe stress response mechanism of *Capsicum annuum* L. *Plant Physiol* 82: 511-517
- Läuchli A** (1972) Translocation of inorganic solutes. *Ann Rev Plant Physiol* 23: 197-219
- Läuchli A** (1976) Apoplastic transport in tissues. In: Lüttge U, Pitman MG, eds, *Encyclopedia of plant physiology*. Vol II. *Transport in Plants. Part B. Tissues and organs*. Springer-Verlag, Berlin Heidelberg. pp 3-34

- Läuchli A, Kramer D, Pitman MG, Lüttge U (1974a)** Ultrastructure of xylem parenchyma cells of barley roots in relation to ion transport to the xylem. *Planta* 119: 85-99
- Läuchli A, Kramer D, Stelzer R (1974b)** Ultrastructure and ion localization in xylem parenchyma cells of roots. In: Zimmermann U, Dainty J, eds, *Membrane transport in plants*. Springer-Verlag, Berlin Heidelberg. pp 363-371
- Läuchli A, Spurr AR, Epstein E (1971a)** Lateral transport of ions into the xylem of corn roots. I. Kinetics and energetics. *Plant Physiol* 48: 111-117
- Läuchli A, Spurr AR, Epstein E (1971b)** Lateral transport of ions into the xylem of corn roots. II. Evaluation of a stellar pump. *Plant Physiol* 48: 118-124
- López-Sáez JF, Gimenez-Martin G, Risueno MC (1966)** Fine structure of the plasmodesm. *Protoplasma* 61: 81-84
- Lou CH (1955)** Protoplasmic continuity in plants. *Acta Bot Sin* 4: 183-222
- Lou CH, Wu SH, Chang WC, Shao LM (1956)** Intercellular movement of protoplasm as a means of translocation of organic material in garlic. *Sci Sin* 6: 139-157
- Lucas WJ (1999)** Plasmodesmata and the cell-to-cell transport of proteins and nucleoprotein complexes. *J Exp Bot* 50 (special issue): 979-987
- Luft JH (1961)** Improvements in epoxy resin embedding methods. *J Biophys Biochem Cytol* 9: 409-414z
- Lüttge U, Laties GG (1966)** Dual mechanisms of salt uptake in relation to compartmentation and long distance transport in plants. *Plant Physiol* 41: 1531-1539
- Luxova M (1990)** Effect of lateral root formation on the vascular pattern of barley roots. *Bot Acta* 103: 305-310
- Ma F, Peterson CA (2000)** Plasmodesmata in onion (*Allium cepa* L.) roots: a study enabled by improved fixation and embedding techniques. *Protoplasma* 211: 103-115
- Mackenzie KAD (1979)** The development of the endodermis and *phi* layer of apple roots. *Protoplasma* 100: 21-32
- Matsubara Y, Uetake Y, Peterson RL (1999)** Entry and colonization of *Asparagus officinalis* roots by arbuscular mycorrhizal fungi with emphasis on changes in host microtubules. *Can J Bot* 77: 1159-1167
- McCully ME (1994)** Accumulation of high levels of potassium in the developing xylem elements in roots of soybean and some other dicotyledons. *Protoplasma* 183: 116-125
- McLean BG, Hempel FD, Zambryski PC (1997)** Plant intercellular communication *via* plasmodesmata. *Plant Cell* 9: 1043-1054
- Mersey B, McCully ME (1978)** Monitoring of the course of fixation of plant cells. *J Microsc* 114: 49-76
- Mizuno A, Kojima H, Katou K, Okamoto H (1985)** The electrogenic protons pumping from parenchyma symplast into xylem - direct demonstration by xylem perfusion. *Plant Cell Environ* 8: 525-529
- Moon GJ, Peterson, CA, Peterson RL (1984)** Structural, chemical, and permeability changes following wounding in onion roots. *Can. J. Bot.* 62: 2253-2257

- Münch E** (1930) Die Stoffbewegungen in der Pflanze. Fischer, Jena.
- Nelson DP, Pan WL, Franceschi VR** (1990) Xylem and phloem transport of mineral nutrients from *Solanum tuberosum* roots. *J Exp Bot* 41: 1143-1148
- O'Brien TP, Carr DJ** (1970) A suberized layer in the cell walls of the bundle sheath of grasses. *Aust J Biol Sci* 23: 275-287
- O'Brien TP, Kuo J** (1975) Development of the suberized lamella in the mestome sheath of wheat leaves. *Aust J Bot* 23: 783-794
- Olesen P** (1978) Studies on the physiological sheaths in roots I. Ultrastructure of the exodermis in *Hoya carnososa* L. *Protoplasma* 94: 325-340
- Olesen P** (1979) The neck constriction in plasmodesmata: evidence for a peripheral sphincter-like structure revealed by fixation with tannic-acid. *Planta* 144: 349-358
- Oparka KJ** (1994) Plasmolysis: new insights into an old process. *New Phytol* 126: 571-591
- Oparka KJ, Boevink P, Santa Cruz S** (1996) Studying the movement of plant viruses using green-fluorescent protein. *Trends Plant Sci* 1: 412-418
- Oparka KJ, Duckett CM, Prior DAM, Fisher DB** (1994) Real-time imaging of phloem unloading in the root tip of *Arabidopsis*. *Plant J* 6: 759-766
- Oparka KJ, Prior DAM** (1992) Direct evidence for pressure-generated closure of plasmodesmata. *Plant J* 2: 741-750
- Overall RL, Gunning BES** (1982) Intercellular communication in *Azolla* roots: II. Electrical coupling. *Protoplasma* 111: 151-160
- Palevitz BA, Hepler PK** (1985) Changes in dye coupling of stomatal cells of *Allium* and *Commelina* demonstrated by microinjection of Lucifer yellow. *Planta* 164: 473-479
- Patrick JW, Offler CE** (1996) Post-sieve element transport of photoassimilates in sink regions. *J Exp Bot* 47: 1165-1177
- Perumalla CJ, Peterson CA** (1986) Deposition of Casparian bands and suberin lamellae in the exodermis and endodermis of young corn and onion roots. *Can J Bot* 64: 1873-1878
- Perumalla CJ, Peterson CA, Enstone DE** (1990) A survey of angiosperm species to detect hypodermal Casparian bands. I. Roots with a uniseriate hypodermis and epidermis. *Bot J Linn Soc* 103: 93-112
- Peterson CA** (1987) The exodermal Casparian band of onion roots blocks the apoplastic movement of sulphate ions. *J Exp Bot* 38: 2068-2081
- Peterson CA** (1988) Exodermal Casparian bands: their significance for ion uptake by roots. *Physiol Plant* 72: 204-208
- Peterson CA** (1989) Significance of the exodermis in root function. In: Loughman BC, Gašpariková O, Kolek J eds, Structural and functional aspects of transport in roots. Kluwer Academic Publishers, Dordrecht. pp 35-40

- Peterson CA** (1998) The exodermis and its interactions with the environment. In: Flores HE, Lynch JP, Eissenstat D, eds, *Radical biology: advances and perspectives on the function of plants roots*. American Society of Plant Physiologists, Rockville. pp 131-138
- Peterson CA, Cholewa E** (1998) Structural modifications of the apoplast and their potential impact on ion uptake. *Z Pflanzenernähr Boden* 161: 521-531
- Peterson CA, Emanuel ME** (1983) Casparian strips occur in onion root hypodermal cells: evidence from band plasmolysis. *Ann Bot* 51: 135-137
- Peterson CA, Emanuel ME, Wilson C** (1982) Identification of a Casparian band in the hypodermis of onion and corn roots. *Can J Bot* 60: 1529-1535
- Peterson CA, Enstone DE** (1996) Function of passage cells in the endodermis and exodermis of roots. *Physiol Plant* 97: 592-598
- Peterson CA, Perumalla CJ** (1984) Development of the hypodermal Casparian band in corn and onion roots. *J Exp Bot* 35: 51-57
- Peterson CA, Perumalla CJ** (1990) A survey of angiosperm species to detect hypodermal Casparian bands. II. Roots with a multiseriate hypodermis or epidermis. *Bot J Linn Soc* 103: 113-125
- Peterson CA, Peterson RL, Robards AW** (1978) A correlated histochemical and ultrastructural study of the epidermis and hypodermis of onion roots. *Protoplasma* 96: 1-21
- Peterson CA, Waite JE** (1996) The effect of suberin lamellae on the vitality and symplastic permeability of the onion root exodermis. *Can J Bot* 74: 1220-1226
- Peterson RL, Farquhar ML** (1996) Root hairs: specialized cells extending root surfaces. *Bot Rev* 62: 1-40
- Peterson RL, Hambleton S** (1978) Guard cell ontogeny in leaf stomata of the fern *Ophioglossum petiolatum*. *Can J Bot* 56: 2836-2852
- Peterson TA, Swanson ES, Hull RJ** (1986) Use of lanthanum to trace apoplastic solute transport in intact plants. *J. Exp. Bot.* 37: 807-822
- Pitman M** (1972) Uptake and transport of ions in barley seedlings. II Evidence for two active stages in transport to the shoot. *Aust J Biol Sci* 25: 243-257
- Radford JE, Vesik M, Overall RL** (1998) Callose deposition at plasmodesmata. *Protoplasma* 201: 30-37
- Radford JE, White RG** (1998) Localisation of a myosin-like protein to plasmodesmata. *Plant J* 14: 743-750
- Rinne PLH, van del Schoot C** (1998) Symplastic fields in the tunica of the shoot apical meristem coordinate morphogenetic events. *Development* 125: 1477-1485
- Robards AW** (1976) Plasmodesmata in higher plants. In: Gunning BES, Robards AW, eds, *Intercellular communication in plants: studies on plasmodesmata*. Springer-Verlag, Berlin. pp 15-57
- Robards AW, Clarkson DT** (1976) The role of plasmodesmata in the transport of water and nutrients across roots. In: Gunning BES, Robards AW, eds, *Intercellular communication in plants: studies on plasmodesmata*. Springer-Verlag, Berlin Heidelberg. pp 181-201



- Robards AW, Clarkson DT, Sanderson J** (1973) The structure of barley roots in relation to the transport of ions into the stele. *Protoplasma* 77: 291-311
- Robards AW, Jackson SM** (1976) Root structure and function - an integrated approach. In: Sunderland N, ed, *Perspectives in experimental biology*, Vol. 2, Botany. Pergamon Press, Oxford. pp 413-422
- Robards AW, Lucas WJ** (1990) Plasmodesmata. *Annu Rev Plant Physiol Plant Mol Biol* 41: 369-419
- Samuels AL, Fernando M, Glass ADM** (1992) Immunofluorescent localization of plasma membrane H<sup>+</sup>-ATPase in barley roots and effects of K nutrition. *Plant Physiol* 99: 1509-1514
- Schmidt HW, Schönherr J** (1982) Fine structure of isolated and non-isolated potato tuber periderm. *Planta* 154: 76-80
- Schmidt W, Bartels M** (1996) Formation of root epidermal transfer cells in *Plantago*. *Plant Physiol* 110: 217-225
- Schreiber L, Hartmann K, Skrabs M, Zeier J** (1999) Apoplastic barriers in roots: chemical composition of endodermal and hypodermal cell walls. *J Exp Bot* 50: 1267-1290
- Schulz A** (1995) Plasmodesmal widening accompanies the short-term increase in symplastic phloem unloading in pea root tips under osmotic stress. *Protoplasma* 188: 22-37
- Scott FM, Hamner KC, Baker E, Bowler E** (1956) Electron microscope studies of cell wall growth in the onion root. *Am J Bot* 43: 313-324
- Scott LI** (1928) The root as an absorbing organ. II. The delimitation of the absorbing zone. *New Phytol* 27: 141-174
- Scott MG, Peterson RL** (1979) The root endodermis in *Ranunculus acris*. I. Structure and ontogeny. *Can J Bot* 57: 1040-1062
- Seagull RW** (1983) Differences in the frequency and disposition of plasmodesmata resulting from root cell elongation. *Planta* 159: 497-504
- Shishkoff N** (1987) Distribution of the dimorphic hypodermis of roots in angiosperm families. *Ann Bot* 60: 1-15
- Sokal RR, Rohlf FJ** (1981) *Biometry*. 2nd ed, W. H. Freeman and Company, San Francisco. pp 208-227
- Spanswick RM** (1972) Electrical coupling between cells of higher plants: a direct demonstration of intercellular communication. *Planta* 102: 215-227
- Spanswick RM** (1976) Symplastic transport in tissues. In: Lüttge U, Pitman MG, eds, *Encyclopedia of plant physiology*. Vol II. Transport in Plants. Part B. Tissues and organs. Springer-Verlag, Berlin Heidelberg. pp 35-53
- Spanswick RM, Costerton JWF** (1967) Plasmodesmata in *Nitella translucens*: structure and electrical resistance. *J Cell Sci* 2: 451-464
- Spurr AR** (1969) A low-viscosity epoxy resin embedding medium for electron microscopy. *J Ultrastruct Res* 26: 31-43

- Stasovski E, Peterson CA** (1993) Effects of drought and subsequent rehydration on the structure, vitality, and permeability of *Allium cepa* adventitious roots. *Can J Bot* 71: 700-707
- Stelzer R, Kuo J, Koyro H-W** (1988) Substitution of  $\text{Na}^+$  by  $\text{K}^+$  in tissues and root vacuoles of barley (*Hordeum vulgare* L. cv. Aramir). *J Plant Physiol* 132: 671-677
- Stelzer R, Läuchli A** (1977) Salt- and flooding tolerance of *Puccinellia peisonis* II. Structural differentiation of the root in relation to function. *Z Pflanzenphysiol* 84: 95-108
- Stelzer R, Läuchli A, Kramer D** (1975) Pathways of intercellular chloride transport in roots of intact barley seedlings. *Cytobiologie* 10: 449-457
- Stelzer R, Läuchli A, Kramer D** (1978) An improved precipitation technique for intracellular  $\text{Cl}^-$  localization in plant tissues by use of picric acid. *J Exp Bot* 29: 729-733
- Steudle E, Peterson CA** (1998) How does water get through roots? *J Exp Bot* 49: 775-788
- Storey R, Walker RR** (1987) Some effects of root anatomy on K, Na and Cl loading of *Citrus* roots and leaves. *J Exp Bot* 38: 1769-1780
- Strugger S** (1957a) Der elektronenmikroskopische Nachweis von Plasmodesmen mit Hilfe der Uranylprägnierung an Wurzelmeristemen. *Protoplasma* 48: 231-236
- Strugger S** (1957b) Elektronenmikroskopische Beobachtungen an den Plasmodesmen des Urmeristems der Wurzelspitze von *Allium cepa*; ein Beitrag zur Kritik der fixation und zur Beurteilung elektronmikroskopischer Grössenangaben. *Protoplasma* 48: 365-367
- Terry BR, Robards AW** (1987) Hydrodynamic radius alone governs the mobility of molecules through plasmodesmata. *Planta* 171: 145-157
- Thomson N, Evert R, Kelman A** (1995) Wound healing in whole potato tubers: a cytochemical, fluorescence, and ultrastructural analysis of cut and bruise wounds. *Can J Bot* 73: 1436-1450
- Tippett JT, O'Brien TO** (1976) The structure of eucalypt roots. *Aust J Bot* 24: 619-632
- Tucker EB** (1990) Calcium-loaded 1,2-bis(2-aminophenoxy) ethane-N,N,N',N'-tetraacetic acid blocks cell-to-cell diffusion of carboxyfluorescein in staminal hairs of *Setcreasea purpurea*. *Planta* 182: 34-38
- Tucker EB, Tucker JE** (1993) Cell-to-cell diffusion selectivity in staminal hairs of *Setcreasea purpurea*. *Protoplasma* 174: 36-44
- Turgeon R** (1996) Phloem loading and plasmodesmata. *Trends Plant Sci* 1: 418-423
- Tyree MT** (1970) The symplast concept: a general theory of symplastic transport according to the thermodynamics of irreversible processes. *J Theor Biol* 26: 181-214
- Tyree MT, Fischer RA, Dainty J** (1974) A quantitative investigation of symplasmic transport in *Chara corallina*. II. The symplasmic transport of chloride. *Can. J. Bot.* 52: 1325-1334
- Vakhmistrov DB** (1981) Specialization of root tissues in ion transport. In: Brouwer R, Gašpariková, O, Kolek J, Loughman BC, eds, *Structure and function of plant roots*. Martinus Nijhoff/Dr. W. Junk Publishers, The Hague. pp 203-208

- Vakhmistrov DB, Kurkova EB, Soloviev VA** (1972) Some characteristics of plasmodesmae and lomasome-like formations in barley roots and their relation to transport of substances. *Fiziol Rast* 19: 951-960
- Van Bel AJE, Gamalei YV, Ammerlaan A, Bik LPM** (1992) Dissimilar phloem loading in leaves with symplastic or apoplastic minor-vein configurations. *Planta* 186: 518-525
- Van Bel AJE, Kempers R** (1990) Symplastic isolation of the sieve element-companion cell complex in the phloem of *Ricinus communis* and *Salix alba* stems. *Planta* 183: 69-76
- Van Bel AJE, van Rijen HVM** (1994) Microelectrode-recorded development of the symplasmic autonomy of the sieve element/companion cell complex in the stem phloem of *Lupinus luteus* L. *Planta* 192: 165-175
- Van den Berg C, Willemsen V, Hage W, Weisbeek P, Scheres, B** (1995) Cell fate in the *Arabidopsis* root meristem determined by directional signaling. *Nature* 378: 62-65
- Van den Berg C, Willemsen V, Hendriks G, Weisbeek P, Scheres, B** (1997) Short-range control of cell differentiation in the *Arabidopsis* root meristem. *Nature* 390: 287-289
- Van der Schoot C, Dietrich MA, Storms M, Verbeke JA, Lucas WJ** (1995) Establishment of a cell-to-cell communication pathway between separate carpels during gynoecium development. *Planta* 195: 450-455
- Van Fleet DS** (1950) A comparison of histochemical and anatomical characteristics of the hypodermis with the endodermis in vascular plants. *Am J Bot* 37: 721-725
- Van Iren F, Boers-van der Sluijs P** (1980) Symplasmic and apoplasmic radial ion transport in plant roots. cortical plasmalemma lose absorption capacity during differentiation. *Planta* 148: 130-137
- Van Iren F, van der Spiegel A** (1975) Subcellular localization of inorganic ions in plant cells by *in vivo* precipitation. *Science* 187: 1210-1211
- Van Steveninck RFM, van Steveninck ME** (1978) Ion localization. In: Hall JL, ed, Electron microscopy and cytochemistry of plant cells. Elsevier/North-Holland Biomedical Press. pp 187-234
- Verdaguer D, Molinas M** (1997) Development and ultrastructure of the endodermis in the primary root of cork oak (*Quercus suber*). *Can J Bot* 75: 769-780
- Von Guttenberg H** (1968) Der Primäre Bau der Angiospermenwurzel. In: Linsbauer K, ed. Handbuch der Pflanzenanatomie, Vol. 8. Gebrüder Borntraeger, Berlin. pp 141-159
- Waimann E, Turner A, Peart J, Roberts K, Zambryski P** (1997) Ultrastructural analysis of leaf trichome plasmodesmata reveals major differences from mesophyll plasmodesmata. *Planta* 203: 75-84
- Walker RR, Sedgley M, Blesing MA, Douglas TJ** (1984) Anatomy, ultrastructure and assimilate concentration of roots of citrus genotypes differing in ability for salt exclusion. *J Exp Bot* 35: 1481-1494
- Wang XL, McCully ME, Canny MJ** (1995) Branch roots of *Zea*. V. Structural features that may influence water and nutrient transport. *Bot Acta* 108: 209-219
- Wang X-Y, Guo G-Q, Nie X-W, Zheng G-C, Zheng G-C (Cheng K-C)** (1998) Cytochemical localization of cellulase activity in pollen mother cells of David lily during meiotic prophase I and its relation to secondary formation of plasmodesmata. *Protoplasma* 204: 128-138

- Warmbrodt RD (1985a)** Studies on the root of *Hordeum vulgare* L.- ultrastructure of the seminal root with special reference to the phloem. *Am J Bot* 72: 414-432
- Warmbrodt RD (1985b)** Studies on the root of *Zea mays* L. - structure of the adventitious roots with respect to phloem unloading. *Bot Gaz* 146: 169-180
- Warmbrodt RD (1986a)** Structural aspects of the primary tissues of the *Cucurbita pepo* L. root with special reference to the phloem. *New Phytol* 102: 175-192
- Warmbrodt RD (1986b)** Solute concentrations in the phloem and associated vascular and ground tissues in the root of *Hordeum vulgare* L. In: Cronshaw J, Lucas WJ, Giaquinta RT, eds. Phloem transport. Alan R. Liss, Inc., New York. pp 435-444
- Warmbrodt RD (1987)** Solute concentrations in the phloem and apex of the root of *Zea mays*. *Am J Bot* 74: 394-402
- Wegner LH, Raschke K (1994)** Ion channels in the xylem parenchyma of barley roots. A procedure to isolate protoplasts from this tissue and a patch-clamp exploration of salt passageways into xylem vessels. *Plant Physiol* 105: 799-813
- White RG, Badelt K, Overall RL, Vesik M (1994)** Actin associated with plasmodesmata. *Protoplasma* 180: 169-184
- Wille AC, Lucas WJ (1984)** Ultrastructural and histochemical studies on guard cells. *Planta* 160: 129-142
- Wilson AJ, Robards AW (1980)** Observation on the pattern of secondary wall development in the hypodermis of onion (*Allium cepa*) roots. *Protoplasma* 104: 149-156
- Winter-Sluiter E, Läubli A, Kramer D (1977)** Cytochemical localization of K<sup>+</sup> stimulated adenosine-triphosphate activity in xylem parenchyma cells of barley roots. *Plant Physiol* 60: 923-927
- Wolf S, Deom CM, Beachy RN, Lucas WJ (1989)** Movement protein of tobacco mosaic virus modifies plasmodesmatal size exclusion limit. *Science* 246: 377-379
- Wright KM, Oparka KJ (1997)** Metabolic inhibitors induce symplastic movement of solutes from the transport phloem of *Arabidopsis* roots. *J Exp Bot* 48: 1807-1814
- Yu GH, Kramer PJ (1967)** Radial salt transport in corn roots. *Plant Physiol* 42: 985-990
- Yu GH, Kramer PJ (1969)** Radial transport of ions in roots. *Plant Physiol* 44: 1095-1100
- Zee S-Y, O'Brien TP (1970)** Studies on the ontogeny of the pigment strand in the caryopsis of wheat. *Aust J Biol Sci* 23: 1153-1171
- Zhu T, Lucas WJ, Rost TL (1998a)** Directional cell-to-cell communication in the *Arabidopsis* root apical meristem I. An ultrastructural and functional analysis. *Protoplasma* 203: 35-47
- Zhu T, O'Quinn RL, Lucas, Rost TL (1998b)** Directional cell-to-cell communication in the *Arabidopsis* root apical meristem II. Dynamics of plasmodesmatal formation. *Protoplasma* 204: 84-93
- Ziegler H (1975)** Nature of transported substances. In: Zimmermann MH, Milburn JA, eds, Encyclopedia of plant physiology, Vol. 1. Transport in plants I, Phloem transport. Springer-Verlag, Berlin Heidelberg. pp 59-100

**Ziegler H, Lüttge U (1967) The salt-glands of *Limonium vulgare* II. The localization of chloride. *Planta* 74: 1-17**

**Ziegler H, Weigl J, Lüttge U (1963) Mikroautoradiographischer Nachweis der Wanderung von  $^{35}\text{S}_4^-$  durch die Tertiarendodermis der *Iris*-Wurzel. *Protoplasma* 56: 362-370**